UFRJ

**Universidade Federal do Rio de Janeiro Instituto de Química**

**Programa de Pós-Graduação em Bioquímica (PPGBq)**

**ERIKA LOURDES VELÁSQUEZ NUÑEZ**

# ANÁLISE PROTEÔMICA APLICADA NA CARACTERIZAÇÃO SUBCELULAR DO CÓRTEX ORBITOFRONTAL DE PACIENTES COM ESQUIZOFRENIA

**Rio de Janeiro – RJ**

**Julho de 2019**

ERIKA LOURDES VELÁSQUEZ NUÑEZ

# ANÁLISE PROTEÔMICA APLICADA NA CARACTERIZAÇÃO SUBCELULAR DO CÓRTEX ORBITOFRONTAL DE PACIENTES COM ESQUIZOFRENIA

Tese de doutorado apresentada ao Programa de Pós-Graduação em Bioquímica do Instituto de Química da Universidade Federal do Rio de Janeiro, como parte dos requisitos necessários à obtenção do título de Doutor em Ciências (Bioquímica).

Orientadores: Prof. Fábio César Sousa Nogueira
Prof. Gilberto Barbosa Domont

**Rio de Janeiro – RJ**

**Julho de 2019**

“*Tuus ego sum, et omnia mea tua sunt, o Virgo super omnia benedicta*”

**AGRADECIMENTO**

A Deus... *“ Tu es Christus, pater meu sanctus, Deus meus pius, rex meus magnus, pastor meus bonus, magister meus unus, adiutor meus optimus, dilectus meus pulcherrimus, panis meus vivus, sacerdos meus in aeternum, dux meus ad patriam, lux mea vera, dulcedo mea sancta, via mea recta, sapientia mea praeclara, simplicitas mea pura, concordia mea pacifica, custodia mea tota, portio mea bona, salus mea sempiterna... Deus cordis mei et pars mea, Christe Iesu, deficiat cor meum spiritu suo, et vivas tu in me, et concalescat in spiritu meo vivus carbo amoris tui et excrescat in ignem perfectum...” (Meditationum lib. I, cap. XVIII, n.2 (inter opera S. Augustini)*

Aos meus pais pelo apoio e incentivo

Ao Bernardo por ser minha benção, meu amor, minha pessoa favorita e companheiro em todos os momentos

A minha família, por sempre acreditar em mim, especialmente a minha tia Ingrid, meu anjo salvador nos momentos de burrice estatística

À Sheila por ter me recebido em seu coração como uma irmã

Ao Jimmy por sua amizade, ajuda, apoio e tantos momentos de risos! Trabalhar no lab sem você não é o mesmo!

Aos meus orientadores, Fábio e o Gilberto por sua paciência, ensinamentos e amizade. Vocês sempre serão um exemplo e inspiração para mim!

A todos os membros da Unidade Proteômica (aos antigos e relativamente novos) pela ajuda, parceria e fazer mais leve o trabalho de cada dia

Ao Prof. György Marko-Varga por me receber em seu laboratório. Gostaria de agradecer especialmente a Melinda por todos os ensinamentos e por ser um exemplo e inspiração de mulher na ciência

Aos membros da banca, por ter aceito convite e sempre estar dispostos a me ajudar.

A todos, muito obrigada!

**RESUMO**

VELÁSQUEZ, Erika. Análise proteômica aplicada na caracterização subcelular do córtex orbitofrontal de pacientes com esquizofrenia. Tese (Doutorado em Bioquímica) – Instituto de Química, Universidade Federal do Rio de Janeiro, Rio de Janeiro, 2019

A esquizofrenia é um distúrbio neuropsiquiátrico crônico caracterizado pelo comprometimento das funções mentais que afeta cerca de 1% da população mundial. A caracterização proteômica de frações subcelulares do córtex orbitofrontal podem fornecer informações valiosas sobre os mecanismos moleculares envolvidos na fisiopatologia desta doença. O proteoma quantitativo de sinaptossomas (SIN), mitocôndrias (MIT), fração nuclear (NUC) e citoplasma (CIT) foi obtido para 12 pacientes com esquizofrenia e para um pool com 8 controles saudáveis livres de doenças mentais usando técnicas quantitativas diferentes como iTRAQ, label-free e targeted (PRM e SRM). Na fração SIN foram identificadas um total de 2018 grupos de proteínas usando uma abordagem label-free e marcação com iTRAQ. Análises estatísticas revelaram a variação significativa na abundância de 12 e 55 proteínas quantificadas por iTRAQ e label-free, respectivamente. As principais proteínas desreguladas estavam relacionadas ao desequilíbrio da via de sinalização do cálcio, estresse do retículo endoplasmático e morte celular programada, refletidas na desregulação de proteínas como o Reticulon-1 e o Citocromo c. Além disso, encontramos um aumento significativo de proteínas associadas à regulação do comportamento humano como a LSAMP e Proteína quinase II dependente de cálcio e calmodulina. Por outro lado, a análises de espectrometria de massas identificou 939 grupos de proteínas na fração MIT, 2021 em NUC e 2433 em CIT. Um total de 358 grupos de proteínas foi encontrado desregulado entre as frações MIT, NUC e CIT. Por meio da análise proteômica quantitativa, detectamos como principais vias biológicas afetadas as relacionadas ao desequilíbrio de cálcio, apoptose, metabolismo de glutamato, ruptura da sinalização celular da ativação de CREB, orientação de axônios e proteínas envolvidas na ativação da sinalização de NF-kB juntamente com o aumento da proteína complemento C3. Com base em nossa análise de dados, sugerimos a ativação do NF-kB como uma possível via que liga a desregulação do glutamato, do cálcio, a apoptose e a ativação do sistema imune em pacientes com esquizofrenia.

Palavras-chave: Esquizofrenia, frações celulares, córtex orbitofrontal, proteômica quantitativa.

**ABSTRACT**

VELÁSQUEZ, Erika. Proteomic analysis applied in the subcellular characterization of the orbitofrontal cortex of patients with schizophrenia. Análise proteômica aplicada na caracterização subcelular do córtex orbitofrontal de pacientes com esquizofrenia. Tese (Doutorado em Bioquímica) – Instituto de Química, Universidade Federal do Rio de Janeiro, Rio de Janeiro, 2019

Schizophrenia is a chronic neuropsychiatric disorder characterized by the impairment of mental functions which affects about one percent of the world population. The proteomic characterization of subcellular fractions from the orbitofrontal cortex is useful for providing valuable information about the molecular mechanisms involved in the physiopathology of these disease. The quantitative proteome of synaptosome (SYN) (MIT), crude nuclear (NUC) and cytoplasm fractions (CIT) were obtained from 12 patients with schizophrenia and a pool of 8 healthy controls free of mental illness using different quantitative techniques such as iTRAQ, label-free and targeted (PRM and SRM). In SYN fraction was identified a total of 2018 protein groups using a Label-free and iTRAQ labelling approach. Statistical analyses reveal the significant variation in the abundance of 12 and 55 proteins by iTRAQ and label-free, respectively. The main dysregulated proteins were related to calcium signaling pathway imbalance, endoplasmic reticulum stress and programmed cell death, reflected through the dysregulation of proteins such as Reticulon-1 and Cytochrome c. Also, we found a significant increase of proteins associated to the regulation of human behaviour as limbic system-associated membrane protein and α-calcium/calmodulin-dependent protein kinase II. On the other hand, mass spectrometry analyses identified 939 protein groups in MIT fraction, 2021 in NUC and 2433 in CYT. A total of 358 protein groups were found dysregulated among MIT, NUC and CYT fractions. Through the quantitative proteomic analysis, we detect as the main biological pathways those related to calcium imbalance, apoptosis, glutamate metabolism, cell signaling disruption of CREB activation, axon guidance and proteins involved in the activation of NF-kB signaling along with the increase of complement proteins C3. Based on our data analysis, we suggest the activation of NF-kB as a possible pathway that links the deregulation of glutamate, calcium, apoptosis and the activation of the immune system in schizophrenia patients

Keywords: Schizophrenia, cellular fractions, orbitofrontal cortex, quantitative proteomics.

**SUMÁRIO**

## ABREVIAÇÕES, SÍMBOLOS E UNIDADES

| | |
|---|---|
| ACC | Córtex cingulado anterior |
| BD-HPP | O projeto proteoma humano orientado à biologia / doença, do inglês, *The biology/disease-driven human proteome Project* |
| C-HPP | Proteoma Humano – Projeto Proteoma Humano Centrado no Cromossomo, do inglês, *Chromosome-Centric Human Proteome Project* |
| CIT | citoplasma |
| CREB | Proteína de ligação ao elemento de resposta cAMP, do inglês *cAMP response element binding protein* |
| CYT | citoplasma, do inglês, cytoplasm |
| DC | Corrente direta |
| DLFL | Lobo frontal dorsolateral |
| DSM-V | Manual Diagnóstico e Estatístico de Transtornos Mentais, do inglês, *Diagnostic and Statistical Manual of Mental Disorders* |
| eIF4G2 | Tradução eucariótica factor de iniciação 4 G gamma 2, do inglês, Eukaryotic *translation initiation factor 4 gamma 2* |
| ERK1 | Quinase regulada por sinal extracelular 1, do inglês, *Extracellular signal–regulated kinase 1* |
| ESI | Ionização por eletrospray, do inglês, *Electospray Ionization* |
| GABA | Ácido gama-aminobutírico |
| GNA13 | Subunidade G da Proteína Alfa 13, do inglês, G Protein Subunit Alpha 13 |
| GRIN2A | Subunidade 2A do receptor ionotrópico do glutamato tipo NMDA, do inglês, *Glutamate ionotropic receptor NMDA type subunit 2A* |
| GWAS | Estudos de associação genômica ampla, do inglês, *genome-wide association study* |
| HCD | Dissociação de colisão por alta energia, do inglês, *High Energy Collision Dissociation* |
| HUPO | Organização do projeto proteoma humano, do inglês, *The Human Proteome Organization* |
| iTRAQ | Marcadores isobáricos de quantificação absoluta e relativa, do inglês, *Isobaric Tags for Relative and Absolute Quantification* |
| LC-MS | Cromatografia líquida com espectrômetro de massa |

| | |
|---|---|
| LSAMP | Proteína de membrana associada ao sistema límbico, do inglês, *Limbic system-associated membrane protein* |
| m/z | Massa–carga |
| MALDI | Ionização e dessorção a laser assistido por matriz, do inglês, *Matrix-Assisted Laser Desorption/Ionization* |
| MIT | mitocôndrias |
| mPC | Córtex pré-frontal medial |
| MS | Espectrometria de massas |
| MS/MS | Espectrometria de massas sequencial ou em tandem |
| nano-LC | Nano-cromatografia |
| NF-κB | Factor nuclear kappa B |
| NMDA | N-metil D-Aspartato |
| NUC | fração nuclear |
| PET | Tomografia por emissão de pósitrons |
| PRM | Monitoramento Paralelo de Reações |
| PSMs | Do inglês, *Peptide-spectrum match* |
| PTMs | Modificações pós-traducionais |
| Q | Quadrupolos |
| RF | Radiofrequência |
| SIN | sinaptossoma |
| SPECT | Tomografia por emissão de fóton único |
| SRM | Monitoramento de Reação Selecionada |
| SRR | Serine racemase |
| SYN | Sinaptossoma, do inglês, synaptosome |

## LISTA DE FIGURAS DA INTRODUÇÃO

## LISTA DE TABELAS DA INTRODUÇÃO

## ORGANIZAÇÃO DA TESE

No primeiro capítulo é apresentada uma introdução geral sobre a esquizofrenia; as principais características clínicas da doença, tratamento farmacológico, a neuroquímica da doença e os principais achados genéticos e proteômicos.

No segundo capítulo são apresentados conceitos gerais da proteômica; as principais estratégias de analises, analisadores de massas e diversas estratégias utilizadas na quantificação relativa de proteínas.

No terceiro capítulo será exposta a justificativa e os objetivos deste projeto de pesquisa. Seguidamente, a metodologia utilizada, os resultados obtidos, a discussão e as conclusões estarão apresentados em conformidade com os manuscritos publicados e em fase de revisão.

No quarto capítulo, descreve-se a través de um capitulo de livro o protocolo detalhado da técnica de marcação com iTRAQ e sua aplicação na quantificação de proteínas de tecido cerebral *post-mortem* para o estudo de doenças psiquiátricas.

No quinto capítulo é apresentada, através de um artigo publicado, as análises proteômicas quantitativas da fração de sinaptossoma utilizando as técnicas de *label-free*, iTRAQ e PRM.

Finalmente no sexto capitulo, através de um artigo submetido, discutimos os principais achados das análises quantitativas das frações de mitocôndria, núcleo e citoplasma utilizando a marcação por iTRAQ e SRM.

# CAPÍTULO I

# INTRODUÇÃO: CARACTERÍSTICAS GERAIS DA ESQUIZOFRENIA

## 1.1. Esquizofrenia: características clínicas, diagnóstico e tratamento

A esquizofrenia é um transtorno neuropsiquiátrico crônico caracterizado pelo comprometimento das funções psíquicas superiores. A doença se manifesta principalmente através dos sintomas positivos caracterizados por delírios, alucinações, distúrbios motores; e negativos como avolição, alogia, apatia substancial, deterioração funcional nas relações interpessoais e cuidado pessoal e déficit cognitivo (GAUR et al., 2008).

Segundo a Organização Mundial da Saúde (2018) a esquizofrenia afeta mais de 23 milhões de pessoas em todo o mundo, sendo mais comum em homens do que em mulheres. A idade média de aparição da enfermidade varia entre os 18 anos nos homens e 25 anos nas mulheres, no caso do sexo feminino existe um risco maior de manifestar a doença nos meados dos 40 anos (SIE, 2011).

O diagnóstico e a categorização da esquizofrenia são baseados nas apreciações subjetivas obtidas nas entrevistas com os pacientes, classificando-se em diferentes subtipos clínicos através da ponderação dos diversos sintomas. De acordo com a última atualização do Manual Diagnóstico e Estatístico de Transtornos Mentais (EROGLU S., TOPRAK S., URGAN O, MD, OZGE E. ONUR, MD, ARZU DENIZBASI, MD, HALDUN AKOGLU, MD, CIGDEM OZPOLAT, MD, EBRU AKOGLU, 1994) a esquizofrenia é classificada em cinco subtipos conforme a Tabela 1.

**Tabela 1. Classificação e principais sintomas da esquizofrenia segundo o DSM-V.**

| Código DMS-V | Subtipo de esquizofrenia | Principais sintomas |
|---|---|---|
| 295.30 | Tipo paranóico | • Delírios Alucinações auditivas frequentesNão apresenta fala desorganizada, comportamento catatônico ou desorganizado, afeto plano ou inadequado |
| 295.10 | Tipo desorganizado | Fala desorganizada Comportamento desorganizado<br>• Afeto plano ou inadequado |
| 295.20 | Tipo | • Imobilidade motora, evidenciada pela catalepsia ou estupor |

| | | |
|---|---|---|
| | catatônico | • Atividade motora excessiva (sem propósito e nãoinfluenciado por estímulos externos)<br>• Negativismo extremo ou mutismo<br>• Peculiaridades do movimento voluntário<br>• Posturas inadequadas ou bizarras, maneirismos proeminentes ou careta proeminente<br>• Ecolalia ou ecopraxia |
| 295.90 | Tipo indiferenciado | • Não são atendidos exclusivamente os critérios de classificação para os de tipo paranoide, desorganizado ou tipo catatônico |
| 295.60 | Tipo residual | • Ausência de delírios proeminentes. Pode apresentar de forma atenuada crenças, experiências perceptuais incomuns, alucinações, fala desorganizada, comportamento desorganizado ou catatônico.<br>• Presença continua de sintomas negativos |

Os antipsicóticos, também conhecidas como neurolépticos, são os medicamentos indicados para o tratamento da esquizofrenia e de outros transtornos com episódios psicóticos (Tabela 2). A eficácia do tratamento antipsicótico apresenta limitações significativas. Apenas 50% dos pacientes tratados respondem positivamente ao tratamento, observando-se principalmente a melhoria dos sintomas positivos concomitantemente com os diversos efeitos colaterais da medicação (LALLY; MACCABE, 2015). Os sintomas negativos e cognitivos permanecem atualmente sem uma opção terapêutica totalmente eficaz (MÖLLER, 2016). Por último, é necessário destacar que 30% dos pacientes com esquizofrenia não respondem a nenhum tratamento farmacológico disponível (NUCIFORA et al., 2018).

**Tabela 2. Antipsicóticos para o tratamento da esquizofrenia. (Adaptado de (STĘPNICKI; KONDEJ; KACZOR, 2018)**

| **Classificação do antipsicótico** | **Mecanismo de ação** | **Efeitos colaterais** |
|---|---|---|
| Antipsicóticos de primeira geração ou típicos.<br>Exemplos: clorpromazina, haloperidol, loxapina | • Antagonista dos receptores D2 | • Efeitos extrapiramidais<br>• Elevação da prolactina<br>• Perturbações do sono, demência, perda dememória e depressão<br>• Afecção no sistema cardiovascular, sistema urinário e reprodutivo, sistema gastrointestinal, fígado, depressão do sistema respiratório e imunológico<br>• Desordens metabólicas como hiperlipidemia, hiperglicemia, aumento de peso |
| Antipsicóticos de segunda geração ou atípicos.<br>Exemplos: clozapina, olanzapine, risperidone | • Antagonistas dos receptores 5-$HT_{2A}$, receptores D4 e D2 (parciais)<br>• Agonistas parciais dos receptores 5-$HT_{1A}$ | • Obesidade<br>• Diabetes<br>• Sedação<br>• Agranulocitose (clozapina) |
| Antipsicóticos de terceira geração.<br>Exemplos: aripiprazol, | • Agonistas parciais dos receptores D1, D2/D3, 5-$HT_{1A}$ | • Insônia, ansiedade, dor de cabeça, constipação ou náusea<br>• Acatisia |

| | | |
|---|---|---|
| brexpiprazole, cariprazine | • Antagonistas dos receptores 5-$HT_{2A}$, 5-$HT_{2B}$ e 5-$HT_7$ | |

## 1.2. Neuroquímica da esquizofrenia

### 1.2.1. Teoria dopaminérgica

A hipótese dopaminérgica da esquizofrenia surgiu inicialmente de várias evidências indiretas, uma delas na década de 1970 com a eficácia clínica dos antipsicóticos antagonistas dos receptores D2 de dopamina no tratamento dos sintomas positivos da doença (SEEMAN et al., 1976). Posteriormente, foi demostrado que a administração de anfetaminas e outros compostos que aumentam as concentrações extracelulares de dopamina podem induzir sintomas psicóticos semelhantes aos observados na esquizofrenia (BREIER et al., 1997).

A teoria clássica da psicose estabelece que na esquizofrenia existe uma hiperatividade da dopamina na via mesolímbica, abundante em receptores de tipo D2 o alvo dos neurolépticos, o que gera a manifestação dos sintomas positivos (BRISCH et al., 2014). Paralelamente, foi observada uma hipoatividade da dopamina na via mesocortical com hipostimulação do receptor da dopamina D1 do córtex pré-frontal, o que é manifestado nos sintomas negativos e cognitivos (CHOHAN et al., 2016). Foi demonstrado que o bloqueio prolongado dos receptores D2 leva à regulação negativados receptores D1 no córtex pré-frontal, resultando na deterioração significativa da memória de trabalho (CASTNER; WILLIAMS; GOLDMAN-RAKIC, 2000).

Recentemente, a meta-análise de estudos utilizando tomografia por emissão de pósitrons (PET) e tomografia por emissão de fótonúnico (SPECT) achou inconsistências na teoria mesolímbica, demonstrando que há um aumento significativo na síntese e liberação da dopamina no corpo estriado dorsal durante as psicoses (MCCUTCHEON et al., 2018). Em tecido cerebral *post-mortem* de pacientes com esquizofrenia, especificamente no *nucleus accumbens* e no corpo estriado dorsal, foram encontradas concentrações de dopamina elevadas assim como aumento dos receptores dopaminérgicos (MCCOLLUM et al., 2015). Finalmente, foi demonstrado que a dopamina do corpo estriado e a dopamina cortical têm uma relação bidirecional, sendo que o incremento da liberação da dopamina na área estriada dorsal pode diminuir a

liberação de dopamina na região mesocortical produzindo alterações cognitivas (SIMPSON; KELLENDONK; KANDEL, 2010).

### 1.2.2. Teoria glutamatérgica

O glutamato é o neurotransmissor excitatório mais comum no cérebro dos mamíferos, os neurônios glutamatérgicos representam aproximadamente 60-80% da atividade metabólica cerebral total (ROTHMAN et al., 2003). Distúrbios na neurotransmissão glutamatérgica, especialmente no funcionamento do receptor N-metil D-Aspartato (NMDA), pode influenciar a plasticidade sináptica e os microcircuitos corticais (HARRISON; WEINBERGER, 2005). Os antagonistas do receptor NMDA, como a fenciclidina e cetamina podem mimetizar a psicose com sintomas semelhantes à esquizofrenia (FARBER NB, 2003). Num estudo *in vivo* utilizado SPECT, foi observado um déficit relativo na atividade do receptor de NMDA no hipocampo de pacientes com esquizofrenia que ainda não tinham recebido tratamento antipsicótico (PILOWSKY et al., 2006). Por outro lado, os níveis de glutamato e glutamina encontra-se aumentados em indivíduos com risco familiar de esquizofrenia (TANDON et al., 2013). No primeiro episódio psicótico de pacientes não medicados, o nível de glutamato foi achado aumentado no núcleo caudado (FUENTE-SANDOVAL et al., 2011). Da mesma forma, pacientes com esquizofrenia resistentes ao tratamento farmacológico, possuem uma maior quantidade de glutamato no córtex cingulado anterior em comparação com o grupo de pacientes com esquizofrenia que responde ao tratamento e ao grupo controle (DEMJAHA et al., 2014).

O papel potencial do glutamato na fisiopatologia da esquizofrenia tem sido reforçado pelas descobertas genéticas recentes, onde se verificou polimorfismos de nucleotídeo único no gene GRIN2A (subunidade 2A do receptor ionotrópico do glutamato tipo NMDA), que codifica para uma subunidade do receptor NMDA, assim como no gene SRR (Serine racemase), que desempenha um papel fundamental nas vias que conduzem à ativação do receptor NMDA (RIPKE et al., 2014). Do mesmo modo, estudos no tecido cerebral *post-mortem* de cérebro de pacientes com esquizofrenia, detectaram alterações na densidade dos receptores do tipo NMDA no córtex pré-frontal e no giro frontal superior (CATTS et al., 2015). Alguns propõe que a anormalidade da densidade deste receptor se deve primariamente a uma localização aberrante e não a um déficit generalizado (J.C. HAMMOND, D. SHAN, 2014).

O mecanismo completo pelo qual os antagonistas do receptor de NMDA geram alterações

no metabolismo do glutamato e neurotóxicidade em modelos animais ainda não foi completamente elucidado. Evidências indicam que a hipofunção dos receptores NMDA dos interneurônios GABAérgicos, implicaria a desinibição dos neurônios piramidais com o aumento da neurotransmissão glutamatérgica (HOMAYOUN; MOGHADDAM, 2008). Porém, também foi proposta a hipóteses de que a hipofunção glutamatérgica dos interneurônios pode ser devida a diminuição da neurotransmissão dos interneurônios parvalbumina-positivos (ROTARU; LEWIS; GONZALEZ-BURGOS, 2013). Outrossim, como parte central deste mecanismo, foram consideradas as alterações nos níveis de espécies reativas de oxigênio induzidas pelos antagonistas do receptor de NMDA, já que a redução dos níveis de superóxido evitou as alterações induzidas pela cetamina na atividade dos interneurônios bloqueando o efeito comportamental em modelos animais (BEHRENS et al., 2007).

### 1.2.3. Teoria serotoninérgica e GABAérgica

A hipótese serotoninérgica da esquizofrenia é derivada das observações sobre o mecanismo de ação da droga alucinógena dietilamida do ácido lisérgico e sua ligação à serotonina (AGHAJANIAN; MAREK, 2000). Além disso, a maioria dos chamados antipsicóticos atípicos, agem como agonistas parciais ou antagonistas sobre os receptores de serotonina do tipo 5-$HT_{1A}$ e 5-$HT_{2A}$ respectivamente (QUEDNOW; GEYER; HALBERSTADT, 2010). Foi sugerido que o incremento na atividade do sistema serotoninérgico no núcleo dorsal da rafe pode perturbar a atividade dos neurônios corticais na esquizofrenia, sendo que se esta hiperatividade for de forma extensa e prolongada, pode impactar o funcionamento do córtex cingulado anterior (ACC) e o lobo frontal dorsolateral (DLFL), gerando os sintomas deste distúrbio psiquiátrico (EGGERS, 2013). Imagens adquiridas por PET demonstraram a desregularão na densidade do receptor da serotonina, comprovando que a alteração no sistema serotoninérgico está presente durante as fases iniciais da doença e antes da exposição aos neurolépticos (NGAN et al., 2000).

Por outro lado, também tem sido postulada a hipótese GABAérgica. O ácido gama-aminobutírico (GABA) é o principal neurotransmissor inibitório no sistema nervoso e o desequilíbrio na sua sinalização causa o desbalanço entre os sinais excitatórios e inibitórios no córtex cerebral, fator chave na fisiopatologia da esquizofrenia (GUIDOTTI et al., 2005). Estudos *post-mortem* apoiam a hipótese de uma transmissão GABAérgica alterada na esquizofrenia, devido à redução na expressão do glutamato

descarboxilase-67, dos interneurônios parvalbumina positivos e do transportador GAT-1 no córtex pré-frontal dorsolateral, ACC e córtex visual primário (JONGE, DE et al., 2017). Pesquisas recentes sugerem que a modulação seletiva do sistema GABAérgico é uma intervenção promissora para o tratamento dos defeitos cognitivos associados à esquizofrenia (XU; WONG, 2018).

### 1.3. Esquizofrenia: neurodesenvolvimento e alterações neuroanatômicas

Por muitos anos, a esquizofrenia tem sido classificada como uma doença do neurodesenvolvimento. Desde o ano 1982, o pesquisador Feinberg (FEINBERG, 1982) observou uma redução importante na densidade sináptica cortical nos pacientes com esquizofrenia, o qual considerou um defeito na maturação análoga à poda sináptica e eliminação programada de elementos neurais nas etapas inicias do desenvolvimento. Os primeiros sintomas da doença geralmente aparecem na adolescência e são eventos estressantes, indicando que fatores ambientais podem contribuir de forma significativa na aparição dos primeiros sintomas da esquizofrenia (SIRIS, 1988).

Os primeiros achados em relação às mudanças estruturais no cérebro de pacientes com esquizofrenia datam da década de 70, detectando-se do volume ventricular em pacientes com esquizofrenia (JOHNSTONE; FRITH; KREEL, 1976). Atualmente, a meta-análise de diversos estudos morfométricos de diferentes áreas do cérebro de pacientes com esquizofrenia determinou que existem alterações significativas. Foi reportada a diminuição na matéria branca, especificamente nas regiões do corpo caloso, ACC, cápsula interna, na área temporal esquerda e no córtex pré-frontal medial (mPC), por outro lado, na matéria cinzenta, houve uma diminuição nas áreas da insula bilateral /giro temporal superior, ACC dorsal e rostral, tálamo e no mPC (BORA et al., 2011).

Diversos estudos longitudinais e transversais apontaram a redução generalizada e progressiva do volume de massa cinzenta principalmente no lobo frontal de pacientes com esquizofrenia (ZHANG et al., 2018). É necessário enfatizar que a primeira fase do desenvolvimento do córtex pré-frontal se dá na gestação, finalizando o amadurecimento na adolescência com a eliminação de sinapses, constituindo dois períodos críticos de vulnerabilidade (PETANJEK et al., 2011). Durante a adolescência, período no qual geralmente se manifestam os primeiros sintomas psicóticos, as situações sociais adversas elevam o estresse e aumentam a estimulação dopaminérgica da via mesocortical levando a uma poda sináptica exagerada (SELTEN et al., 2013). Num modelo primata, comprovou-se que a hiperestimulação dopaminérgica diminui a densidade dos neurônios

piramidais do córtex pré-frontal provocando disfunção cognitiva (SELEMON et al., 2007).

### 1.4. Genômica e proteômica na esquizofrenia

A taxa de herdabilidade da esquizofrenia está estimada em 64-81%, no entanto, a importância da influência dos fatores ambientais é importante nesta doença (DONGEN, VAN; BOOMSMA, 2013). Existe uma herança genética como parte importante da etiologia da esquizofrenia (RIPKE et al., 2014). Atualmente são conhecidos pelo menos 108 loci por estudos de associação genômica ampla (GWAS) relacionados a genes envolvidos na neurotransmissão glutamatérgica, plasticidade sináptica, receptor de dopamina D2, subunidades de canais de cálcio voltagem-dependentes e também o complexo de histocompatibilidade principal, um candidato consistente encontrado em outros estudos de GWAS (RIPKE et al., 2014) (GIEGLING et al., 2017) Embora as análises de GWAS gerem dados importantes, esses não respondem completamente às perguntas elementares sobre a fisiopatologia da doença, nem tampouco contribuem na identificação de biomarcadores com valor preditivo para o risco da doença ou resposta terapêutica. Na última década, os esforços foram centrados nos estudos de transcriptômica baseados em microarranjos usando tecido cerebral *post-mortem* de pacientes com esquizofrenia e indivíduos-controle. Os dados mostraram que existem várias vias moleculares afetadas na esquizofrenia, incluindo inflamação, metabolismo energético, função sináptica e via da mielinização. Um fator limitante de tais pesquisas é a ocorrência de mudanças sutis na expressão dos genes que, nem sempre, podem ser extrapoladas à expressão de proteínas (PENNINGTON; COTTER; DUNN, 2005).

Na última década, estudos de proteômica tentaram contribuir na elucidação da fisiopatologia da esquizofrenia a analisando diferentes áreas de tecidos cerebrais *post-mortem* de pacientes esquizofrênicos em comparação com controles livres de doenças mentais. Atualmente, a caracterização proteômica de áreas cerebrais, como o córtex pré-frontal, revelou alteração de proteínas envolvidas no metabolismo energético e dos oligodendrócitos (MARTINS-DE-SOUZA; GATTAZ; SCHMITT; REWERTS; MARANGONI et al., 2009) nas vias de sinalização comprometidas com a formação de axônios e plasticidade sináptica, como GNA13-ERK1-eIF4G2 (HIRAYAMA-KUROGI et al., 2017) desequilíbrio na homeostase do cálcio e no sistema imunológico (MARTINS-DE-SOUZA; GATTAZ; SCHMITT; REWERTS; MACCARRONE et al., 2009) e aumento significativo da expressão de proteínas sinápticas como a proteína de união à

sintaxina e a proteína de membrana associada ao sistema límbico (LSAMP) (BEHAN et al., 2009). A análise proteômica do lobo temporal (MARTINS-DE-SOUZA; GATTAZ; SCHMITT; NOVELLO; MARANGONI et al., 2009) tálamo mediodorsal (MARTINS-DE-SOUZA et al., 2010) e corpo caloso (SAIA-CEREDA et al., 2015) também reportaram a desregulação das proteínas envolvidas no metabolismo energético, oligodendrócito, homeostase do cálcio e regulação do citoesqueleto. No caso do córtex cingulado anterior, apresenta variação na abundância de proteínas vinculadas ao processo de endocitose mediada por clatrina e dos receptores NMDA (FÖCKING et al., 2015). Até o momento, foram realizados poucos estudos utilizando uma abordagem proteômica subcelular, entre os quais podemos mencionar a caraterização do proteoma nuclear de tecido cerebral do corpo caloso e lobo temporal anterior (SAIA-CEREDA et al., 2017), no qual se reportaram as proteínas do *spliceosome* e à sinalização cálcio/calmodulina como os principais processos biológicos afetados.

# CAPÍTULO II
# INTRODUÇÃO: ANÁLISE PROTEÔMICA

## 2.1. Análises proteômica e suas diferentes abordagens

O proteoma pode ser definido como o complemento proteico do genoma e consiste no conjunto de proteínas expressas por um sistema biológico num momento determinado (WILKINS et al., 1996). A proteômica, é um conjunto de técnicas cujo fim é o estudo do proteoma ; (HUBER, 2003). A análise proteômica fornece informação sobre o conjunto de proteínas expressas por um organismo em condições determinadas (EIDHAMMER et al., 2007).

O estudo do proteoma pode ser abordado através de três estratégias diferentes, a primeira delas, através da análise direta de proteínas intactas, chamada *top-down* (CATHERMAN; SKINNER; KELLEHER, 2015) e a segunda, denominada *bottom-up*, onde as proteínas são hidrolisadas por uma enzima de clivagem específica, geralmente a tripsina, a partir de amostras em solução ou previamente separadas numa corrida eletroforética (WOLTERS; WASHBURN; YATES, 2001). Esta última estratégia é a mais comum, fornecendo a detecção indireta das proteínas através de análises, identificação e quantificação de seus respectivos peptídeos (ZHAN et al., 2013). E finalmente, a terceira estratégia chamada de middle-down, é aplicada na analises peptídeos longos naturais ou gerados através da digestão da amostra com enzimas com sítios de clivagem menos frequentes que a tripsina como GluC ou AspN. Uma aplicação clássica desta abordagem é no estudo das caudas das histonas, com a finalidade de obter mais informações sobre modificações pós-traducionais (PTMs) coexistentes (SIDOLI; GARCIA, 2017).

## 2.2. Espectrometria de massa

Atualmente, a espectrometria de massas (MS) é a ferramenta analítica que permite a identificação do analito em função de sua relação massa–carga (m/z). Na proteômica, o MS é constituído por três elementos essências: (1) fonte de ionização branda, geralmente acoplada a um sistema de nano-cromatografia (nano-LC), (2) analisador de massas, que seleciona e fragmenta os analíticos para serem analisados em função da sua razão m/z (3) detector que permite captar e registrar a informação dos espectros obtidos (JAYARAM, 2013). Em seguida, descrever-se-á cada um dos elementos separadamente

### 2.2.1. Fonte de ionização

A aplicação da MS na análise de amostras biológicas como as proteínas foi possível graças ao desenvolvimento de técnicas eficazes de ionização branda, como a

ionização por *electrospray* (ESI) e a dessorção/ionização por laser assistida por matriz (MALDI), onde as moléculas ionizadas alcançam a fase gasosa sem sofrer uma fragmentação excessiva.

Na ionização por ESI, as amostras em solução são dispersas em forma de aerossol, gerando gotículas carregadas (LOO; UDSETH; SMITH, 1989). Uma vez aplicado o potencial elétrico no capilar onde se encontra retida a amostra, sobre o líquido agem duas forças a saber, a tensão superficial e as forças de Coulomb, o que conduz à formação do "Cone de Taylor". O analito carregado emerge do cone através de um processo de "brotamento" no qual a força eletrostática aplicada supera à tensão superficial (BANERJEE; MAZUMDAR, 2012). Uma vez expelidas do cone, tem-se proposto que as gotículas carregadas sofrem um processo de evaporação e fissão por meio de explosões de Coulomb até a formação eventual de gotículas contendo um único íon (GASKELL, 1997) ou através da evaporação progressiva do solvente das gotículas até a ejeção dos íons solvatados (WILM, 2011).

Por outro lado, na técnica de ionização por MALDI, a amostra é co-cristalizada em conjunto com uma matriz geralmente composta por ácidos orgânicos fracos de baixo peso molecular, cuja função principal é assistir à ionização do analito através da doação de prótons (LEWIS; WEI; SIUZDAK, 2006). O cristal formado é bombardeado comum laser UV que permite a volatilização da amostra junto com a matriz; dois modelos principais foram postulados para este tipo de ionização (1) o modelo de ionização fotoquímica, onde os íons são produzidos a partir de um processo de protonação ou desprotonação envolvendo uma molécula de analito colidindo com íons da matriz na fase gasosa (2) O modelo de ionização por cluster de íons, onde o analito carregado é dessorvido por forte foto absorção pelas moléculas da matriz (CHANG et al., 2007).

### 2.2.2. Analisadores de massa

Neste momento encontram-se no mercado diversos tipos de analisadores de massa como os instrumentos de tempo de vôo, o triplo quadrupolo, a armadilha de íons linear, o analisador por ressonância ciclotrônica de íons e o Orbitrap, que utilizam diferentes técnicas de fragmentação para as análises das amostras. Nesta secção serão apenas descritos os métodos de fragmentação e instrumentos utilizados nesta pesquisa de tese, o analisador Orbitrap nos instrumentos LTQ Orbitrap Velos (espectrômetro de massa híbrido) e no Q Exactive Plus e o TSQ Quantiva, um triplo quadrupolo.

O Orbitrap consiste em uma armadilha com um eletrodo externo em forma de barril e um eletrodo central fusiforme ao longo do eixo (Figura 1A). Os íons são injetados tangencialmente no campo elétrico entre os eletrodos, movimentando-se em trajetórias estáveis de rotação e oscilação ao longo do eixo; a frequência dessa oscilação harmônica é independente da velocidade do íon e é inversamente proporcional à raiz quadrada da relação m/z (MAKAROV, 2000). A aquisição de imagens, que procedem do sinal da tensão induzida pelas oscilações dos íons e registrada em forma de transientes e transformada rapidamente mediante as transformações de Fourier para obter o espectro de massa (HU et al., 2005). Geralmente o Orbitrap, utiliza uma técnica de fragmentação exclusiva chamada de dissociação de colisão por alta energia (*High Energy Collision Dissociation* – HCD). A fragmentação por HCD é realizada com gás nitrogênio numa câmara de colisão ou octopolo; o peptídeo é transportado e acelerado por um gradiente de pressão que provoca sua aceleração e colisão com o nitrogênio, gerando fragmentos que posteriormente são analisados no Orbitrap (THERMO FISHER SCIENTIFIC, 2009).

No caso do triplo quadrupolo, como o nome indica, é uma seria linear de três quadrupolos Q1, Q2 e Q3 onde cada um consiste em quatro hastes de metal dispostas de forma paralela (GROSS; GROSS, 2011) (Figura 1B). Q1 e Q3 agem com filtros de massas, que no caso do TSQ Quantiva (ThermoScientific), utiliza uma relação variável de tensão de radiofrequência (RF) assimétrica que aumenta a sensibilidade e a transmissão iônica e de tensão de corrente direta (DC) gerando um campo elétrico que dá oscilações estáveis aos íons com um m/z específico. O Q2 atua como cela de colisão cheia de argônio de alta pressão onde uma determinada RF cria um campo elétrico que fornece oscilações estáveis aos íons numa janela de valores m/z; no eixo axial uma DC acelera o trânsito de íons dentro da célula (THERMO FISHER SCIENTIFIC, 2017).

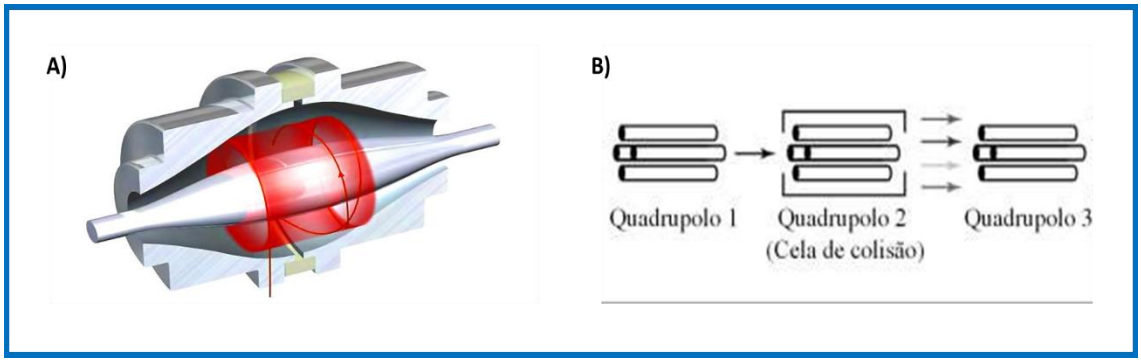


**Figura 1. A)** Desenho básico de um analisador Orbitrap. **B)** Representação do um analisador triplo quadrupolo.
**Disponível em:** A) http://analyteguru.com/resources/intact-monoclonal-antibody-characterization-using-a-bench-top-orbitrap-mass-spectrometer/. B) www.researchgate.net/figure/Figura-1-Esquema-de-um-analisador-triplo-quadrupolo_fig1_297659998**Acesso:** 15 fevereiro 2019.

### 2.3. Proteômica quantitativa

Para uma maior compreensão dos sistemas biológicos, a proteômica desenvolveu várias estratégias para efetuar com precisão a análise quantitativa tanto absoluta como relativa da expressão de proteínas num proteoma determinado. Assim, através da proteômica podemos efetuar uma quantificação exata de uma proteína, por exemplo, em termos de ng ou nmoles. Contudo, uma das estratégias mais amplamente implementadas, são aquelas que visam à quantificação relativa das proteínas, isto é, a relação de duas o mais condições (por exemplo, paciente versus controle) calculada em termos de razão para determinar quantas vezes aumenta ou diminui uma condição experimental com relação à outra (LI et al., 2017). A seguir, serão apresentadas as técnicas de quantificação relativa mais empregada nos estudos proteômica e na presente teses de pesquisa.

#### 2.3.1. Quantificação por marcação com isóbaros (iTRAQ)

A marcação química por iTRAQ é um método de quantificação relativa que permite quantificar ao mesmo tempo várias condições experimentais, através da introdução de uma modificação química nas amostras. O reagente iTRAQ, constituído por diferentes combinações de isótopos $^{13}C$, $^{15}N$ e $^{18}O$ é formado por um grupo repórter (N-metilpiperazina) unido a um grupo de equilíbrio de massa (carbonil) e um grupo amino-reativo (éster NHS) o qual se une aos grupos Ɛ-amino de lisina e à porção N-terminal dos peptídeos(ROSS et al., 2004) (Figura 2A). As diversas combinações de

isótopos, permite estabelecer várias etiquetas isóbaras com grupos repórter de massas diferentes sem mudar a massa total do reagente (Figura 2B).

Por essa razão, as amostras de várias condições podem ser analisadas simultaneamente no espectrômetro de massas, já que, após sofrer o processo de fragmentação MS2, a estrutura do reagente de iTRAQ é clivada, e o grupo repórter é liberado permitindo calcular a concentração relativa dos peptídeos a partir das intensidades obtidas dos íons repórteres correspondentes (Figura 2C) (ROSS et al., 2004).

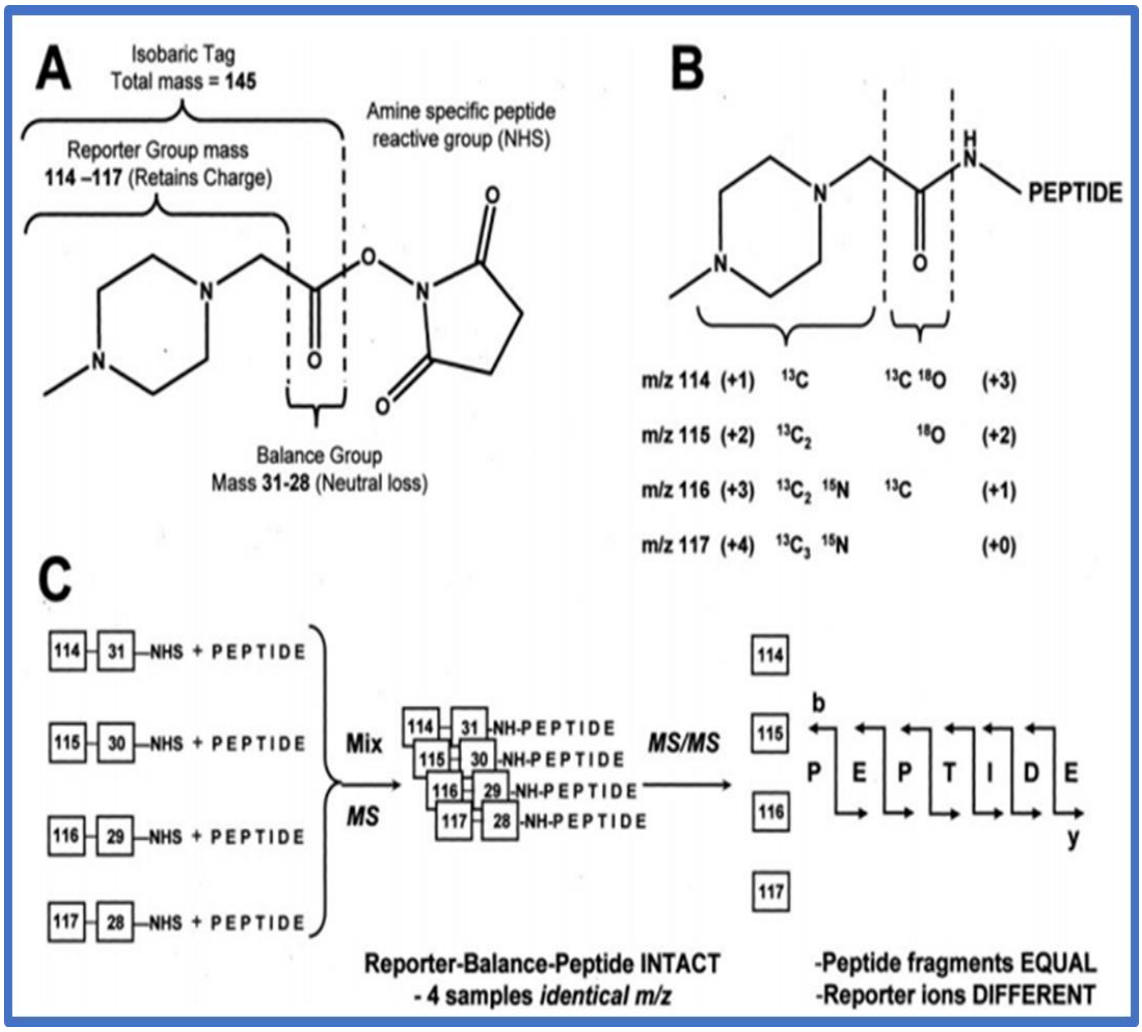


**Figura 2.** Marcação com iTRAQ. a) Estrutura do reagente de iTRAQ. b) A molécula de reagente de iTRAQ utiliza isótopos $^{13}C$, $^{15}N$ e$^{18}O$ para manter as mesmas massas. c) Em uma varredura inicial as massas para cada grupo repórter são iguais. Uma vez fragmentados, cada repórter é liberado e sua intensidade é proporcional à abundância relativa desse peptídeo em cada amostra. (Figura adaptada de ROSS et. al, 2004)

Uma das principais vantagens da marcação com o iTRAQ é a diminuição do tempo de análises no espectrômetro de massas e a melhora na reprodutibilidade entre as diferentes réplicas experimentais. Por outro lado, entre as desvantagens encontra-se o elevado custo dos reagentes e a restrição no número de canais disponíveis para efetuar a marcação limitando a comparação ao número de amostras. Primeiramente, foi desenvolvido o reagente de iTRAQ 4-plex de quatro canais (ROSS et al., 2004) e posteriormente o iTRAQ 8-plex (CHOE et al., 2007). Atualmente, encontram-se disponíveis no mercado outras estratégias de marcação com isóbaros como TMT2-plex, 6-plex, 10-plex e 11-plex, mas estudos sinalizam que o reagente iTRAQ- 4plex se destaca por ser mais eficiente em termos de identificação e quantificação de peptídeos e proteínas (PICHLER et al., 2010).

### 2.3.2. Quantificação livre de marcação

Em contraste com os métodos quantitativos por marcação química, nos métodos livres de marcação, cada amostra é preparada separadamente e submetida à análise individual por LC-MS. Geralmente são utilizadas duas estratégias para este tipo de quantificação relativa, a primeira delas, baseada no valor da área do pico obtida no LC-MS. Cada íon de uma determinada m/z possui uma intensidade que é detectada e registrada num momento determinado da análise. Nos primeiros testes para avaliar esta metodologia, foram utilizadas diversas concentrações de mioglobina. Verificou-se que na medida em que aumentava a concentração do analito, a intensidade do sinal e a áreas cromatográficas dos picos procedentes dos peptídeos de mioglobina, aumentavam guardando uma correlação linear com a concentração de proteína (CHELIUS; BONDARENKO, 2002). Esta abordagem apresenta diversas limitações, uma destas é a variabilidade da intensidade dos picos entre cada corrida de LC-MS, além disso, o tempo de retenção também pode variar após múltiplas injeções de amostra numa mesma coluna, gerando imprecisões na quantificação (LAI; WANG; WITZMANN, 2013).

Outra estratégia de quantificação relativa consiste na contagem espectral. A quantificação da proteína é obtida comparando o número de PSMs da mesma proteína em cada um dos conjuntos de corridas. Segundo este método, quanto mais abundante o peptídeo, maior é a probabilidade de ser selecionado para análise MS / MS, resultando no aumento da cobertura da sequência proteica, no número de peptídeos únicos identificados e no número de espectros MS / MS totais identificados para cada proteína (WONG; CAGNEY, 2009). A contagem espectral ofereceu uma ampla faixa dinâmica de

quantificação e com boa reprodutibilidade, no entanto, várias considerações devem ser levadas em conta, como por exemplo, a influência de parâmetros experimentais como a exclusão dinâmica de íons precursores, velocidade de varredura do instrumento MS, distribuição do comprimento dos peptídeos gerados que determina quantos peptídeos diferentes podem ser detectados dentro da uma faixa de massa, a variabilidade na quantificação de proteínas curta se o efeito de saturação em altas concentrações de proteína (BANTSCHEFF et al., 2012).

### 2.3.3. Quantificação alvo direcionada: Monitoramento de Reação Selecionada (SRM) e Monitoramento Paralelo de Reações (PRM)

A quantificação alvo direcionada é uma estratégia que permite a análise de um conjunto específico de proteínas ou uma proteína de interesse. No caso do SRM, este é realizado em espectrômetros de massa triplo quadrupolo onde o primeiro analisador de massa está configurado para filtrar um íon peptídeo precursor de interesse numa janela de isolamento estreita. O peptídeo isolado é fragmentado no Q2, e cada transição ou par precursor/íon produto é analisada separadamente no Q3 (BORRÀS; SABIDÓ, 2017) (Figura 3A). A probabilidade de dois fragmentos peptídicos terem a mesma massa, derivar de dois peptídeos isobáricos diferentes, com exatamente o mesmo tempo de retenção é muito baixa, portanto, o método do uso de transições torna esta estratégia de quantificação altamente específico e sensível (LANGE et al., 2008).

Uma das principais diferenças entre o PRM e o SRM é a análise simultânea de todos os fragmentos gerados do peptídeo de interesse. Neste método, o primeiro analisador de massa (um quadrupolo) é definido para filtrar numa janela de m/z estreita e isolar o íon de interesse. O peptídeo selecionado é fragmentado e os íons resultantes são analisados simultaneamente no analisador de massa de alta resolução (Figura 3B) (PETERSON et al., 2012). Estudos utilizando SRM e PRM demostraram que ambos métodos têm sensibilidade, linearidade e faixa dinâmica comparáveis, com alta precisão e reprodutibilidade e na quantificação de proteínas, contudo, o PRM tem certas vantagens sobre o SRM, devido a que é mais simples construir o método de aquisição de dados, fornece alta especificidade porque os dados MS/MS são adquiridos em alta resolução sendo capaz de incluir nas análises todos os íons potenciais derivados do peptídeo alvo e confirmar sua identidade (RAUNIYAR, 2015).

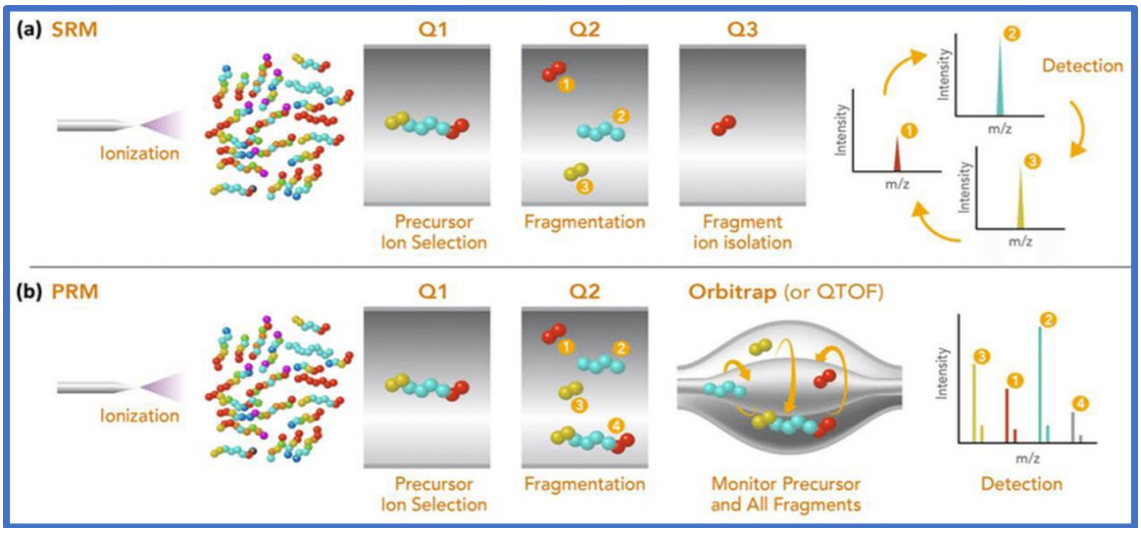


**Figura 3.** a) Representação do esquema geral do SRM. b) Representação do PRM. (Figura adaptada de BURNUM-JOHNSON et. al, 2016)

## 2.4. Análise de dados

A informação dos espectros obtidos está contida num arquivo RAW o qual é utilizado para as análises de dados. Atualmente, as buscas dos espectros são automatizadas, implementando para interpretação de dados estratégias de alinhamento entre o espectro teórico, gerado *in silico* utilizam do banco de dados, e o espectro experimental, atribuindo-se um score para essa associação. Esta estratégia de alinhamento é chamada de *Peptide Spectrum Match* (PSM) e existem diversos algoritmos disponíveis como o SEQUEST (ENG; ASHLEY, MCCORMACK L. AND YATES, 1994), Mascot (PERKINS et al., 1999), ProLuCID (XU et al, 2006), Comet (ENG; JAHAN; HOOPMANN, 2013) entre outros, que usam a PSM como estratégia de busca.

Contudo, diferença entre os dados experimentais e os peptídeos preditos *in silico*, como a presença de modificações pós-traducionais, modificações na sequência peptídica, problemas na digestão e fragmentação dos peptídeos, não geram nenhuma identificação (ZHAN et al., 2013). Geralmente, os algoritmos de buscas consideram parâmetros como modificações inerentes à preparação da amostra, tolerância de massa, enzima utilizada, presença de PTMs ou o uso de técnicas de quantificação por marcação como o iTRAQ, para identificação correta dos espectros. Do mesmo modo, quando se investiga por proteômica um organismo com genoma não-sequenciado, a análise por PSM é menos eficaz, sendo necessário recorrer a outro tipo de estratégia como o uso de sequenciamento de novo dos espectros MS/MS e busca por similaridade de sequência de proteínas nas bases de dados para validar as identificações pouco confiáveis geradas por PSM (SHEVCHENKO; VALCU; JUNQUEIRA, 2009); (LEPREVOST et al., 2014).

# CAPÍTULO III
# JUSTIFICATIVA E OBJETIVOS

## 3.1-Justificativa

A esquizofrenia é uma doença incurável com episódios recorrentes de internação dos pacientes em centros de saúde especializados, tornando-a a doença psiquiátrica de maior custo com uma despesa anual estimada de U$ 2,3 bilhões (ASCHER-SVANUM et. al, 2010). A terapia farmacológica disponível está dirigida na melhora dos sintomas positivos, sendo ineficazes no tratamento dos sintomas negativos e cognitivos, indicadores importantes da função social (STEEDS, CARHART-HARRIS e STONE, 2015). Além disso, há uma perda de 50-75% da eficácia dos tratamentos convencionais e cerca de 30% dos pacientes não respondem aos antipsicóticos (LALLY E MACCABE, 2015). Outro problema associado a esta doença são as altas taxas de ideação suicida; 40% dos pacientes com esquizofrenia tenta suicídio pelo menos uma vez e 15% morrem por esta causa (HOR e TAYLOR, 2010).

Apesar dos esforços da comunidade científica, a fisiopatologia da esquizofrenia ainda não é totalmente compreendida. Foram desenvolvidos diferentes modelos biológicos, porém esses modelos são limitados na avaliação de sintomas negativos e ideação suicida (FILIOU et al., 2011) Por essa razão, o estudo do tecido cerebral post-mortem ainda pode fornecer informações valiosas sobre a fisiopatologia deste transtorno. O primeiro objetivo deste estudo é realizar a caracterização proteômica das frações de sinaptossoma, mitocôndria, núcleo e citoplasma de uma das áreas cerebrais menos compreendidas, como é o córtex orbitofrontal, cuja função está envolvida na regulação da resposta emocional adequada, participando na aprendizagem, na previsão e tomada de decisões em relação aos comportamentos emocionais e relacionados à recompensa (Hospital &Kringelbach, 2005). Por outro lado, é conhecido que a função proteica está relacionada à localização subcelular e essas mudanças na localização das proteínas regulam a atividade de diversos processos biológicos (Itzhak, Tyanova, Cox, &Borner, 2016). Neste contexto, a identificação e quantificação das proteínas das frações subcelulares utilizando as técnicas de iTRAQ, *label-free*, PRM e SRM, abre a possibilidade de observar alterações dinâmicas do proteoma subcelular, com uma abordagem diferente ao reportado na literatura para este tipo de amostras, que possa sugerir novos mecanismos celulares na fisiopatologia desta doença. Finalmente, este projeto contribui na construção de um mapa abrangente do proteoma humano dentro do projeto do Proteoma Humano – Projeto Proteoma Humano Centrado no Cromossomo, (C-HPP) criado pela Organização do projeto proteoma humano (HUPO) sendo o Brasil responsável pelo cromossomo 15. Estudos de GWAS relacionam o cromossomo 15

(regiões 15q11.2 e 15q13.3) com a esquizofrenia (GIEGLING et al., 2017). O objetivo do C-HPP é inicialmente mapear e anotar pelo menos uma proteína codificada pelos genes de cada cromossomo humano incluindo as "missing proteins", que são aquelas que possuem alguma evidência por transcriptômica, anticorpos e/ou por homologia, mas não possuem evidência por espectrometria de massas, e correlacioná-las às doenças (projeto proteoma humano orientado à biologia / doença, BD-HPP) para compreender os processos moleculares na presença ou ausência de determinada patologia (AEBERSOLD et al., 2013).

### 3.2.- Objetivos

#### 3.2.1.- Geral

1. Caracterizar e comparar o proteoma subcelular do córtex orbitofrontal de pacientes com esquizofrenia e grupo controle.

#### 3.2.2.- Específicos

1.- Quantificar por marcação com iTRAQ as proteínas das frações de núcleo, citoplasma, mitocôndria e sinaptossoma de pacientes com esquizofrenia e controles.

2.- Quantificar por *label-free* as proteínas da fração de sinaptossoma de pacientes com esquizofrenia e controles.

3- Validar por SRM e PRM os peptídeos das proteínas de interesse nas diferentes frações.

4- Detectar as possíveis "*missing proteins*" com ênfase no cromossomo 15.

## CAPÍTULO IV

## APLICAÇÃO DO ITRAQ *SHOTGUN PROTEOMICS* PARA A MEDIÇÃO DE PROTEÍNAS CEREBRAIS EM ESTUDOS DE DISTÚRBIOS PSIQUIÁTRICOS

Capítulo de livro publicado na Proteomic Methods in Neuropsychiatric Research
Adv Exp Med Biol. 2017;974:219-227. doi: 10.1007/978-3-319-52479-5_18.

## Chapter 18

## Application of iTRAQ Shotgun Proteomics for Measurement of Brain Proteins in Studies of Psychiatric Disorders

Erika Velásquez Núñez, Paul C. Guest, Daniel Martins-de-Souza, Gilberto Barbosa Domont, and Fábio César Sousa Nogueira

### 18.1 Introduction

Psychiatric disorders are a leading cause of medical disability throughout the world, affecting one out of every three people at some point in their lifetime [1]. Despite the fact that years of intensive research have led to a better understanding of the biological pathways that are perturbed in people with these disorders, none of this information has led to newer and better approaches for patient management, particularly in the area of improved diagnosis and treatment. Thus far, this has been hindered by a poor understanding of the molecular pathways affected in these diseases and may also be a direct cause of disease complexity and overlap of symptoms across the supposedly different disorders [2, 3]. The current state-of-the-art diagnosis is based on evaluation of symptoms during clinical interviews, but this is only subjective and can vary depending on the experience, training, and methodology of the attending clinician and the validity of information given by the patient. Taken together, this can make effective disease management a difficult prospect.

The availability of biomarker tests based on the pathologies underlying psychiatric disorders would help to overcome some of these difficulties. Using biomarker tests targeting the affected pathways would give empirical readings, which could be used in combination with the standard methods for improved accuracy and timeliness of diagnosis. In turn, this would allow the access of patients to earlier and more efficient treatment options. In the initial discovery stages, it is important that brain tissue is analyzed in order to identify potential biomarkers, considering that this is likely to be the direct cause of symptoms due to effects on neuronal pathways [4].

---

E.V. Núñez • G.B. Domont • F.C.S. Nogueira (*)

Laboratory of Protein Chemistry – Proteomics Unit, Chemistry Institute, Federal University of Rio de Janeiro, Rio de Janeiro, Brazil

e-mail: fabiocsn@ufrj.br

P.C. Guest • D. Martins-de-Souza

Department of Biochemistry and Tissue Biology, Laboratory of Neuroproteomics, Institute of Biology, University of Campinas, CidadeUniversitáriaZeferinoVaz, Campinas, Brazil

P.C. Guest (ed.), Proteomic Methods in Neuropsychiatric Research, Advances in Experimental Medicine and Biology, DOI 10.1007/978-3-319-52479-5_18

Furthermore, proteomic-based biomarkers are likely to be the most useful for development of diagnostic and prognostic tests considering the dynamic nature of proteins in general in response to changing environmental stimuli [5].

Mass spectrometry (MS) profiling is one of the key proteomic techniques in the study of disease biomarkers [6], and the incorporation of isobaric labeling methods in MS approaches, such as isobaric tags for relative and absolute quantitation (iTRAQ), has allowed measurement of multiple proteomes simultaneously [7]. Although the iTRAQ labels have an indistinguishable mass in MS mode, reporter fragment ions of different masses are released in MS/MS mode in the collision chamber. This enables peptides from different samples to be differentiated and quantitated based on the intensity of their specific reporter ions [8]. The iTRAQ approach has now been used for analysis of up to four [7] or eight samples [9]. In comparison to label-free MS techniques, the multiplexing potential of the iTRAQ approach allows a simultaneous analysis of different biological samples, decreases the inherent variations in chromatographic analysis between the samples, and requires fewer technical replicates to obtain a good accuracy in the measurement. In the iTRAQ 4-plex approach, the reagent contains an N-methylpiperazine reporter, carbonyl balance, and NHS-ester reactive groups. Each reagent has the same mass (145 Da) achieved by a combination of 13C, 15N, and 18O in the reporter (114–117 Da) and balance groups (31–28 Da). The labeled peptides have identical retention times during chromatographic separation, and the peptides appear as a single peak with the same m/z in MS spectra. However, fragmentation of the precursor ion produces MS/MS spectra with reporter ion peaks at low mass region (114, 115, 116, and 117 Da) and peptide fragmentation ion peaks of higher masses. The intensity of the reporter ion peaks directly reflects the abundance of the peptide in each sample (Fig. 18.1).

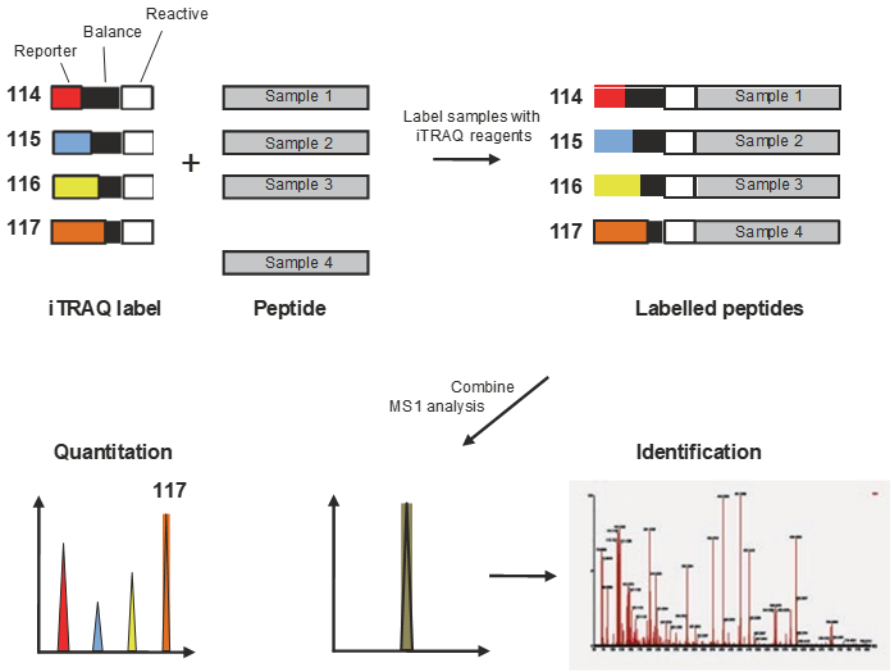


**Fig. 18.1 Schematic diagram of the iTRAQ4-plex mass spectrometry approach**

Here, we describe a detailed sample preparation and iTRAQ 4-plex labeling protocol for relative quantification of postmortem brain samples from patients with psychiatric disorders such as schizophrenia compared to those from controls. In addition, we outline a strategy for peptide fractionation after the iTRAQ-labeling procedure.

## 18.1 Materials (See Note 1)

### *18.1.1 Protein Extraction of Brain Tissues (See Note 2)*

**Procedure 1**

1. RapiGest® (Waters Corporation; Milford, MA, USA)
2. 1 M triethylammonium bicarbonate (TEAB; Sigma-Aldrich; Sao Paulo, Brazil)

**Procedure 2**

1. Extraction solution: 7 M urea/2 M thiourea and 2% sodium deoxycholate (Sigma-Aldrich)

2. Cold acetone

### *18.1.2 Enzymatic Digestion*

1. Qubit® 2.0 fluorometric assay kit for protein analysis (Invitrogen; Waltham, MA, USA)
2. Reducing solution: 100 mM dithiothreitol (DTT) or 50 mM tris(2-carboxyethyl) phosphine (TCEP) (*see Notes 3 and 4*)
3. Alkylating solution: 400 mM iodoacetamide (IAA) (*see Note 5*)
4. Sequencing grade modified trypsin (Promega; Madison, WI, USA)
5. Acetic acid
6. 10% trifluoroacetic acid (TFA)

### *18.1.3 iTRAQ Peptide Labeling*

1. 0.1% TFA
2. 0.1% TFA, 50% acetonitrile (ACN) 3. 0.1% TFA, 70% CAN
3. iTRAQ reagent 4-plex kit (Applied Biosystems Sciex; Foster City, CA, USA)
4. C18 macro-spin column (Harvard Apparatus; Holliston, MA, USA) (*see Note 6*)
5. Strong cation exchange (SCX) macro-spin column (Harvard Apparatus) (*see Note 7*)
6. Buffer A: 5 mM $KH_2PO_4$, 25% ACN (pH 3)
7. Buffer B: 1 M KCl stock solution
8. LC-20AT high-performance liquid chromatography (HPLC) instrument for hydrophilic interaction chromatography (HILIC) (Shimadzu Corporation; Kyoto, Japan) (*see Note 8*)
9. 3 μm x 5 cm x 2 mm TSKgel® amide-80 column (Sigma-Aldrich) for use with the LC-20AT instrument (*see Note 9*)
10. Solvent A (HILIC-A): 90% ACN, 0.1% TFA
11. Solvent B (HILIC-B): 0.1% TFA

### *18.1.4 Labeled Peptide Analysis by Nano LC-MS/MS*

1. Trap column: 2 cm length, 200 μm inner diameter
2. Analytical capillary column: 18 cm length, 100 μm inner diameter, 5 μm resin ReproSil-Pur C18 (Dr. Maisch GmbH; Ammerbuch, Germany)
3. Phase A: 0.1% formic acid, 5% ACN
4. Phase B: 0.1% formic acid, 95% CAN

5. Nano LC EASY II (Thermo Fisher Scientific; Waltham, MA, USA)
6. LTQ Orbitrap Velos mass spectrometer (Thermo Fisher Scientific)

#### *18.1.5 Data Analysis*

1. Data inspection: Xcalibur 2.1 software (Thermo Fisher Scientific)
2. Database searches: Proteome Discoverer 2.1 software (Thermo Fisher Scientific) with the SEQUEST algorithm
3. Databases: UniProt (www.uniprot.org/), NCBI (www.ncbi.nlm.nih.gov/), and neXtProt (www.nextprot.org/)

### 18.3 Methods

#### *18.3.1 Protein Extraction in Brain Tissues*

1. Pulverize and macerate the tissues in liquid nitrogen [10].
2. Add 0.1% RapiGest in 50 mM TEAB (*see Note 10*) or extraction solution.
3. Vortex the samples and centrifuge 30 min at 20,000 × g at 4 °C.
4. Transfer the supernatant to another tube and take one aliquot for protein quantification.
5. When using the extraction solution, precipitate the proteins with 4 volumes of cold acetone overnight and centrifuge at 20,000 × g at 4 °C for 30 min.
6. Wash the pellet three times with cold acetone followed by centrifugation at 20,000 × g at 4 °C for 10 min.
7. Remove the acetone excess and dry the pellet.
8. Solubilize the pellet in 7 M urea and 2 M thiourea solution.

#### *18.3.2 Protein Digestion with Trypsin*

1. Quantitate proteins using the Qubit 2.0 fluorometric assay kit according to the manufacturer's instructions.
2. Carry out reduction of disulfide bonds in proteins by incubating samples with DTT or TCEP solution at a final concentration of 10 mM for 1 h at 30 °C.
3. Alkylate thiol groups in proteins by incubating samples with IAA solution at a final concentration of 40 mM for 30 min at room temperature in the dark.
4. Add trypsin at a 1:50 enzyme/protein ratio and incubate 12–18 h at 37 °C (*see Note 11*).
5. Stop the reaction by adding 10% TFA to give a final concentration of 0.1% (*see*

*Note 12*).

### *18.3.3 iTRAQ Peptide Labeling [11, 12]*

1. For peptide cleaning, incubate C18 spin columns with 500 μL 100% ACN for 15 min and centrifuge at 2000 × g for 1 min.
2. Add the same amount of ACN and repeat the centrifugation step.
3. Equilibrate columns with 150 μL 0.1% TFA and centrifuge at 2000 × g as above.
4. Repeat this step three times.
5. Add 75–150 μL sample and centrifuge at 2000 × g as above.
6. Wash the columns using 0.1%TFA and centrifuge at 2000 × g as above.
7. Repeat the wash/centrifugation cycle three times.
8. Elute the peptides in two successive steps into the same collection tube by add- ing 0.1% TFA/50% ACN and 0.1% TFA/70% ACN followed by centrifugation at 2000 × g as above.
9. Dry the peptides by vacuum centrifugation.
10. Suspend peptides in 30 μL 20 mM TEAB (pH 8.5) (*see Note 13*) and quantify using the Qubit 2.0 fluorometric assay to normalize peptide amounts in each condition (20–100 μg).
11. Briefly centrifuge the iTRAQ reagent solution vial at room temperature to collect the content in the bottom of the tube and add 70 μL ethanol to each vial.
12. Vortex the vials and centrifuge briefly as above.
13. Transfer the contents of each vial to the specific sample tube, vortex, and centrifuge again (*see Note 14*).
14. Incubate samples at room temperature for 1 h.
15. Stop the reaction by adding formic acid at a final concentration of 1% and vor- tex and centrifuge as above (*see Note 15*).
16. Combine the contents of all samples labeled with different iTRAQ tags into one tube, vortex, and centrifuge.
17. Dry the contents in a vacuum centrifuge but stop before complete dryness is reached (*see Note 16*).

### *18.3.4 iTRAQ-Labeled Peptide Fractionation*

1. SCX fractionation: suspend the semidry pellets in 100 μL of 5 mM $KH_2PO_4$, 25% ACN solution to give an approximate 1 μg peptides/μL concentration and vortex.

2. Incubate the SCX spin column with 500 μL of the same solution for 15 min at room temperature.

3. Centrifuge at 2000 × g until all solution has passed through the column and repeat this step.

4. Add the sample to the spin column, centrifuge at 2000 × g, and collect the col- umn flow through.

5. Carry out four sequential elution steps using 150 μL of the 5 mM $KH_2PO_4$/25% ACN solution, containing 75, 150, 250, and 500 mMKCl, followed by centrifu- gation each time at 2000 × g, and collect the eluates in separate tubes.

6. Desalt the samples using the peptide cleaning step above (3.4.1–3.4.9).

7. Suspend the samples in 0.1% formic acid and quantify as above.

8. For HILIC fractionation [13, 14], suspend the samples in 100 μL of HILIC-A solution at approximately 1 μg/μL, vortex, centrifuge briefly, and collect the supernatant.

9. Load samples at a flow rate of 0.2 mL/min into the TSKgel Amide-80 column on the LC-20AT HPLC system.

10. Fractionate peptides by applying 100% HILIC-A (0% HILAC-B) for 10 min, 12% HILIC-B for 2 min, 20% HILIC-B for 30 min, 30% HILIC-B for 30 min, 100% HILIC-B for 5 min, and return into 100% HILIC-A for 5 min.

### *18.3.5 Labeled Peptide Analysis by Nano LC-MS/MS*

1. Load 1 μg labeled peptides onto the trap and capillary columns on the nanoLC system coupled online to LTQ Orbitrap Velos mass spectrometer.

2. For peptide elution, apply a gradient from 100% phase A to 35% phase B over 120 min at a flow rate of 200 nL/min.

3. After each run, wash the column with 90% phase B and re-equilibrate with phase A.

4. Acquire spectra in positive mode applying a data-dependent automatic survey MS scan and MS/MS (*see Note 17*).

5. Set the resolution of the Orbitrap mass analyzer at 60,000 at m/z 400, automatic gain control target at $1 \times 10^6$, and maximum ion injection at 500 ms.

6. Acquire MS/MS spectra at a resolution of 7500 at 400 m/z, a signal threshold of 30,000, normalized collision energy of 40, and dynamic exclusion enabled for 30 s with a repeat count of 1.

7. Place an Eppendorf tube covered with 5% ammonia water solution under the nano

ESI needle (*see Note 18*).

### *18.3.6 Data Analysis*

1. Inspect raw data using the Xcalibur software.
2. Perform database searches against target and decoy (reverse) databases from UniProt, NCBI, and neXtProt using the following search parameters: MS accuracy = 10 ppm, MS/MS accuracy = 0.1 Da, trypsin digestion with two missed cleavages allowed, fixed carbamidomethyl modification of cysteine, and variable modification of oxidized methionine.
3. For identification of iTRAQ-labeled peptides, also include the iTRAQ 4-plex monoisotopic mass = 144.102 and variable modification for N-terminus, lysine, and tyrosine.
4. Accept false discovery rates of less than 1% and peptide rank = 1.

## 18.4 Notes

1. Reagents should be of analytical grade, solvents HPLC or LC-MS grade and solutions should be prepared with ultrapure water (18 MΩ-cm at 25 °C). LC-MS solutions should be made with LC-MS grade water.
2. It is advisable to use protease inhibitors in this step to prevent degradation of proteins caused by proteases in the sample. In addition, for phosphoproteomics, it is necessary to use phosphatase inhibitors to prevent dephosphorylation during preparation and handling of samples.
3. It is recommended to use a fresh DTT stock solution.
4. TCEP has the advantage of being a more powerful reducing agent than DTT, by providing an irreversible reaction. In addition, it is more hydrophilic, active in alkaline and acidic conditions, and more resistant to air oxidation. Also, it does not reduce metals and is significantly more stable than DTT in the absence of a metal chelator.
5. It is necessary to prepare the IAA solution immediately before use and keep it protected from light because it is unstable and light sensitive.
6. The C18 macro-spin column has a binding capacity of 30–300 μg of sample, accepting a sample volume of 70–150 μL. Review the manufacturer's specifica- tions before use.
7. The SCX macro-spin column has an ion capacity of 0.18–0.25 mmol (Cl)/mL, has a binding capacity of 30–300 μg of protein sample, and accepts a sample volume of 70–

150 μL. Review the manufacturer's specifications before use.

8. It is possible to use a HPLC instrument with an equivalent configuration.

9. HILIC is recommended to remove excess iTRAQ reagent from iTRAQ-labeled peptides to increase compatibility with mass spectrometry analysis. This elimi- nates an additional step of sample cleaning.

10. We recommend addition of 200 μL of 0.1% RapiGest per 100 mg of tissue.

11. Samples in 7 M urea, 2 M thiourea must be diluted to final concentrations lower than 1 M urea using 100 mM TEAB and heating must be avoided. Check the pH to ensure that it is close to 8.

12. For RapiGest samples, acidify the samples with TFA to a final concentration of 1% to stop the reaction and incubate 40 minutes at room temperature. Centrifuge for 30 min at 20,000 × g to remove the insoluble material.

13. Before peptide labeling, ensure that the pH is close to 8.5.

14. It is advisable to use commercial peptides (e.g., Glu-1-fibrinopeptide B) at a known concentration at the time of labeling to serve as an internal control and to facilitate data normalization.

15. It is advisable to analyze a peptide sample aliquot by mass spectrometry before making the final mix of all iTRAQ labels in order to confirm the presence of labeled peptides with the appropriate m/z peaks for each reporter ion. If the labeling process was not successful, repeat the labeling procedure.

16. The peptide pellets are easier to resuspend if they are not completely dry.

17. The data-dependent acquisition method consisted of the selection and fragmen- tation of the tenth most intense precursor ions by high-energy collision disso- ciation. The $MS^2$ spectra range must include the m/z of the reporter ions.

18. The presence of 5% ammonia during analysis avoids the supercharge effect of the iTRAQ 4-plex tag [15].

**Acknowledgments** National Council of Technological and Scientific Development (CNPq) (Grant number: 477325/2013-0) and Rio de Janeiro State Foundation for Research Support (FAPERJ) (Grant number: E-26/202.801/2015).

**References**


1. Patel V, Chisholm D, Parikh R, Charlson FJ, Degenhardt L, Dua T et al (2016) Addressing the burden of mental, neurological, and substance use disorders: key messages from disease con- trol priorities, 3rd edition. Lancet 387:1672–1685

2. Cosgrove VE, Suppes T (2013) Informing DSM-5: biological boundaries between bipolar I disorder, schizoaffective disorder, and schizophrenia. BMC Med 11:127

3. Filiou MD, Turck CW (2011) General overview: biomarkers in neuroscience research. Int Rev Neurobiol 101:1–17. Rauniyar N, Yates JR 3rd (2014) Isobaric labeling-based relative quanti- fication in shotgun proteomics. J Proteome Res 13:5293–5309

4. Martins-de-Souza D (2015) Brainproteomics. Proteomics ClinAppl 9:795. doi:10.1002/ prca.201570053

5. Guest PC, Guest FL, Martins-de Souza D (2015) Making sense of blood-based proteomics and metabolomics in psychiatric research. Int J Neuropsychopharmacol. pii: pyv138. doi: 10.1093/ ijnp/pyv138. [Epub ahead of print]

6. Ross PL, Huang YN, Marchese JN, Williamson B, Parker K, Hattan S et al (2004) Multiplexed protein quantitation in *Saccharomyces cerevisiae* using amine-reactive isobaric tagging reagents. Mol Cell Proteomics 3:1154–1169

7. Nogueira FC, Domont GB (2014) Survey of shotgun proteomics. Methods MolBiol 1156:3–23

8. Rauniyar N, Yates JR 3rd (2014) Isobaric labeling-based relative quantification in shotgun proteomics. J Proteome Res 13:5293–5309

9. Choe L, D'Ascenzo M, Relkin NR, Pappin D, Ross P, Williamson B et al (2007) 8-plex quan- titation of changes in cerebrospinal fluid protein expression in subjects undergoing intravenous immunoglobulin treatment for Alzheimer's disease. Proteomics 7:3651–3660

10. Aquino PF, Lima DB, Fischer JSG, Melani RD, Nogueira FC, Chalub SR et al (2014) Exploring the proteomic landscape of a gastric cancer biopsy with the shotgun imaging ana- lyzer. J Proteome Res 13:314–320

11. Nogueira FC, Palmisano G, Schwämmle V, Campos FA, Larsen MR, Domont GB et al (2012) Performance of isobaric and isotopic labeling in quantitative plant proteomics. J Proteome Res 11:3046–3052

12. Nogueira FC, Palmisano G, Schwämmle V, Soares EL, Soares AA, Roepstorff P et al (2013) Isotope labeling-based quantitative proteomics of developing seeds of castor oil seed (*Ricinus communis* L.). J Proteome Res 12:5012–5024

13. Palmisano G, Lendal SE, Engholm-Keller K, Leth-Larsen R, Parker BL, Larsen MR (2010) Selective enrichment of sialic acid-containing glycopeptides using titanium dioxide chroma- tography with analysis by HILIC and mass spectrometry. Nat Protoc 5:1974–1982

14. Melo-Braga MN, Verano-Braga T, León IR, Antonacci D, Nogueira FC, Thelen JJ et al (2012) Modulation of protein phosphorylation, N-glycosylation and Lys-acetylation in grape (Vitisvinifera) mesocarp and exocarp owing to Lobesiabotrana infection. Mol Cell Proteomics 11:945–956

15. Thingholm TE, Palmisano G, Kjeldsen F, Larsen MR (2010) Undesirable charge-enhancement of isobaric tagged phosphopeptides leads to reduced identification efficiency. J Proteome Res 9:4045–4052

**CAPÍTULO V**

**ANÁLISES PROTEÔMICA DO SINAPTOSSOMA DO CÓRTEX ORBITOFRONTAL DE PACIENTES COM ESQUIZOFRENIA USANDO *LABEL-FREE* E iTRAQ**

Artigo publicado na edição especial da revista *Journal of Proteome Research*

J Proteome Res. 2017 Dec 1;16(12):4481-4494. doi: 10.1021/acs.jproteome.7b00422. Epub 2017 Oct 13.

**Synaptosomal proteome of the orbitofrontal cortex from schizophrenia patients using quantitative label-free and iTRAQ-based shotgun proteomics**

Erika Velásquez[1], Fabio CS Nogueira[1,2], Ingrid Velásquez[3], Andrea Schmitt[4], Peter Falkai[4], Gilberto B Domont[1*] and Daniel Martins-de-Souza[5,6*]

[1]Proteomics Unit, Department of Biochemistry, Institute of Chemistry, Federal University of Rio de Janeiro.

[2]Laboratory of Proteomics, LADETEC, Institute of Chemistry, Federal University of Rio de Janeiro.

[3]University of Carabobo, Venezuela.

[4]Department of Psychiatry and Psychotherapy, Ludwig Maximilian University of Munich (LMU), Munich, Germany.

[5]Laboratory of Neuroproteomics, Department of Biochemistry, Institute of Biology, University of Campinas (UNICAMP).

[6]UNICAMP's Neurobiology Center, Campinas, Brazil.

Corresponding authors: dmsouza@unicamp.br; gilberto@iq.ufrj.br

ABSTRACT: Schizophrenia is a chronic and incurable neuropsychiatric disorder which affects about one percent of the world population. The proteomic characterization of the synaptosome fraction of the orbitofrontal cortex is useful for providing valuable information about the molecular mechanisms of synaptic functions in these patients. Quantitative analyses of synaptic proteins were made with 8 paranoid schizophrenia patients and a pool of 8 healthy controls free of mental diseases. Label-free and iTRAQ labeling identified a total of 2018 protein groups. Statistical analyses revealed 12 and 55 significantly dysregulated proteins by iTRAQ and label-free, respectively. Quantitative proteome analyses showed an imbalance in the calcium signaling pathway and proteins such as Reticulon-1 and Cytochrome c, related to endoplasmic reticulum stress and programmed cell death. Also, it was found that there is a significant increase of limbic system-associated membrane protein and α-calcium/calmodulin-dependent protein kinase II, associated to the regulation of human behavior. Our data contribute to a better understanding about apoptosis as a possible pathophysiological mechanism of this disease, as well as neural systems supporting social behavior in schizophrenia. This study also is a joint effort of the Chr 15 C-HPP team and the Human Brain Proteome Project of

B/D-HPP. All MS proteomics data are deposited in the ProteomeXchange Repository under PXD006798.

Keywords: Schizophrenia, synaptosome, orbitofrontal cortex, quantitative proteomics

## 1. INTRODUCTION

Considered chronic and incurable neuropsychiatric disorder schizophrenia affects about one percent of the world population. Typical clinical manifestations of this disease are the positive symptoms as hallucinations, delusions, disordered thoughts and speech, negative symptoms like anhedonia, apathy, blunting of affect, social withdrawal with substantial functional deficiency in interpersonal relationships, work or personal care along and cognitive deficit with difficulty in attention and working memory [1 2]**.** Around 30% of patients with schizophrenia will not respond satisfactorily to the use of antipsychotics[3] and current pharmacological therapy is largely ineffective for the treatment of cognitive impairments and negative symptoms[4]. Schizophrenia inheritance is passed along by several genetic variations each with small effects**.** The genome-wide association studies (GWA) made by the Schizophrenia Working Group of Psychiatric Genomics Consortium[5] revealed in a total of 128 significant independent single nucleotide polymorphisms distributed in 108 independent loci are related to schizophrenia**,** highlighting genes involved in glutamatergic neurotransmission, synaptic plasticity, dopamine receptor D2, voltage-gated calcium channel subunits, and also the major histocompatibility complex, a consistent candidate found in other GWA studies[6]. However, the underlying causes and pathophysiological mechanisms of this disease are still not fully elucidated.

The evidence of synaptic dysfunction present in the etiology of schizophrenia was indirectly demonstrated after the discovery of the antipsychotic properties and mechanism of action of dopamine D2-like receptor antagonists, which ameliorated psychotic symptoms through their action upon neurotransmitter systems[7]. In the last decade, proteomics studies have tried to elucidate the pathophysiology of schizophrenia using different areas of post-mortem brain tissue from schizophrenia patients and comparing the results to mentally healthy controls[8]. Already, proteomic characterization of different brain areas has revealed the following biochemical alterations: energy metabolism[9]; oligodendrocyte function[10]; signaling pathways associated with axon formation and synaptic plasticity[11]; calcium homeostasis and the immune system[12]; expression of

synaptic proteins like syntaxin-binding protein, brain abundant membrane-attached signal protein 1, and limbic system-associated membrane protein[13]; and in the clathrin-mediated endocytosis and N-methyl-D-aspartate proteins, which are part of the endocytic and long-term potentiation pathways, respectively[14].

Despite the development of animal[15] and *in vitro*[16] biological models for understanding the interactions between neurotransmitter systems and correlating their relationship with schizophrenia symptoms, these models are limited in the evaluation of pathophysiological processes of negative symptoms and suicidal ideation[17]. However, the study of post-mortem brain tissue can still provide valuable information about the pathophysiology of schizophrenia[18]. The objective of this study was to perform a proteomic characterization of the synaptosome fraction of the orbitofrontal cortex, which was still unexplored. This brain region receives connections from the medial prefrontal cortex, amygdala, hypothalamus, insula/operculum, and dopaminergic midbrain, as well as areas of the basal ganglia, like the ventral and dorsal striatum[19 20]. Its function regulates appropriate emotional responses in association with learning, prediction, and decision-making for emotional- and reward-related behaviors[19]. Additionally, protein functions are related to subcellular localization, because organelles offer different interaction partners and chemical environments; these changes in protein localization regulate the activity of the biological pathways involved[21]. In this context, synaptosomes are useful for studying the molecular mechanisms of synaptic function and the identification. The quantification of synaptic proteins using label-free and iTRAQ labeling will be helpful to unravel new cellular mechanisms for this disease, providing a better understanding of schizophrenia pathogenesis and allowing the identification of possible candidates as new therapeutic targets.

Finally, this research improved the characterization of disease-associated proteins that will contribute to the construction of a comprehensive map of the entire human proteome following the goal of the Chromosome-centric and Biology/ Diseases Human Proteome Projects.

## 2. EXPERIMENTAL PROCEDURES

### 2.1. Brain samples

Brain tissue samples (Orbitofrontal, Prefrontal cortex, PFC) were collected postmortem from 8 chronic schizophrenia patients diagnosed antemortem by an experienced psychiatrist according to the Diagnostic and Statistical Manual of Mental

Disorders (DSM-IV) criteria as residual schizophrenia, with paranoid episodes (295.6) and 8 controls (Table S-1). Patient samples were collected at the State Mental Hospital in Wiesloch, and control samples from the Institute of Neuropathology, Heidelberg University, in Heidelberg, both in Germany. Controls were free from any brain or somatic diseases and had not taken antidepressants or antipsychotics during their lifetime. All brains analyzed here were submitted for neuropathological characterization to rule out any other associated brain disorders. Braak staging was required to be less than II for all brains. Schizophrenia patients have a record of antipsychotic treatment, so chlorpromazine equivalents (CPE) could be calculated. For typical neuroleptics and clozapine, we used Jahn and Mussgay's algorithm [22]. All patients and controls were white Germans with no history of alcohol or drug abuse, according to subjects and familial information. All assessments, postmortem evaluations, and procedures were approved by the ethics committee of the Faculty of Medicine, Heidelberg University, Heidelberg, Germany.

**2.2. Subcellular enrichment.**

PFC brain tissue (50mg) was homogenized in 10 volumes of buffer A (0.32M sucrose, 4mM HEPES pH 7.4, protease cocktail inhibitor tablet (Roche) and phosphatase inhibitor cocktail I and II (Sigma). All procedures were performed at 4 $^{0}$C. The homogenate was centrifuged at 1,000 x *g* for 10 min, the supernatant was transferred to a new tube (S1) and the pellet (P1) was resuspended in 10 volumes of buffer A and centrifuged at 1,000 x *g* for 10 min (S2, P2). S1 and S2 (S) were combined and centrifuged at 17,000 x *g* for 55 min (S3, P3). P3 was resuspended in 0.32M sucrose and laid on top of a discontinuous sucrose density gradient (1ml 0.32/1ml 0.8/1ml 1.2) and ultracentrifuged at 25,000 rpm for 2h. The synaptosomal fraction was (SYN) extracted from 1.2/0.8 interphase, diluted 1:1 (v/v) in water and ultracentrifuged at 40,000 rpm for 60 min (S4, P4). P4 was diluted in 10 µl distilled water and stored at -20 $^{0}$C. Efficiency of cellular compartment enrichment was verified by Western blot (Figure 1). Once enriched, proteins from each of the compartments were extracted as described in the study of Saia-Cereda and collaborators [23].

**2.3. Western blot**

Protein lysates had their protein concentrations determined using a Bradford assay (BioRad; Munich, Germany). Protein extracts (20 µg) from each sample were

electrophoresed in 12% SDS-PAGE (BioRad; Hercules, CA, USA). Proteins were then transferred electrophoretically to Immobilon-FL polyvinyldiphenyl fluoride (PVDF) membranes (Millipore; Bedford, MA, USA) at 100 V for 1 h, using a cooling system. PVDF membranes containing the transferred proteins were treated with 5% Carnation instant non-fat dry milk powder in Tris buffered saline (pH 7.4) containing 0.1% Tween −20 (TBS-T) for 4 h, rinsed in TBS-T three times for a total of 20 min and incubated with collapsin 2 for cytosolic proteins, ATP5A1 for mitochondrial proteins, PSD95 for synaptosomal proteins, and HDAC1 for nuclear proteins, at a dilution of 1:1000 in TBS-T overnight at 4 $^{0}$C (all antibodies were from Abcam; Cambridge, UK). Following the overnight incubation, the membranes were washed twice with TBS-T for 15 min per wash. Next, the membranes were incubated with anti-c-MYC-peroxidase antibody 1:10000 (GE Healthcare; Uppsala, Sweden) for 40 min at room temperature, washed with water and TBS-T, and incubated with Enhanced Chemiluminescence (ECL) solution (GE Healthcare) for 1 min. The membranes were scanned using a Gel DocTM XR+ System (Silk Scientific Incorporated; Orem, UT, USA) and the optical densities of the immunoreactive bands were measured using Quantity One software (Bio-Rad). Protein loading was determined by staining PVDF membranes with Ponceau S to ensure equal loading in each gel lane.

**2.4. Enzymatic digestion.**

Ten µg of SYN proteins were reduced with 5 mM tris(2-carboxyethyl)phosphine (1 hour at 30 $^{0}$C), alkylated with 10 mM iodoacetamide (30 min at room temperature), and diluted 1:10 with 50 mM triethylammonium bicarbonate (TEAB) pH 8, followed by digestion with trypsin (1:50) for 18 hours at 35 $^{0}$C. Peptides were desalted in C18 micro columns (Harvard apparatus), dried in a vacuum centrifuge, resuspended in 30 µl of 20 mM TEAB pH 8,0 and quantified by Qubit® protein assay (Invitrogen) for iTRAQ labeling, following the manufacturer’s recommendations. In label-free analyses the peptides were resuspended in 0.1% formic acid, quantified by Qubit® protein assay, and analyzed by mass spectrometry.

**2.5. iTRAQ Labeling**

Following manufacturer's instructions, 5 µg of peptides were labeled with iTRAQ® Reagents – 4-plex. The organization of iTRAQ 4-plex was made up as follows: three channels (114, 115 and 116) were labeled with one different schizophrenia

preparation and one channel (117) containing a pool of control samples (n=8). The pool of controls was the common element used for normalization and comparison between the iTRAQ sets **.**Labeled peptides were dried to 20 µl and diluted to a final volume of 100 µl with $KH_2PO_4$ 5 mM / ACN 25% pH 3 for SCX chromatography (*Harvard apparatus*) by one-step peptide elution with 500 mM KCl[24]. Samples were cleaned in a C18 column, dried, and resuspended in 0.1% formic acid for quantification (Qubit®) and LC-MS/MS analyses.

**2.6. LC-MS/MS analyses**

Two µg of peptides were analyzed in technical triplicate after three hours of gradient (5% to 40% B / 167 minutes; 40% to 95% B / 5 min; 95% B / 8 minutes). nanoLC solvent A consisted of (95% $H_2O$ / 5% acetonitrile (ACN) / 0.1% formic acid) and solvent B of (95% ACN / 5% $H_2O$ / 0.1% formic acid). Trap-column length was 3 cm with an internal diameter of 200 µm (5 µm spheres-Reprosil Pur C18, Dr. Maish) and analytical column of 15 cm and internal diameter of 75 µm (3 µm spheres- Reprosil Pur C18, Dr. Maish). In iTRAQ analyses, nanoESI was carried out under steam atmosphere provided by 5% ammonium hydroxide using a nLC Proxeon EASY-II system (Thermo Scientific) on-line with LTQ Orbitrap Velos (Thermo Scientific) mass spectrometer; label-free quantification was performed in an Easy-nLC 1000 (Thermo Scientific) coupled to a QExactive Plus (Thermo Scientific).

LTQ Orbitrap Velos settings for data-dependent acquisition mode (DDA) were: dynamic exclusion list of 90 s, spray voltage at 2.5 kV, and no auxiliary gas flow. Full MS scan was acquired at a resolution of 60,000 and at m/z 400 in the Orbitrap analyzer, and the ten most intense ions were selected for fragmentation by higher-energy collision dissociation (HCD) with normalized collision energy of 40. $MS^2$ spectra were analyzed in the Orbitrap (resolution of 7,500at m/z 400). QExactive Plus in FullScan-DDA $MS^2$ mode used a dynamic exclusion list of 45 s and spray voltage at 2.30 kV. Full scan was acquired at a resolution of 70,000 at m/z 200, with a m/z range of 350-2000, AGC of $1x10^6$, and injection time of 50 ms. Selection of the twenty most intense ions for HCD fragmentation used a normalized collision energy of 30, precursor isolation window of m/z 1.2 and 0.5 off-set, a resolution of 17,500 at m/z 200, AGC at $5x10^5$, and injection time of 100 ms.

**2.7. Data analysis**

Data were analyzed by the Proteome Discoverer 2.1 software using a human database downloaded from neXtprot (May 2017). The parameters used were: full-tryptic search space, up to two missed cleavages allowed for trypsin, precursor mass tolerance of 10 ppm, and fragment mass tolerance of 0.1 Da. Carbamidomethylation of cysteine was included as fixed modification, and methionine oxidation and protein N-terminal acetylation as dynamic modifications in Label-free quantification. iTRAQ modifications (K, Y, and N-terminal) were additionally considered as dynamic modifications for the iTRAQ labeled samples.

Spectra analyses used a target-decoy strategy considering maximum delta CN of 0.05, all available peptide-spectrum matches, and a target false discovery rate (FDR) 0.01 (strict). Parameters in the peptide filter were set up for high confidence with a minimum peptide length of 6 aminoacids. For protein filter was considered the minimum number of peptide sequence as 1, counting only rank 1 peptides. Peptide shared between multiple proteins was counted for the top scoring protein. The confidence thresholds in FDR protein validator were 0.01 for target FDR (strict). The strategy for protein grouping was strict parsimony. In the peptide and protein quantification module, for iTRAQ and label-free analysis, unique peptides were considered. The calculation of fold-change was made using the patients as numerator and pool of controls as denominator. For iTRAQ quantification, reporter abundance was automatic, applying the correction for the impurity reporter and a filter to do not report quantitative values for a single-peak in the precursor isotope pattern. Extraction ion chromatography strategy was used for label-free quantification.

### 2.8. Statistical analyses

Statistical evaluation of the data was performed by the *Inferno RDN* program (Polpitiya et al., 2008), unique peptides being normalized using Central Tendency and the absolute deviation of adjusted median (MAD). The peptides were extrapolated to their corresponding protein through RRollup using the Grubbs test, with a minimum of three peptides and p-value $<0.05$. To determine the statistical significance of dysregulated proteins the z-score and the p-value associated with a 95% confidence level were calculated using robust estimators such as the median and median absolute deviation (MAD).

### 2.9. Bioinformatics Functional Analysis

Comparative analyses were carried out with the program Venny 2.1[25]. For the cellular component, biological processes, and molecular function of quantified proteins, we used the program DAVID 6.8[26] , Human Protein Reference Database[27] and Reactome Pathways[28]. Proteins whose variation in abundance was statistically significant, STRING 10[29] (considering high-confidence interactions) and KEGG program[30], were used for protein-protein interaction analyses and evaluations of functional enrichment in the network.

### 2.10. PRM analysis

We have used 2 µg of peptides from patients and control samples spiked with the heavy version of the peptide VAGALQAQVK (K:13C(6)15N(2)) (JPT Peptide Technologies). Peptide separation were carried out using an EASY-nLC 1000 (Thermo Scientific), trap column (2 cm x 100 µm ID, 5 µm spheres-Reprosil Pur C18, Dr. Maish) and analytical column (30 cm x 75 µm ID, 3 µm spheres- Reprosil Pur C18, Dr. Maish). Peptide elution was performed by applying a flow of 300 nL/min and gradient of 5 to 40% of solvent B (95% acetonitrile, 0.1% formic acid) over 100 min followed by 10 min of 40-95% solvent B and 10 min of washing at 95% solvent B. Solvent A is composed by 5% of acetonitrile and 0.1% of formic acid. PRM mode was performed in a QExactive Plus (*Thermo Scientific*) using an inclusion list for the target ions with 2-Th window, resolution of 35,000 (at m/z 200), AGC of $5x10^5$, injection time of 150 ms, spray voltage at 2.30 kV, and MS/MS scans were acquired with a starting mass of m/z 100 and normalized collision energy of 27. We analyzed the PRM data using the Skyline software (64-bit, 3.6.0.10493).

## 3. RESULTS AND DISCUSSION

### 3.1. General proteome analysis

Our strategy consisted of a synaptosome enrichment of postmortem PFC brain tissue from patients with schizophrenia and from controls. Label-free and iTRAQ-based quantitative proteomics were employed as complementary approaches to characterize the synaptosome proteome (Figure 2). In the total synaptosome proteome, 2018 proteins were identified, combining results from the iTRAQ and label-free techniques (Figure 3A and 3B, Table S-2 and Table S-3). Quantitative analysis by iTRAQ identified 1176 proteins

comprising 513 groups, 127 of them with robust quantification (Figure 3A). The selection criteria for up- and down-regulated proteins included, besides p-value, the same quantitative behavior in at least half of the patients studied (n≥3) (Table 1 and Table S-4). Statistical analysis of iTRAQ data revealed 12 significantly dysregulated proteins. On the other hand, label-free quantification identified 4904 proteins in 1917 groups (Figure 3A); and of the 341 quantified proteins, 55 showed statistically significant variations in their abundance (Table 1 and Table S-4). They were found 3 deregulated proteins in common between iTRAQ and Label-free data (Table S-4).

GO analyses of the synaptosome proteome, using DAVID for all identified proteins showed the cellular component distribution of proteins expected for a synaptosome fraction (Figure 3D, Table S-5). Important biological processes in this total proteome were related to signal transduction and cell-cell adhesion, whereas the most important molecular functions of proteins were ATP and protein binding, and cell- cell adhesion. In more detailed analyses, Reactome pathway highlighted axon guidance and membrane trafficking as principal biological processes (Table S-5).

### 3.2. Label free qualitative analysis

The label-free comparative analysis of patients and control groups (Figure 3C) showed that 161 proteins were identified only in the control, but only 10 of those were identified with two or more unique peptides (Table S-6). Proteins detected only in the control condition were involved in the biological processes of neural cell adhesion, protein binding, molecular chaperones, and the activation of the GABA A receptor (Table S-7). Deficiencies in GABA function in the prefrontal cortex result in neurotransmissive and cognitive impairments in schizophrenia patients[31]. It was shown that Disrupted-in-schizophrenia 1 gene (DISC1) participates in the dynamic regulation and trafficking of GABAAR, and the knockdown of DISC1 significantly reduced changes of GABAAR-mediated synaptic inducing in surface expression[32].

On the other hand, 741 proteins were identified in the patient group; but only 6 proteins of these were present in all patients and identified with two or more unique peptides (Table S-6). The biological functions of the proteins identified only in patients are associated with membrane traffic processes and chemical synaptic transmission (Table S-7). Moreover, among these proteins the Programmed cell death 6-interacting protein, HSP70 and the adhesion protein Cadherin-13 stand out.

Cadherin-13 mediates cell–cell adhesion and is involved in intracellular signaling

pathways such as synaptogenesis, early embryonic patterning to circuit formation, and synaptic plasticity in the mature brain[33]. Cadherin-13 is associated with neuropsychiatric disease, suggesting that it may contribute to the genetic risk of schizophrenia[34]. Recently, a relationship between the Cadherin-13 and the GABA system was demonstrated. Cadherin-13 is located at GABA synapses and Cdh13$^{-/-}$ mice show an increase in inhibitory activity without changes in excitatory input, resulting in an excitatory–inhibitory imbalance[35], but the relationship and the impact of the interaction of these proteins in the pathophysiology of schizophrenia has not been determined.

### 3.3. Quantitative analysis of iTRAQ and Label free data

In relation to proteins with robust quantification, the functional analyses of these with DAVID and Reactome Pathways software, revealed that most of these proteins contribute mainly to cell adhesion processes, membrane trafficking, and vesicle-mediated transport (Table S-8). However, the proteins that presented statistically significant variation and met the criteria to be considered as dysregulated (Table 1) are mostly associated with synaptic activity and signaling pathways associated with calcium (Figure 4A, Table S-9). PRM analysis confirmed the quantification of SERCA, MARCKS, CAM1, CYCS, RTN1-C, LSAMP and PDCD6IP proteins in four patients (Table S-10), obtaining similar results regarding quantitative iTRAQ and Label-free techniques. Figure 5 shows XIC for the top 6 fragments of the internal standard (Figure 5A) and the peptide EAFSLFDKDGDGTITTK from calmodulin-1 (Figure 5B). This protein presents a lower abundance in patients with schizophrenia compared with the control group, which confirm our finds of the label-free and iTRAQ labeling data.

The protein-protein interaction analysis of dysregulated proteins (Figure 4B) showed that the main point of interaction converges on CaM, an important intracellular calcium sensor that converts the $Ca^{2+}$ signal into a variety of biochemical changes, whereby regulating important proteins for synaptic plasticity[36]. CaM is downregulated in this study and it was shown that the knockdown of CaM decreased the probability of synaptic vesicle release[37]. Moreover, a significant decrease was reported through immunostaining in the Brodmann area 9, layer III of schizophrenia patients, indicating a loss of CaM in pyramidal cells, which suggests that calcium/CaM-dependent pathways may be affected in the pyramidal cells of the prefrontal cortex [38].

In the analysis of network associations, it was observed that CaM interacts with relevant proteins in the processes of synaptic plasticity such as MARCKS and αCaMKII

(Figure 4B). CaM binds to MARCKS, removing it from membranes [39]. Curiously, in our study, MARCKS is found to be up-regulated in the SYN fraction simultaneously with a down-regulation of CaM. MARCKS acts to modulate actin-dependent processes by regulating the membrane-associated phospholipid $PIP_2$ availability[40], to participate in neuronal migration, proliferation, and neurite outgrowth, and is known for its importance for memory and maintenance in synaptic plasticity [40]. It was shown that the upregulation of MARCKS is able to produce significant impairments in spatial learning [41]. In addition, MARCKS is increased in the membrane fraction of postmortem hippocampal tissue from patients with suicidal behavior, with and without major depressive disorder [42]. In dorsolateral prefrontal cortices from schizophrenia and bipolar disorder patients, MARCKS mRNA expression was increased. Rats with chronic administration of haloperidol or clozapine did not show significant changes in the relative expression of MARCKS mRNA [43], or protein expression in the frontal cortex[44]. On the other hand, CaMKII is important for interaction with the NMDA receptor and long-term potentiation. Reduction of CaMKII activity is related to synaptic plasticity impairment, whereas its overexpression increases synaptic strength [45]. However, recently, studies have reported that the overexpression of specific isoforms of αCaMKII in mutant mice induced a significant increase in anxiety and detrimental changes in social behavior, suggesting that changes in αCaMKII expression levels strongly affect emotional state [46].

Parallel to the network association analysis, KEGG pathway was used to highlight the activation of G-protein coupled receptors and PLCβ activation in the calcium signaling route (Figure 6). PLCβ activation is involved in a variety of cellular functions associated with the hydrolysis of phosphatidylinositol 4,5-bisphosphate to produce secondary messengers such as inositol 1,4,5-trisphosphate ($IP_3$)[47]. IP3 mediates an increase in cytosolic $Ca^{2+}$ releasing intracellular stores through $IP_3$ receptor channel activation[48]. In response to calcium release from the ER, the up-regulation of SERCA and plasma membrane $Ca^{2+}$ ATPase (PMCA) was observed in this signaling pathway (Figure 6). Their main functions are to deplete the excess of cytosolic calcium into ER lumen and outside the cell respectively, restoring the $Ca^{2+}$ [49] to basal levels.

An excess of intracellular calcium is associated with ER stress and activation of cell death pathways [50]. In that sense, the up-regulation of Reticulon-1 (RTN1-C) protein (Table 1) was found in our data. RTN1-C is localized on the ER membrane, and its overexpression also results in elevated cytosolic $Ca^{2+}$ levels due to ER store depletion, resulting in ER stress-induced cell death with ultrastructural changes in the mitochondria

[51]. In fact, the increase of RTN1-C protein levels resulted in ER stress-induced cell death, mediated by an increase of cytosolic $Ca^{2+}$, and significantly sensitized cells to different ER-stress inducers. Also, the Programmed cell death 6-interacting protein (PDCD6IP) was identified only in schizophrenia patients (Table S-6). When calcium imbalance from homeostasis occurs and ER stress is generated, PDCD6IP takes part in apoptosis as a crucial mediator of Caspase-9 activation [52]. The overexpression of PDCD6IP *in vivo* is sufficient to induce cell death [53].

There is a link between ER stress-mediated apoptosis and the mitochondria transition pore [5]. The $Ca^{2+}$ flux activates mitochondrial permeability transition pore stimulating the apoptosis with the release of cytochrome c and other pro-apoptotic factors [54]. Indeed, the second main point of the network association analysis (Figure 4) included proteins involved with apoptosis such as SLC25A6 and VDAC2, which participated in the formation of the permeability transition pore complex, controlling mitochondrial permeability[55]. During the activation of apoptosis, SLC25A6 overexpression increases caspases 9 and 3[56] and VDAC2 facilitates Bax stabilization in the mitochondrial outer membrane [57]. Another important and classical indicator of apoptosis, CYCS, is part of this interaction network. When mitochondrial membrane permeability is altered, CYCS released into the cytosol triggers apoptotic processes. The overexpression of CYCS enhances Caspase activation[58] forming the apoptosome through interaction with the Apoptotic protease activating factor-1 and subsequent activation of the caspase-9 death pathway[59]. Furthermore, the Serine/threonine-protein phosphatase PGAM5, a novel partner of Apoptosis-inducing factor, was also increased in schizophrenia patients and its overexpression induced caspase activation and cell death [60]. Also, anti-apoptotic proteins were identified, such as BAG3, induced by stressful stimuli, which acted synergistically with Bcl-2 on the inhibition of apoptosis processes mediated by Bax and Fas[61 62], Hsp70 protein, identified only in patients (Table S-6), enhanced cell survival under ER stress conditions, preventing the formation of an active apoptosome [63] ; and 14-3-3η which conferred neuroprotection in NMDA-induced cellular stress and cell death [64]

There is a link between ER stress-mediated apoptosis and the mitochondria transition pore [5]. The $Ca^{2+}$ flux activates mitochondrial permeability transition pores, stimulating apoptosis with the release of cytochrome c and other pro-apoptotic factors [54]. Indeed, the second main point of the network association analysis (Figure 4) included proteins involved with apoptosis such as SLC25A6 and VDAC2, which participated in the formation of the permeability transition pore complex, controlling mitochondrial

permeability[55]. During the activation of apoptosis, SLC25A6 overexpression increases caspases 9 and 3[56] and VDAC2 facilitates Bax stabilization in the mitochondrial outer membrane [57]. Another important and classical indicator of apoptosis, CYCS, is part of this interaction network. When mitochondrial membrane permeability is altered, CYCS released into the cytosol triggers apoptotic processes. The overexpression of CYCS enhances Caspase activation[58] forming the apoptosome through interaction with the Apoptotic protease activating factor-1 and subsequent activation of the caspase-9 death pathway [59]. Furthermore, the Serine/threonine-protein phosphatase PGAM5, a novel partner of Apoptosis-inducing factor, was also increased in schizophrenia patients and its overexpression induced caspase activation and cell death [60]. Also, anti-apoptotic proteins were identified, such as BAG3, induced by stressful stimuli, which acted synergistically with Bcl-2 on the inhibition of apoptosis processes mediated by Bax and Fas[61 62]. Hsp70 protein, identified only in patients, enhanced cell survival under ER stress conditions, preventing the formation of an active apoptosome [63] ; and 14-3-3η which conferred neuroprotection in NMDA-induced cellular stress and cell death [64].

Apoptosis has been proposed as a process in the pathophysiology of schizophrenia. There is evidence including reduced gray matter volume, synaptic markers, and neuropil, that suggests a form of programmed cell death in the progressive gray matter volume loss during the course of illness in the frontal, parietal and temporal areas [65]. A longitudinal study that determined the long-term effects of antipsychotic treatment in brain volumes proposed the possibility that antipsychotic treatment is not efficient in counteracting the pathophysiologic processes of schizophrenia, rather aggravating the progressive brain tissue volume reductions [66]. In fact, an increase in caspase-3 activity was reported as a delayed effect of typical and atypical antipsychotic treatment; but there was no evidence of DNA fragmentation, indicating that antipsychotic treatment did not induce apoptosis by itself but could still contribute to the progressive cortical gray matter loss in the early stages of schizophrenia[65]. On the other hand, in fibroblast cultures from first-episode schizophrenia patients, there is an increased susceptibility to apoptosis, displaying a correlation between regional brain volume and changes in levels of brain glutamate and *N*-acetylaspartate in the anterior cingulate and the left thalamus [67]. Besides this, the serum levels of apoptotic markers were significantly higher in deficit schizophrenia syndrome patients than in non-deficit schizophrenia patients and healthy controls[68] suggesting the importance of apoptotic processes in the negative symptoms of schizophrenia.

The third most important point of protein-protein interaction network revealed the dysregulation of oligodendrocyte proteins connected to myelin sheath formation (Figure 4B). We found three main proteins: myelin basic protein (MBP), a calmodulin binding protein whose main function is related to the adhesion of multi-lamellar compact myelin into the plasma membrane; the proteolipid protein (PLP), a principal component of compact myelin; and the myelin oligodendrocyte glycoprotein (MOG), a specific constituent of CNS myelin, mostly present on the outer loop of the myelin sheath[10 69]. MBP, PLP, and MOG are expressed during the beginning of myelin sheath formation around axons[70]. However, PLP increase and sequestration of MOG have been associated to myelin degeneration and the axonopathy observed in PLP1-transgenic animals and Pelizaeus-Merzbacher patients[71]. The overexpression of PLP in transgenic animals leads to ER stress is associated with inefficient transport of PLP from the ER to the myelin sheath, causing a blockage of transport for other myelin proteins such as MOG[71]. ER stress induces apoptosis with a loss of myelin and the death of oligodendrocytes in gray matter of the central nervous system.[71] Moreover, expression of Contactin-1, a cell adhesion molecule, is also increased in our study. Contactin-1 is implicated in axon growth and guidance, neural differentiation, synapse formation, myelination formation, organization, and as a critical signal for axon–glia communication in CNS myelin[72] . *In vitro* experiments of unmyelinated axons have associated the up-regulation of Contactin-mediated signals with trigger events that orchestrate the expression of proteins such as PLP, MBP, and MGO for myelin formation [73]. Also, it was demonstrated that calmodulin regulation of MPB modifies cytoskeleton-mediated events in myelinogenesis[74]

The dysregulation of oligodendrocyte proteins has already been described in previous proteomic studies[10] and a qualitative electron microscopy study of the prefrontal cortex from patients with schizophrenia or bipolar disorder confirmed ultrastructural changes in oligodendrocytes corresponding to apoptosis[75]. Findings associated with myelin must be accepted cautiously and require validation, as these proteins (or their fragments) could be contaminants to the synaptosomal fraction, which is supposed to be separated from the myelin fraction.

In the last group of dysregulated proteins, it is necessary to highlight variations in the abundance of proteins related to cell adhesion processes and cytoskeletal organization (Table 1). One of these proteins is LSAMP, increased in all patients analyzed by iTRAQ strategy. LSAMP is a glycosylated protein with three immunoglobulin (Ig) domains integrated into membranes via a glycosyl-phosphatidyl-inositol (GPI) anchor[76]. It is

predominantly expressed on the surface of proximal dendrites and soma, and acts in neural cell adhesion and neuritis formation and outgrowth [77]. The LSAMP gene is linked to human behavior and it has been shown that a transcript level increment in the amygdaloid area, periaqueductal gray, raphe, hippocampus, and frontal cortex is connected with acute fear reaction, fear conditioning, and higher trait anxiety [78]. Allelic variants located in the intronic region of the LSAMP gene are correlated with the pathoetiology of suicidal behavior[79] and there is a significant allelic and haplotype association between the LSAMP gene and schizophrenia [80]. Also, in a proteomic study of membrane microdomains of postmortem brain tissue in the dorsolateral prefrontal cortex from schizophrenia patients, LSAMP expression appeared significantly increased exclusively in the brains of patients with schizophrenia and not in the brains of patients with bipolar disorder (Behan et. al, 2008)[13] , indicating that this protein may play an important role in the pathophysiology of schizophrenia. Currently, LSAMP has been suggested to have a possible role in the mechanisms of psychiatric disorders, specifically in the regulation of emotional behavior[77]. Another protein, alpha-internexin is also up-regulated in this fraction. Primarily expressed in the CNS axons of neurons undergoing differentiation and maturation, this suggests that it has important role in the regulation of the outgrowth and shape of neurites, thus maintaining the network of intermediate filaments in mature neurons [81]. Previously, alpha-internexin was found to be increased in the synaptic membrane fraction of the left dorsolateral prefrontal cortex of patients with schizophrenia[82]. The overexpression of this protein causes a deficit in motor coordination in transgenic mice with varying degrees of neuronal dysfunction and degeneration proportional to the levels of mis-accumulated neuronal intermediate filaments[83] ; however the exact relationship between this protein and the impairments in motor coordination in schizophrenia must be investigated.

### 3.4. Missing proteins candidates

Finally, through this study, it was possible to suggest the existence of two missing proteins (Figure S-1). Protein unc-79 homologous isoform Iso 3 located on chromosome 14, initially with evidence only at transcript level, was identified with 2 unique peptides. The second protein, putative cytochrome b-c1 complex subunit Rieske-like protein 1 isoform Iso 1, belonging to chromosome 22, with evidence classified as uncertain, was identified with 1 unique peptide (Table S-11).

## 4. CONCLUSION

The orbitofrontal cortex, a subdivision of the prefrontal cortex, is directly involved in the regulation of emotions. Neuropsychology and neurophysiology studies, as well as structural and functional neuroimaging, indicate that this area of the brain plays an important role in the development of diseases such as mood, anxiety, and personality disorders; drug addiction; and schizophrenia; [84] which makes proteomic characterization important for the comprehension of this diseases.

The calcium signaling pathway was one of the main dysregulated routes in this brain area in schizophrenia patients. Imbalance in the calcium signaling pathway has been implicated in the development of psychiatric diseases, reported to play a major role in regulating several neuronal processes like transmitter release, neuronal excitability, and synaptic plasticity [85]. Cognitive impairment is a common symptom that prevails after treatment with currently available antipsychotics; and, in association, this study shows a higher level of MARCKS protein in patients. The abnormal expression of MARCKS may contribute to impairments in the synaptic plasticity in schizophrenia patients.

Since long time, apoptosis has been proposed as one possible mechanism that contributes to the pathophysiology of schizophrenia. A great deal of evidence indicates progressive clinical deterioration and neurostructural changes in schizophrenia patients, and recent studies have linked apoptosis with the negative symptoms of schizophrenia [86] [68]**.** This research found for the first time in post-mortem brain tissues in an important brain area involved in the regulation of emotions as the orbitofrontal cortex, evidences of deregulated apoptotic proteins related to ER stress and programmed cell death triggering such as reticulon-1 and cytochrome C. In here we propose as a potential mechanism, based on the deregulation of these proteins, the apoptosis mediated by ER stress in the orbitofrontal area

Finally, schizophrenia patients are characterized by social interaction difficulties that do not improve after standard treatments[87]. Two important proteins, previously related with the regulation of human behavior in other studies were found significantly increased in this study: LSAMP whose increment was previously correlated with abnormal response to fear, panic, and suicidal behavior [78] [79] [80] and αCaMKII linked to an increase in anxiety and detrimental effects on social behavior in mouse model[46] .The increment of these proteins in the orbitofrontal cortex could be related to the aberrant social behavior in these patients. We propose these proteins as potentials markers of social impairment.

Authors recognize that the protein-level FDR is an estimate based on several imperfect assumptions, and present the FDR with appropriate precision and acknowledge that not all proteins surviving the threshold are “confidently identified”.

All MS proteomics data are deposited in the ProteomeXchange Repository under PXD006798.

**ACNOWLEDGEMENTS**

Authors thank Bradley J. Smith for proof-reading the article and LADETEC (Chemistry Institute, UFRJ) for the Q-Exactive Plus (Thermo Scientific) analysis. DMS is supported by São Paulo Research Foundation (FAPESP), grants 2013/08711-3 and 2014/10068-4 and the Brazilian National Council for Scientific and Technological Development (CNPq) grant 460289/2014-4. EV thanks CNPq for her PhD scholarship; FCSN for grant E-26/202.801/2015 from the Rio de Janeiro State Foundation for Science Support (FAPERJ); and GBD for CNPq grant 306316/2015-3. Authors acknowledge FAPERJ for grant E-26/110.138/2013.

## REFERENCES


(1) Gaur, N.; Gautam, S.; Gaur, M.; Sharma, P.; Dadheech, G.; Mishra, S. THE BIOCHEMICAL WOMB OF SCHIZOPHRENIA : A REVIEW. **2008**, *23* (4), 307–327.

(2) Kambarova, D. K.; Golubev, A. G. Biochemical and Genetic Aspects of Pathogenesis of Schizophrenia. **2011**, *47* (5).

(3) Lally, J.; MacCabe, J. H. Antipsychotic medication in schizophrenia: A review. *Br. Med. Bull.* **2015**, *114* (1), 169–179.

(4) Steeds, H.; Carhart-Harris, R. L.; Stone, J. M. Drug models of schizophrenia. *Ther. Adv. Psychopharmacol.* **2015**, *5* (1), 43–58.

(5) Ripke, S.; Neale, B. M.; Corvin, A.; Walters, J. T. R.; Farh, K.-H.; Holmans, P. A.; Lee, P.; Bulik-Sullivan, B.; Collier, D. A.; Huang, H.; et al. Biological insights from 108 schizophrenia-associated genetic loci. *Nature* **2014**, *511* (7510), 421–427.

(6) Giegling, I.; Hosak, L.; Mössner, R.; Serretti, A.; Bellivier, F.; Claes, S.; Collier, D. A.; Corrales, A.; DeLisi, L. E.; Gallo, C.; et al. Genetics of schizophrenia: A consensus paper of the WFSBP Task Force on Genetics. *World J. Biol. Psychiatry* **2017**, *0* (0), 1–14.

(7) Iritani, S. What happens in the brain of schizophrenia patients?: an investigation from the viewpoint of neuropathology. *Nagoya J. Med. Sci.* **2013**, *75* (1–2), 11–28.

(8) Nascimento, J. M.; Martins-de-Souza, D. The proteome of schizophrenia. *npj Schizophr.* **2015**, *1* (1), 14003.

(9) Saia-Cereda, V. M.; Cassoli, J. S.; Martins-de-Souza, D.; Nascimento, J. M. Psychiatric disorders biochemical pathways unraveled by human brain proteomics. *Eur. Arch. Psychiatry Clin. Neurosci.* **2017**, *267* (1), 3–17.

(10) Cassoli, J. S.; Guest, P. C.; Malchow, B.; Schmitt, A.; Falkai, P.; Martins-de-Souza, D. Disturbed macro-connectivity in schizophrenia linked to oligodendrocyte dysfunction: from structural findings to molecules. *npj Schizophr.* **2015**, *1* (1), 15034.

(11) English, J. A.; Pennington, K.; Dunn, M. J.; Cotter, D. R. The neuroproteomics of schizophrenia. *Biol. Psychiatry* **2011**, *69* (2), 163–172.

(12) Martins-De-Souza, D.; Gattaz, W. F.; Schmitt, A.; Rewerts, C.; Maccarrone, G.; Dias-Neto, E.; Turck, C. W. Prefrontal cortex shotgun proteome analysis reveals altered calcium homeostasis and immune system imbalance in schizophrenia. *Eur. Arch. Psychiatry Clin. Neurosci.* **2009**, *259* (3), 151–163.

(13) Behan, Á.; Byrne, C.; Dunn, M. J.; Cagney, G.; Cotter, D. R. Proteomic analysis of membrane microdomain-associated proteins in the dorsolateral prefrontal cortex in schizophrenia and bipolar disorder reveals alterations in LAMP, STXBP1 and BASP1 protein expression. *Mol. Psychiatry* **2009**, *14* (6), 601–613.

(14) Föcking, M.; Lopez, L. M.; English, J. A.; Dicker, P.; Wolff, A.; Brindley, E.; Wynne, K.; Cagney, G.; Cotter, D. R. Proteomic and genomic evidence implicates the postsynaptic density in schizophrenia. *Mol. Psychiatry* **2015**, *20* (4), 424–432.

(15) Gottschalk, M. G.; Sarnyai, Z.; Guest, P. C.; Harris, L. W.; Bahn, S. Translational neuropsychiatry of genetic and neurodevelopmental animal models of schizophrenia. *Rev. Psiquiatr. Clin.* **2013**, *40* (1), 41–

50.

(16) Cassoli, J. S.; Iwata, K.; Steiner, J.; Guest, P. C.; Turck, C. W.; Nascimento, J. M.; Martins-de-Souza, D. Effect of MK-801 and Clozapine on the Proteome of Cultured Human Oligodendrocytes. *Front. Cell. Neurosci.* **2016**, *10* (March), 1–14.

(17) Filiou, M. D.; Turck, C. W.; Martins-De-Souza, D. Quantitative proteomics for investigating psychiatric disorders. *Proteomics - Clin. Appl.* **2011**, *5* (1–2), 38–49.

(18) Harrison, P. J. Using our brains: The findings, flaws, and future of postmortem studies of psychiatric disorders. *Biol. Psychiatry* **2011**, *69* (2), 102–103.

(19) Hospital, J. R.; Kringelbach, M. L. and FMRIB, Oxford Centre for Functional Magnetic Resonance Imaging of the Brain THE HUMAN ORBITOFRONTAL CORTEX: LINKING REWARD TO HEDONIC EXPERIENCE. **2005**, *6* (September), 691–702.

(20) Rempel-Clower, N. L. Role of orbitofrontal cortex connections in emotion. *Ann. N. Y. Acad. Sci.* **2007**, *1121*, 72–86.

(21) Itzhak, D. N.; Tyanova, S.; Cox, J.; Borner, G. H. H. Global, quantitative and dynamic mapping of protein subcellular localization. *Elife* **2016**, *5* (JUN2016), 1–36.

(22) Jahn T, M. L. Die statistische Kontrolle moeglicher Medikamenteneinfluesse in experimentalpsychologischen Schizophreniestudien: Ein Vorschlag zur Berechnung von Chlorpromazina aequivalenten. *Z Klin Psychol Psychother* **1989**, *18:10.*

(23) Saia-Cereda, V. M.; Cassoli, J. S.; Schmitt, A.; Falkai, P.; Martins-de-Souza, D. Differential proteome and phosphoproteome may impact cell signaling in the corpus callosum of schizophrenia patients. *Schizophr. Res.* **2016**, *177* (1–3), 70–77.

(24) Núñez, E. V.; Guest, P. C.; Martins-de-souza, D. Proteomic Methods in Neuropsychiatric Research. **2017**, *974*, 219–227.

(25) Oliveros, J. C. NoVENNY. An interactive tool for comparing lists with Venn Diagrams Title http://bioinfogp.cnb.csic.es/tools/venny/index.html.

(26) Huang, D. W.; Sherman, B. T.; Lempicki, R. A. Systematic and integrative analysis of large gene lists using DAVID bioinformatics resources. *Nat. Protoc.* **2008**, *4* (1), 44–57.

(27) Peri, S.; Navarro, J. D.; Kristiansen, T. Z.; Amanchy, R.; Surendranath, V.; Muthusamy, B.; Gandhi, T. K. B.; Chandrika, K. N.; Deshpande, N.; Suresh, S.; et al. Human protein reference database as a discovery resource for proteomics. *Nucleic Acids Res.* **2004**, *32* (Database issue), D497–D501.

(28) Fabregat, A.; Sidiropoulos, K.; Garapati, P.; Gillespie, M.; Hausmann, K.; Haw, R.; Jassal, B.; Jupe, S.; Korninger, F.; McKay, S.; et al. The reactome pathway knowledgebase. *Nucleic Acids Res.* **2016**, *44* (D1), D481–D487.

(29) Szklarczyk, D.; Franceschini, A.; Wyder, S.; Forslund, K.; Heller, D.; Huerta-Cepas, J.; Simonovic, M.; Roth, A.; Santos, A.; Tsafou, K. P.; et al. STRING v10: Protein-protein interaction networks, integrated over the tree of life. *Nucleic Acids Res.* **2015**, *43* (D1), D447–D452.

(30) Ogata, H.; Goto, S.; Sato, K.; Fujibuchi, W.; Bono, H.; Kanehisa, M. KEGG: Kyoto encyclopedia of genes and genomes. *Nucleic Acids Res.* **1999**, *27* (1), 29–34.

(31) Yoon, J. H.; Maddock, R. J.; Rokem, A.; Silver, M. a; Michael, J.; Ragland, J. D.; Carter, C. S. Gamma-Aminobutyric Acid Concentration is Reduced in Visual Cortex in Schizophrenia and Correlates

with Orientation-Specific Surround Suppression. *J Neurosci.* **2010**, *30* (10), 3777–3781.

(32) Wei, J.; Graziane, N. M.; Gu, Z.; Yan, Z. DISC1 Regulates GABAA Receptor Trafficking and Inhibitory Synaptic Transmission in Cortical Neurons. *J. Biol. Chem.* **2015**, *290* (46), jbc.M115.656173.

(33) Redies, C.; Hertel, N.; Hübner, C. A. Cadherins and neuropsychiatric disorders. *Brain Res.* **2012**, *1470*, 130–144.

(34) Otsuka, I.; Watanabe, Y.; Hishimoto, A.; Boku, S.; Mouri, K.; Shiroiwa, K.; Okazaki, S.; Nunokawa, A.; Shirakawa, O.; Someya, T.; et al. Association analysis of the Cadherin13 gene with schizophrenia in the Japanese population. *Neuropsychiatr. Dis. Treat.* **2015**, *11*, 1381–1393.

(35) Rivero, O.; Selten, M. M.; Sich, S.; Popp, S.; Bacmeister, L.; Amendola, E.; Negwer, M.; Schubert, D.; Proft, F.; Kiser, D.; et al. Cadherin-13, a risk gene for ADHD and comorbid disorders, impacts GABAergic function in hippocampus and cognition. *Transl. Psychiatry* **2015**, *5* (10), e655.

(36) Xia, Z.; Storm, D. R. The role of calmodulin as a signal integrator for synaptic plasticity. *Nat. Rev. Neurosci.* **2005**, *6* (4), 267–276.

(37) Pang, Z. P.; Cao, P.; Xu, W.; Sudhof, T. C. Calmodulin Controls Synaptic Strength via Presynaptic Activation of Calmodulin Kinase II. *J. Neurosci.* **2010**, *30* (11), 4132–4142.

(38) Broadbelt, K.; Jones, L. B. Evidence of altered calmodulin immunoreactivity in areas 9 and 32 of schizophrenic prefrontal cortex. *J. Psychiatr. Res.* **2008**, *42* (8), 612–621.

(39) Kim, J.; Shishido, T.; Jiang, X.; Aderem, A.; McLaughlin, S. Phosphorylation, high ionic strength, and calmodulin reverse the binding of MARCKS to phospholipid vesicles. *J. Biol. Chem.* **1994**, *269* (45), 28214–28219.

(40) Brudvig, J. J.; Weimer, J. M. X MARCKS the spot: myristoylated alanine-rich C kinase substrate in neuronal function and disease. *Front. Cell. Neurosci.* **2015**, *9* (October), 1–10.

(41) McNamara, R. K.; Hussain, R. J.; Simon, E. J.; Stumpo, D. J.; Blackshear, P. J.; Abel, T.; Lenox, R. H. Effect of myristoylated alanine-rich C kinase substrate (MARCKS) overexpression on hippocampus-dependent learning and hippocampal synaptic plasticity MARCKS transgenic mice. *Hippocampus* **2005**, *15* (5), 675–683.

(42) Pandey, G. N.; Dwivedi, Y.; Ren, X.; Rizavi, H. S.; Roberts, R. C.; Conley, R. R.; Tamminga, C. Altered expression and phosphorylation of myristoylated alanine-rich C kinase substrate (MARCKS) in postmortem brain of suicide victims with or without depression. *J. Psychiatr. Res.* **2003**, *37* (5), 421–432.

(43) Konopaske, G. T.; Subburaju, S.; Coyle, J. T.; Benes, F. M. Altered prefrontal cortical MARCKS and PPP1R9A mRNA expression in schizophrenia and bipolar disorder. *Schizophr. Res.* **2015**, *164* (1–3), 100–108.

(44) Anita L. Pinner1,*, Vahram Haroutunian2, and J. H. M.-W. Alterations of the myristoylated, alanine-rich C kinase substrate (MARCKS) in prefrontal cortex in schizophrenia. *Schizophr Res* **2014**, *154* ((0)), 36–41.

(45) Griffith, L. C. Regulation of Calcium/Calmodulin-Dependent Protein Kinase II Activation by Intramolecular and Intermolecular Interactions. *J. Neurosci.* **2004**, *24* (39), 8394–8398.

(46) Hasegawa, S.; Furuichi, T.; Yoshida, T.; Endoh, K.; Kato, K.; Sado, M.; Maeda, R.; Kitamoto, A.; Miyao, T.; Suzuki, R.; et al. Transgenic up-regulation of alpha-CaMKII in forebrain leads to increased anxiety-like behaviors and aggression. *Mol. Brain* **2009**, *2* (1), 6.

(47) Szebenyi, S. A.; Ogura, T.; Sathyanesan, A.; AlMatrouk, A. K.; Chang, J.; Lin, W. Increases in intracellular calcium via activation of potentially multiple phospholipase C isozymes in mouse olfactory neurons. *Front. Cell. Neurosci.* **2014**, *8* (October), 336.

(48) Decuypere, J. P.; Monaco, G.; Bultynck, G.; Missiaen, L.; De Smedt, H.; Parys, J. B. The IP3 receptor-mitochondria connection in apoptosis and autophagy. *Biochim. Biophys. Acta - Mol. Cell Res.* **2011**, *1813* (5), 1003–1013.

(49) Glazner, G. W.; Fernyhough, P. Neuronal survival in the balance : are endoplasmic reticulum membrane proteins the fulcrum ? **2002**, *32*, 421–433.

(50) Ghibelli, L.; Cerella, C.; Diederich, M. The dual role of calcium as messenger and stressor in cell damage, death, and survival. *Int. J. Cell Biol.* **2010**, *2010*.

(51) Di Sano, F.; Fazi, B.; Tufi, R.; Nardacci, R.; Piacentini, M. Reticulon-1C acts as a molecular switch between endoplasmic reticulum stress and genotoxic cell death pathway in human neuroblastoma cells. *J. Neurochem.* **2007**, *102* (2), 345–353.

(52) Strappazzon, F.; Torch, S.; Chatellard-Causse, C.; Petiot, A.; Thibert, C.; Blot, B.; Verna, J. M.; Sadoul, R. Alix is involved in caspase 9 activation during calcium-induced apoptosis. *Biochem. Biophys. Res. Commun.* **2010**, *397* (1), 64–69.

(53) Mahul-Mellier, A.-L. Alix, Making a Link between Apoptosis-Linked Gene-2, the Endosomal Sorting Complexes Required for Transport, and Neuronal Death In Vivo. *J. Neurosci.* **2006**, *26* (2), 542–549.

(54) Marchi, S.; Patergnani, S.; Pinton, P. The endoplasmic reticulum – mitochondria connection : One touch , multiple functions ☆ Author â€™ s personal copy. *Biochim. Biophys. Acta* **2014**, *1837*, 461–469.

(55) Tsujimoto, Y.; Nakagawa, T.; Shimizu, S. Mitochondrial membrane permeability transition and cell death. *Biochim. Biophys. Acta - Bioenerg.* **2006**, *1757* (9–10), 1297–1300.

(56) Zamora, M.; Granell, M.; Mampel, T.; Viñas, O. Adenine nucleotide translocase 3 (ANT3) overexpression induces apoptosis in cultured cells. *FEBS Lett.* **2004**, *563* (1–3), 155–160.

(57) Ma, S. B.; Nguyen, T. N.; Tan, I.; Ninnis, R.; Iyer, S.; Stroud, D. A.; Menard, M.; Kluck, R. M.; Ryan, M. T.; Dewson, G. Bax targets mitochondria by distinct mechanisms before or during apoptotic cell death: a requirement for VDAC2 or Bak for efficient Bax apoptotic function. *Cell Death Differ.* **2014**, *21* (12), 1925–1935.

(58) Chandra, D.; Liu, J. W.; Tang, D. G. Early mitochondrial activation and cytochrome c up-regulation during apoptosis. *J. Biol. Chem.* **2002**, *277* (52), 50842–50854.

(59) Xiong, S.; Mu, T.; Wang, G.; Jiang, X. Mitochondria-mediated apoptosis in mammals. *Protein Cell* **2014**, *5* (10), 737–749.

(60) Lenhausen, A. M.; Wilkinson, A. S.; Lewis, E. M.; Dailey, K. M.; Scott, A. J.; Khan, S.; Wilkinson, J. C. Apoptosis Inducing Factor Binding Protein PGAM5 Triggers Mitophagic Cell Death That Is Inhibited by the Ubiquitin Ligase Activity of X-Linked Inhibitor of Apoptosis. *Biochemistry* **2016**, *55* (23), 3285–3302.

(61) Lee, J.-H.; Takahashi, T.; Yasuhara, N.; Inazawa, J.; Kamada, S.; Tsujimoto, Y. Bis, a Bcl-2-binding protein that synergizes with Bcl-2 in preventing cell death. *Oncogene* **1999**, *18* (46), 6183–6190.

(62) Rosati, A.; Graziano, V.; De Laurenzi, V.; Pascale, M.; Turco, M. C. BAG3: a multifaceted protein

that regulates major cell pathways. *Cell Death Dis.* **2011**, *2* (4), e141.

(63) Gupta, S.; Deepti, A.; Deegan, S.; Lisbona, F.; Hetz, C.; Samali, A. HSP72 protects cells from ER stress-induced apoptosis via enhancement of IRE1??-xbp1 signaling through a physical interaction. *PLoS Biol.* **2010**, *8* (7).

(64) Chen, J.; Lee, C. T.; Errico, S. L.; Becker, K. G.; Freed, W. J. Increases in expression of 14-3-3 eta and 14-3-3 zeta transcripts during neuroprotection induced by Δ9-tetrahydrocannabinol in AF5 cells. *J. Neurosci. Res.* **2007**, *85* (8), 1724–1733.

(65) Glantz, L. A.; Gilmore, J. H.; Lieberman, J. A.; Jarskog, L. F. Apoptotic mechanisms and the synaptic pathology of schizophrenia. *Schizophr. Res.* **2006**, *81* (1), 47–63.

(66) Ho, B.-C.; Andreasen, N. C.; Ziebell, S.; Pierson, R.; Magnotta, V. Long-term Antipsychotic Treatment and Brain Volumes. *Arch. Gen. Psychiatry* **2011**, *68* (2), 128.

(67) Batalla, A.; Bargalló, N.; Gassó, P.; Molina, O.; Pareto, D.; Mas, S.; Roca, J. M.; Bernardo, M.; Lafuente, A.; Parellada, E. Apoptotic markers in cultured fibroblasts correlate with brain metabolites and regional brain volume in antipsychotic-naive first-episode schizophrenia and healthy controls. *Transl. Psychiatry* **2015**, *5* (8), e626-.

(68) Albayrak, Y.; Beyazyuz, M.; Kufeciler, T.; Bulut, L.; Unsal, C.; Baykal, S.; Soydas Akyol, E.; Kuloglu, M.; Hashimoto, K. Increased serum levels of apoptosis in deficit syndrome schizophrenia patients: a preliminary study. *Neuropsychiatr. Dis. Treat.* **2016**, 1261.

(69) Holz, A.; Schwab, M. E. Developmental expression of the myelin gene MOBP in the rat nervous system. *J. Neurocytol.* **1997**, *26* (7), 467–477.

(70) Baumann, N.; Pham-Dinh, D. Biology of oligodendrocyte and myelin in the mammalian central nervous system. *Physiol. Rev.* **2001**, *81* (2), 871–927.

(71) Bauer, J.; Bradl, M.; Klein, M.; Leisser, M.; Deckwerth, T. L.; Wekerle, H.; Lassmann, H. Endoplasmic reticulum stress in PLP-overexpressing transgenic rats: gray matter oligodendrocytes are more vulnerable than white matter oligodendrocytes. *J. Neuropathol. Exp. Neurol.* **2002**, *61* (1), 12–22.

(72) Bizzoca, A.; Corsi, P.; Polizzi, A.; Pinto, M. F.; Xenaki, D.; Furley, A. J. W.; Gennarini, G. F3/Contactin acts as a modulator of neurogenesis during cerebral cortex development. *Dev. Biol.* **2012**, *365* (1), 133–151.

(73) Colakoglu, G.; Bergstrom-Tyrberg, U.; Berglund, E. O.; Ranscht, B. Contactin-1 regulates myelination and nodal/paranodal domain organization in the central nervous system. *Proc. Natl. Acad. Sci.* **2014**, *111* (3), E394–E403.

(74) Hill, C. M. D.; Harauz, G. Charge effects modulate actin assembly by classic myelin basic protein isoforms. *Biochem. Biophys. Res. Commun.* **2005**, *329*, 362–369.

(75) Uranova, N.; Orlovskaya, D.; Vikhreva, O.; Zimina, I.; Kolomeets, N.; Vostrikov, V.; Rachmanova, V. Electron microscopy of oligodendroglia in severe mental illness. *Brain Res. Bull.* **2001**, *55* (5), 597–610.

(76) Pimenta, A. F.; Zhukareva, V.; Barbe, M. F.; Reinoso, B. S.; Grimley, C.; Henzel, W.; Fischer, I.; Levitt, P. The limbic system-associated membrane protein is an Ig superfamily member that mediates selective neuronal growth and axon targeting. *Neuron* **1995**, *15* (2), 287–297.

(77) Innos, J.; Koido, K.; Philips, M.-A.; Vasar, E. Limbic system associated membrane protein as a

potential target for neuropsychiatric disorders. *Front. Pharmacol.* **2013**, *4* (March), 1–3.

(78) Philips, M. A.; Lillev??li, K.; Heinla, I.; Luuk, H.; Hundahl, C. A.; Kongi, K.; Vanaveski, T.; Tekko, T.; Innos, J.; Vasar, E. Lsamp is implicated in the regulation of emotional and social behavior by use of alternative promoters in the brain. *Brain Struct. Funct.* **2015**, *220* (3), 1381–1393.

(79) Must, A.; Tasa, G.; Lang, A.; Vasar, E.; Kõks, S.; Maron, E.; Väli, M. Association of limbic system-associated membrane protein (LSAMP) to male completed suicide. *BMC Med. Genet.* **2008**, *9* (1), 34.

(80) Koido, K.; Janno, S.; Traks, T.; Parksepp, M.; Ljubajev, Ü.; Veiksaar, P.; Must, A.; Shlik, J.; Vasar, V.; Vasar, E. Associations between polymorphisms of LSAMP gene and schizophrenia. *Psychiatry Res.* **2014**, *215* (3), 797–798.

(81) Lee, W. C.; Kan, D.; Chen, Y. Y.; Han, S. K.; Lu, K. S.; Chien, C. L. Suppression of extensive neurofilament phosphorylation rescues α-internexin/peripherin-overexpressing PC12 cells from neuronal cell death. *PLoS One* **2012**, *7* (8).

(82) Smalla, K.-H.; Mikhaylova, M.; Sahin, J.; Bernstein, H.-G.; Bogerts, B.; Schmitt, a; van der Schors, R.; Smit, a B.; Li, K. W.; Gundelfinger, E. D.; et al. A comparison of the synaptic proteome in human chronic schizophrenia and rat ketamine psychosis suggest that prohibitin is involved in the synaptic pathology of schizophrenia. *Mol. Psychiatry* **2008**, *13* (9), 878–896.

(83) Ching, G. Y.; Chien, C. L.; Flores, R.; Liem, R. K. Overexpression of alpha-internexin causes abnormal neurofilamentous accumulations and motor coordination deficits in transgenic mice. *J. Neurosci.* **1999**, *19* (8), 2974–2986.

(84) Jackowski, A. P.; Araújo Filho, G. M. de; Almeida, A. G. De; Araújo, C. M. De; Reis, M.; Nery, F.; Batista, I. R.; Silva, I.; Lacerda, A. L. T. The involvement of the orbitofrontal cortex in psychiatric disorders: an update of neuroimaging findings. *Rev. Bras. Psiquiatr.* **2012**, *34* (2), 207–212.

(85) Berridge, M. J. Calcium signalling and psychiatric disease: Bipolar disorder and schizophrenia. *Cell Tissue Res.* **2014**, *357* (2), 477–492.

(86) Jarskog, L. F.; Glantz, L. A.; Gilmore, J. H.; Lieberman, J. A. Apoptotic mechanisms in the pathophysiology of schizophrenia. *Prog. Neuro-Psychopharmacology Biol. Psychiatry* **2005**, *29* (5), 846–858.

(87) Dodell-Feder, D.; Tully, L. M.; Hooker, C. I. Social impairment in schizophrenia: new approaches for treating a persistent problem. *Curr. Opin. Psychiatry* **2015**, *28* (3), 236–242.

## TABLE AND FIGURES

**Table 1:** Dysregulated proteins and their biological process.

**Figure 1: A.** Polyacrylamide Gel Electrophoresis (SDS-PAGE 12%.) **B.** Western blot evaluation of cellular compartment enrichment efficiency using collapsin 2 (CRMP2) for cytosolic (Cyto), histone deacetylase 1(HDAC1) for nuclear (Nuc), postsynaptic density protein 95 (PSD95) for synaptosomal (Syn) and ATP synthase subunit alpha (ATP5A1) for mitochondrial proteins (Mito).

**Figure 2:** Experimental pipeline for iTRAQ labeling and label-free

quantifications.

**Figure 3: A**. Proteins identified and quantified by iTRAQ and label-free analysis. **B.** Total coverage of proteins identified by iTRAQ and label-free. **C.** Qualitative analysis of label-free data. **D.** GO cellular component analyses of all proteins identified by iTRAQ and label-free.

**Figure 4: A.** Reactome pathway analysis of proteins with statistically significant variation. **B.** Protein-protein interaction network analysis of dysregulated proteins. The first hub is calmodulin-1 (CaM) that interacts with proteins responsible for synaptic plasticity such as αCa2 + proteins / calmodulin-dependent protein kinase II (αCaMKII) and MARCK related protein (MARCKS). The second main interaction point discloses proteins involved in apoptosis as ADP/ATP translocase 3 (SLC25A6), voltage-dependent anion-selective channel protein 2 (VDAC2) and cytochrome c (CYCS). The third hub is around myelin basic protein (MBP), which interacts with proteolipid protein (PLP) and the myelin oligodendrocyte glycoprotein (MOG), associated with cell-cell adhesion and formation of myelin sheath.

**Figure 5:** PRM analysis using the software Skyline. Chromatogram of the internal standard (Figure 5A) and the peptide EAFSLFDKDGDGTITTK from calmodulin-1 (Figure 5B) from patient (Pat_1. Pat_2, Pat_3, and Pat_8) and control (Ctrl) samples.

**Figure 6:** Adapted from KEGG pathway. The biological function of the main dysregulated proteins converges around the regulation of calcium signaling pathways and the apoptotic process. CALM1 modulates proteins related to synaptic plasticity as αCaMKII and the MARCKS. On the other hand, the activation of receptors GPCR generates second messengers as IP3 by Phospholipase C beta with the release of $Ca^{2+}$ into the cytoplasm. The increment of RTN1-C also increases the cytoplasmic $Ca^{2+}$ levels inducing ER stress and cell death. It is also observed, the dysregulation of pro-apoptotic proteins as PGAM5, SLC25A6, VDAC and CYCS and anti-apoptotic proteins as HSP70 and BAG3. **Red:** Down-regulated proteins. **CALM1:** Calmodulin-1. **Yellow:** Up-regulated proteins. **PMCA**: The plasma membrane $Ca^{2+}$ ATPase, **HSP70**: The 70 kilodalton heat shock proteins, **Gq**: heterotrimeric G protein subunit, **PLCβ:** Phospholipase C beta, **CYCS**: cytochrome c, **BAG3:** Bcl2-associated athanogene 3, **PGAM5**: Serine/threonine-protein phosphatase PGAM5, mitochondrial, **SLC25A6:** ADP/ATP translocase 3, **VDAC**: Voltage-dependent anion-selective channel protein. **SERCA**: Sarcoplasmic/endoplasmic reticulum calcium ATPase, **RTN1-C:** Reticulon-1, **MARCKS**: Myristoylated alanine-rich C-kinase substrate, **αCaMKII**: $Ca^{2+/}$Calmodulin-

dependent Protein Kinase II α. **Green:** Quantified proteins with no significant variation in their abundance. **CaV2:** calcium voltage-gated channel, **PKC**: Protein kinase C. **Blue:** Proteins and second messengers that were not identified but are part of the metabolic pathway. **GPCR:** G-protein-coupled receptors, **IP3**: inositol 1,4,5-trisphosphate, **IP3R**: Inositol trisphosphate receptor, **AIF**: Apoptosis-inducing factor. **ER**: Endoplasmic reticulum, **MIT:** Mitochondria

## SUPPORTING INFORMATION

**Supporting Table S-1: Clinical data of patients and control.** This file contains all the information related to the clinical history of the patients, such as type of schizophrenia, duration of illness, time and type of antipsychotic treatment etc.

**Supporting Table S-2: Proteins identified by iTRAQ labeling.** The supporting information contains the table of proteins identified by iTRAQ strategy, as well as the groups of peptides per protein and their respective quantification.

**Supporting Table S-3: Proteins identified by label-free.** This file contains all the information related to the proteins identified by Label-free strategy, as well as the groups of peptides per protein and their respective quantification.

**Supporting Table S-4: Up- and down regulated proteins by iTRAQ labeling and label-free**. In this file is finding the information about the dysregulated proteins quantified by iTRAQ and Label-free in all patients analyzed.

**Supporting Table S-5: GO and Reactome analysis of the synaptosome proteome.** The supporting file contains gene ontology analyses, biological processes, cellular function and Reactome pathway analyses of the total proteome of synaptosome fraction.

**Supporting Table S-6: Proteins specifically identified by label-free in patient or control groups.** The supporting table has the label free qualitative analysis of proteins identified in all patients or control groups with two or more unique peptides.

**Supporting Table S-7: GO and Reactome analysis of proteins specifically identified by label-free in patient or control groups.** Gene ontology analyses, biological processes, cellular function and Reactome pathway analyses of label free qualitative analysis of proteins identified in patients or control groups

**Supporting Table S-8: GO and Reactome analysis of quantified proteins.** Gene ontology analyses, biological processes, cellular function and Reactome pathway analyses of proteins with robust quantification

**Supporting Table S-9: Reactome analysis of up- and down regulated proteins.** This file contains the information about the Reactome pathway analyses of dysregulated proteins quantified by iTRAQ and Label-free strategy.

**Supporting Table S-10: PRM data.** Parallel reaction monitoring analysis confirming the quantification of proteins as SERCA, MARCKS, CAM1, CYCS, RTN1-C, LSAMP and PDCD6IP protein in four patients and control pool.

**Supporting Table S-11: Missing protein candidates.** The table contains the information of missing protein candidates as description, annotated sequences of peptides etc provided by Proteome discoverer software 2.1.

**Supporting Figure S-1:** Spectra of missing proteins candidates. **A.** Spectrum of Putative cytochrome b-c1 complex subunit Rieske-like protein 1 isoform Iso 1. **B, C**. Spectra of Protein unc-79 homolog isoform Iso 3.

**Table 1. Dysregulated proteins and their biological process.**

| ID | Description | Regulation | GO: Biological process |
|---|---|---|---|
| **nxp:NXP62158-1** | Calmodulin isoform Iso 1 | Down | Cell communication; Signal transduction |
| **nxp:NXO14880-1** | Microsomal glutathione S-transferase 3 isoform Iso 1 | Up | Metabolism; Energy pathways |
| **nxp:NXP02686-6** | Myelin basic protein isoform Iso 6 | Up | Immune response; Neurogenesis |
| **nxp:NXP05023-1** | Sodium/potassium-transporting ATPase subunit alpha-1 isoform Iso 1 | Up | Transport |
| **nxp:NXP12036-1** | Neurofilament heavy polypeptide isoform Iso 1 | Up | Cell growth and/or maintenance |
| **nxp:NXP12236-1** | ADP/ATP translocase 3 isoform Iso 1 | Up | Transport |
| **nxp:NXP37840-1** | Alpha-synuclein isoform Iso 1 | Up | Protein metabolism |
| **nxp:NXP51674-1** | Neuronal membrane glycoprotein M6-a isoform Iso 1 | Up | Neurogenesis |
| **nxp:NXP60201-1** | Myelin proteolipid protein isoform Iso 1 | Up | Cell growth and/or maintenance |
| **nxp:NXQ13449-1** | Limbic system-associated membrane protein isoform Iso 1 | Up | Cell communication; Signal transduction |
| **nxp:NXQ16352-1** | Alpha-internexin isoform Iso 1 | Up | Cell growth and/or maintenance |
| **nxp:NXQ16653-1** | Myelin-oligodendrocyte glycoprotein isoform Iso 1 | Up | Immune response |
| **nxp:NXO14827-1** | Ras-specific guanine nucleotide-releasing factor 2 isoform Iso 1 | Up | Cell communication; Signal transduction |
| **nxp:NX** | Synapsin-3 isoform Iso 1 | Up | Transport |

| | | | |
|---|---|---|---|
| **O14994-1** | | | |
| **nxp:NX O43426-2** | Synaptojanin-1 isoform Iso 2 | Up | Metabolism |
| **nxp:NX O43581-3** | Synaptotagmin-7 isoform Iso 3 | Up | Regulation of exocytosis |
| **nxp:NX O75396-1** | Vesicle-trafficking protein SEC22b isoform Iso 1 | Up | Cell communication; Signal transduction |
| **nxp:NX O75899-1** | Gamma-aminobutyric acid type B receptor subunit 2 isoform Iso 1 | Up | Cell communication; Signal transduction |
| **nxp:NX O75964-1** | ATP synthase subunit g, mitochondrial isoform Iso 1 | Up | Metabolism; Energy pathways |
| **nxp:NX O94760-1** | N(G),N(G)-dimethylarginine dimethylaminohydrolase 1 isoform Iso 1 | Up | Metabolism; Energy pathways |
| **nxp:NX O94967-4** | WD repeat-containing protein 47 isoform Iso 4 | Up | Cell communication; Signal transduction |
| **nxp:NX O95817-1** | BAG family molecular chaperone regulator 3 isoform Iso 1 | Up | Apoptosis |
| **nxp:NX O95837-1** | Guanine nucleotide-binding protein subunit alpha-14 isoform Iso 1 | Up | Cell communication; Signal transduction |
| **nxp:NX P00568-1** | Adenylate kinase isoenzyme 1 isoform Iso 1 | Up | Metabolism; Energy pathways |
| **nxp:NX P00918-1** | Carbonic anhydrase 2 isoform Iso 1 | Up | Metabolism; Energy pathways |
| **nxp:NX P06733-1** | Alpha-enolase isoform alpha-enolase | Up | Metabolism; Energy pathways |
| **nxp:NX P07437-1** | Tubulin beta chain isoform Iso 1 | Up | Cell growth and/or maintenance |
| **nxp:NX P11137-1** | Microtubule-associated protein 2 isoform Iso 1 | Up | Cell growth and/or maintenance |

| | | | |
|---|---|---|---|
| **nxp:NX P12532-2** | Creatine kinase U-type, mitochondrial isoform Iso 2 | Up | Energy pathways |
| **nxp:NX P13637-3** | Sodium/potassium-transporting ATPase subunit alpha-3 isoform Iso 3 | Up | Transport |
| **nxp:NX P13637-3** | Sodium/potassium-transporting ATPase subunit alpha-3 isoform Iso 3 | Up | Transport |
| **nxp:NX P13861-1** | cAMP-dependent protein kinase type II-alpha regulatory subunit isoform Iso 1 | Up | Cell communication; Signal transduction |
| **nxp:NX P14618-2** | Pyruvate kinase PKM isoform M1 | Up | Energy pathways; Metabolism |
| **nxp:NX P15104-1** | Glutamine synthetase isoform Iso 1 | Up | Metabolism; Energy pathways |
| **nxp:NX P16615-1** | Sarcoplasmic/endoplasmic reticulum calcium ATPase 2 isoform Iso 1 | Up | Transport |
| **nxp:NX P18669-1** | Phosphoglycerate mutase 1 isoform Iso 1 | Up | Metabolism; Energy pathways |
| **nxp:NX P19086-1** | Guanine nucleotide-binding protein G(z) subunit alpha isoform Iso 1 | Up | Cell communication; Signal transduction |
| **nxp:NX P24539-1** | ATP synthase F(0) complex subunit B1, mitochondrial isoform Iso 1 | Up | Metabolism; Energy pathways |
| **nxp:NX P29966-1** | Myristoylated alanine-rich C-kinase substrate isoform Iso 1 | Up | Cell growth and/or maintenance |
| **nxp:NX P31930-1** | Cytochrome b-c1 complex subunit 1, mitochondrial isoform Iso 1 | Up | Energy pathways; Metabolism |
| **nxp:NX P37840-1** | Alpha-synuclein isoform Iso 1 | Up | Protein metabolism |
| **nxp:NX P45880-1** | Voltage-dependent anion-selective channel protein 2 isoform Iso 1 | Up | Transport |
| **nxp:NX P68366-1** | Tubulin alpha-4A chain isoform Iso 1 | Up | Cell growth and/or maintenance |
| **nxp:NX** | Disks large homolog 4 isoform Iso 2 | Up | Cell communication |

| | | | |
|---|---|---|---|
| **P78352-2** | | | |
| **nxp:NX P99999-1** | Cytochrome c isoform Iso 1 | Up | Metabolism; Energy pathways |
| **nxp:NX Q01814-2** | Plasma membrane calcium-transporting ATPase 2 isoform WA | Up | Transport |
| **nxp:NX Q04917-1** | 14-3-3 protein eta isoform Iso 1 | Up | Cell communication; Signal transduction |
| **nxp:NX Q07960-1** | Rho GTPase-activating protein 1 isoform Iso 1 | Up | Cell communication; Signal transduction |
| **nxp:NX Q08495-1** | Dematin isoform Iso 1 | Up | Cell growth and/or maintenance |
| **nxp:NX Q13449-1** | Limbic system-associated membrane protein isoform Iso 1 | Up | Cell communication; Signal transduction |
| **nxp:NX Q13509-1** | Tubulin beta-3 chain isoform Iso 1 | Up | Cell growth and/or maintenance |
| **nxp:NX Q13885-1** | Tubulin beta-2A chain isoform Iso 1 | Up | Cell growth and/or maintenance |
| **nxp:NX Q15286-1** | Ras-related protein Rab-35 isoform Iso 1 | Up | Cell communication; Signal transduction |
| **nxp:NX Q16352-1** | Alpha-internexin isoform Iso 1 | Up | Protein metabolism |
| **nxp:NX Q16720-1** | Plasma membrane calcium-transporting ATPase 3 isoform XB | Up | Transport |
| **nxp:NX Q16799-1** | Reticulon-1 isoform RTN1-A | Up | Cell communication; Signal transduction |
| **nxp:NX Q16851-1** | UTP--glucose-1-phosphate uridylyltransferase isoform Iso 1 | Up | Metabolism; Energy pathways |
| **nxp:NX** | AP2-associated protein kinase 1 isoform | Up | Transport |

| | | | |
|---|---|---|---|
| **Q2M2I8-1** | Iso 1 | | |
| **nxp:NX Q3ZCQ8-2** | Mitochondrial import inner membrane translocase subunit TIM50 isoform Iso 2 | Up | Cell communication; Signal transduction |
| **nxp:NX Q86UX6-1** | Serine/threonine-protein kinase 32C isoform Iso 1 | Up | Cell communication; Signal transduction |
| **nxp:NX Q96HS1-1** | Serine/threonine-protein phosphatase PGAM5, mitochondrial isoform Iso 1 | Up | Metabolism; Energy pathways |
| **nxp:NX Q9H115-1** | Beta-soluble NSF attachment protein isoform Iso 1 | Up | Transport |
| **nxp:NX Q9NQ66-1** | 1-phosphatidylinositol 4,5-bisphosphate phosphodiesterase beta-1 isoform A | Up | Signal transduction |
| **nxp:NX Q9UHC6-1** | Contactin-associated protein-like 2 isoform Iso 1 | Up | Cell communication; Signal transduction |
| **nxp:NX Q9UPV7-1** | PHD finger protein 24 isoform Iso 1 | Up | Biological_process unknown |
| **nxp:NX Q9UQM7-1** | Calcium/calmodulin-dependent protein kinase type II subunit alpha isoform A | Up | Cell communication; Signal transduction |
| **nxp:NX Q9Y2T3-3** | Guanine deaminase isoform Iso 3 | Up | Metabolism; Energy pathways |

**FIGURE 1**

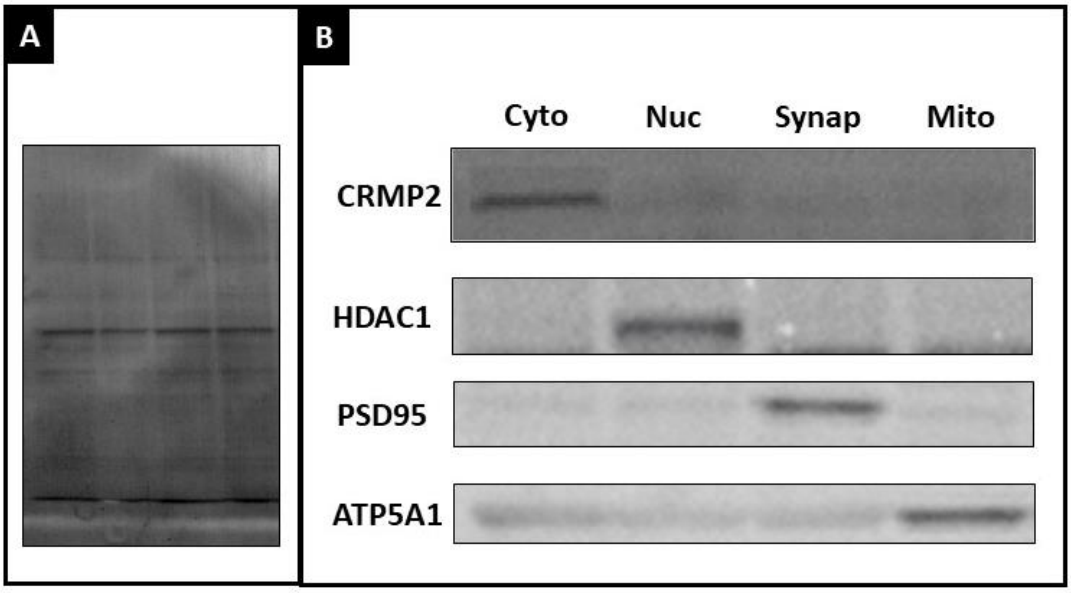

**FIGURE 2**

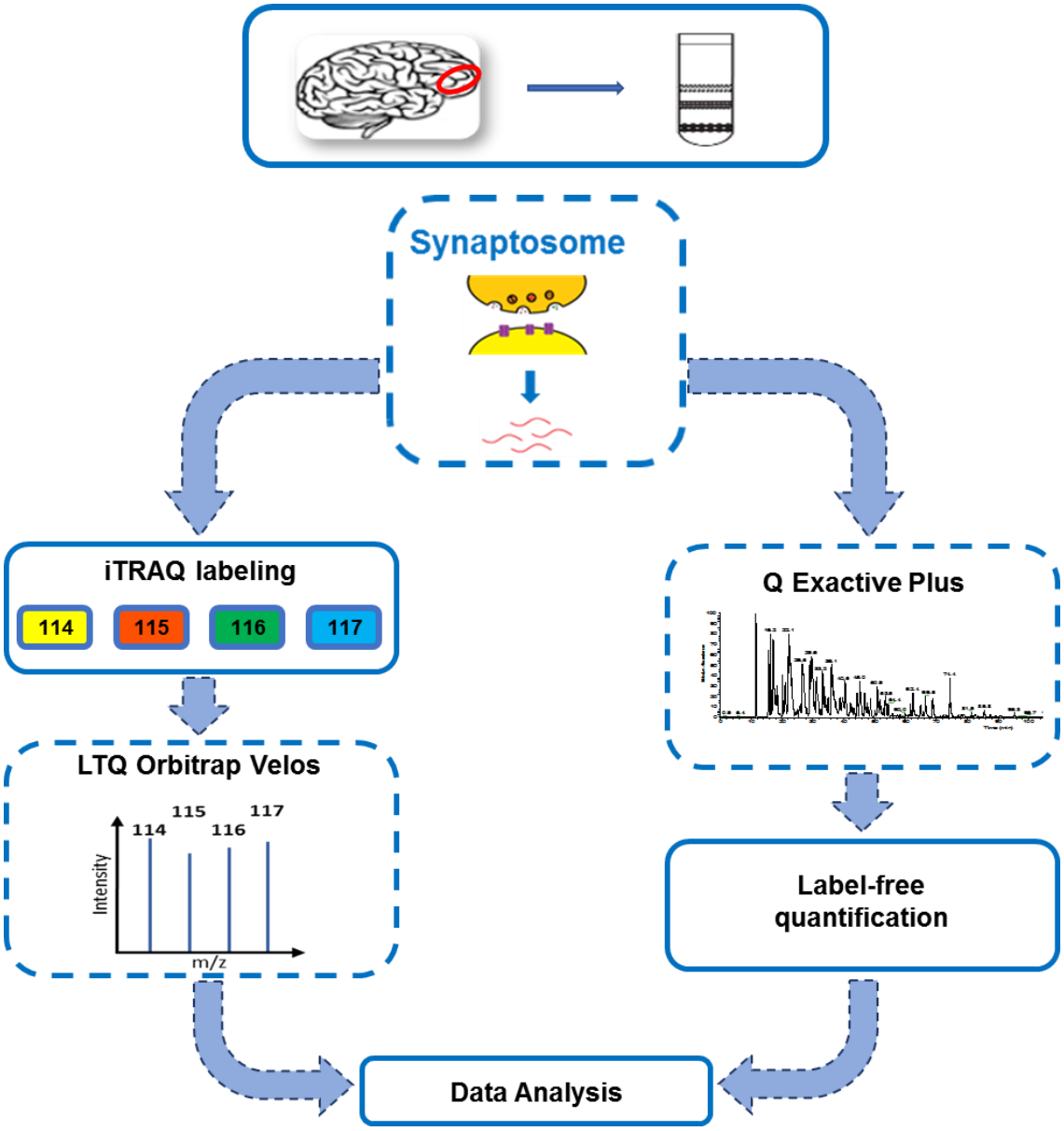
Synaptosome
iTRAQ labeling
114
115
116
117
LTQ Orbitrap Velos
114
115
116
117
Intensity
m/z
Q Exactive Plus
Label-free quantification
Data Analysis

## FIGURE 3

| A | Unique peptides | Proteins | Protein groups | Quantified Proteins | Differentially expressed proteins (p-value ≤ 0.05) |
|---|---|---|---|---|---|
| iTRAQ analysis | 1254 | 1176 | 513 | 127 | 12 |
| Label-free analysis | 5109 | 4904 | 1917 | 341 | 55 |

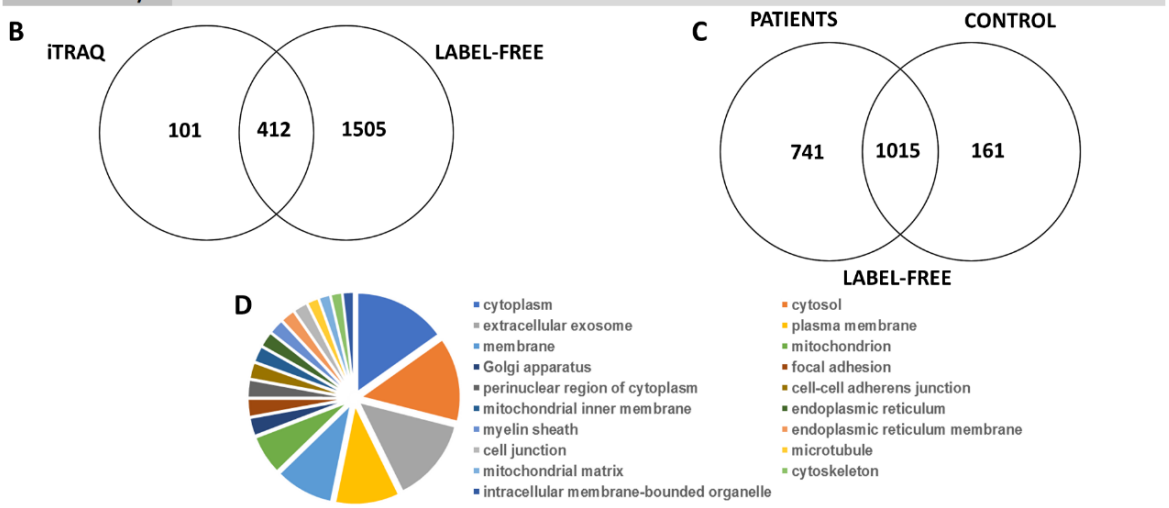


## FIGURE 4

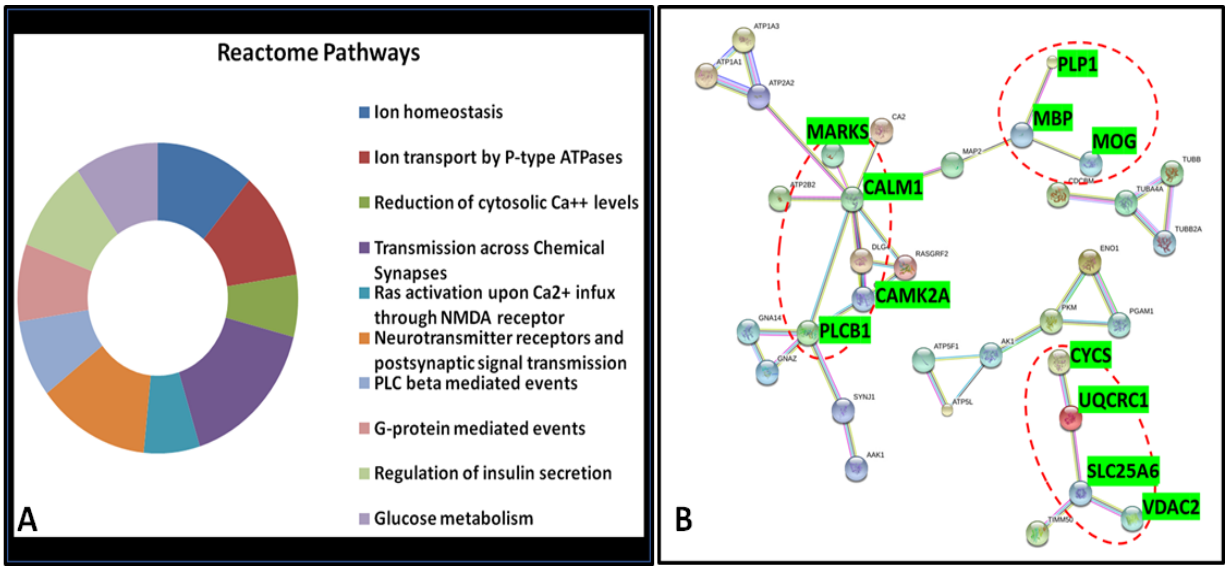

# FIGURE 5

**A) VAGALQAQVK (PI)**

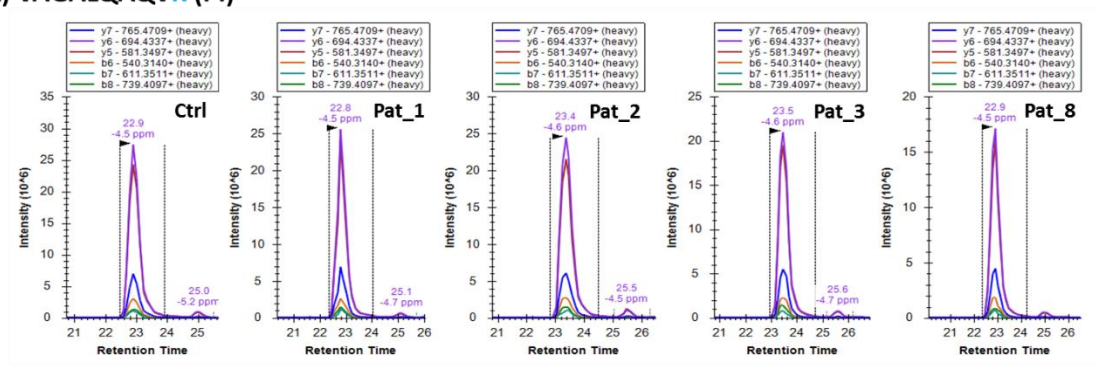


**B) EAFSLFDKDGDGTITTK (Calmodulin-1)**

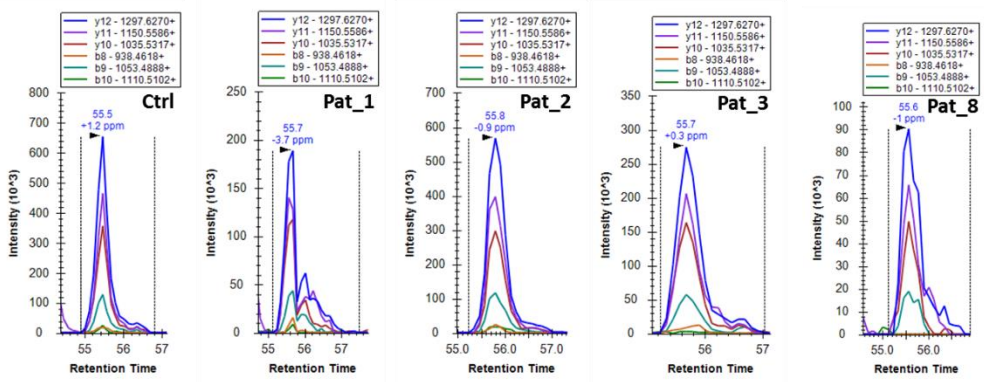

**FIGURE 6**

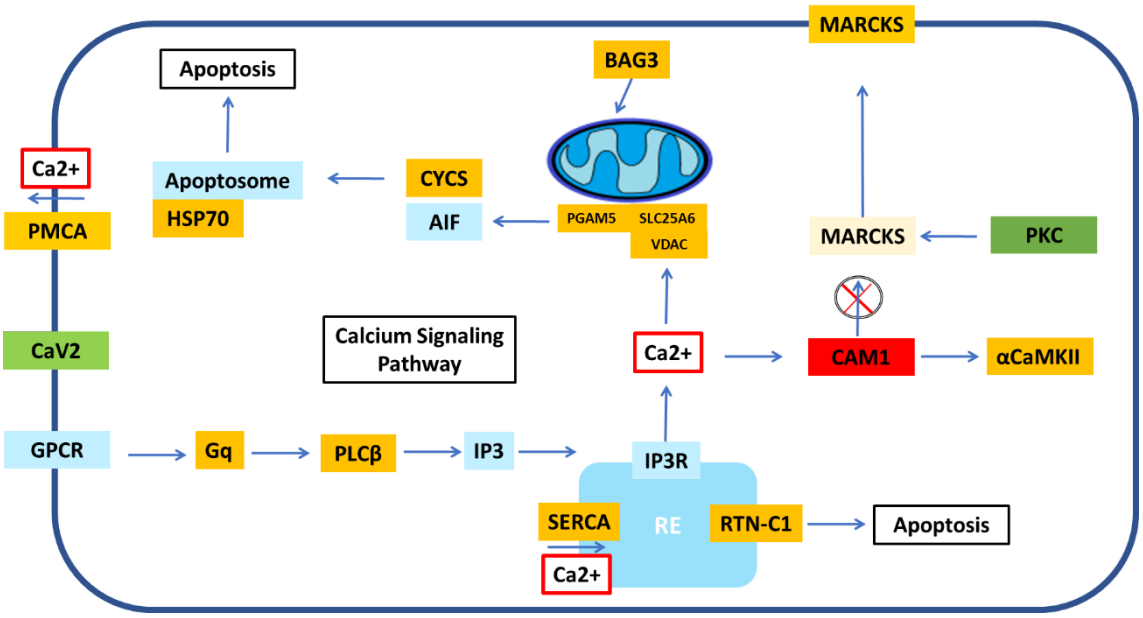
MARCKS
Apoptosis
BAG3
Ca2+
Apoptosome
CYCS
HSP70
AIF
PGAM5
SLC25A6
VDAC
PMCA
MARCKS
PKC
CaV2
Calcium Signaling Pathway
Ca2+
CAM1
αCaMKII
GPCR
Gq
PLCβ
IP3
IP3R
SERCA
RE
RTN-C1
Apoptosis
Ca2+

**CAPITULO VI**

**ANÁLISES PROTEÔMICA DA FRAÇÃO MITOCONDRIAL, NÚCLEO E CITOPLASMA DO CÓRTEX ORBITOFRONTAL DE PACIENTES COM ESQUIZOFRENIA**

Artigo submetido na edição especial da revista *Journal of Proteome Research*

# QUANTITATIVE SUBCELLULAR PROTEOMICS OF THE ORBITOFRONTAL CORTEX OF SCHIZOPHRENIA PATIENTS

| | |
|---|---|
| Journal: | *Journal of Proteome Research* |
| Manuscript ID | Draft |
| Manuscript Type: | Article |
| Date Submitted by the Author: | n/a |
| Complete List of Authors: | Velásquez, Erika; Universidade Federal do Rio de Janeiro, Institute of Chemistry, Department of Biochemistry<br>Martin de Souza, Daniel ; Universidade Estadual de Campinas Instituto de Biologia, Departamento de Bioquimica e Biologia Tecidual<br>Velásquez, Ingrid; University of Carabobo<br>Carneiro, Gabriel; Universidade Federal do Rio de Janeiro, Institute of Chemistry, LADETEC<br>Schmitt, Andrea; Ludwig Maximilians University Munich, Department of Psychiatry and Psychotherapy<br>Falkai, Peter; Ludwig Maximilians University Munich, Department of Psychiatry and Psychotherapy<br>Domont, Gilberto; Universidade Federal do Rio de Janeiro, Proteomics Unit, Department of Biochemistry, Institute of Chemistry;<br>Nogueira, Fabio; Universidade Federal do Rio de Janeiro, Institute of Chemistry, Department of Biochemistry |
| | |

# QUANTITATIVE SUBCELLULAR PROTEOMICS OF THE ORBITOFRONTAL CORTEX OF SCHIZOPHRENIA PATIENTS

Erika Velásquez[1], Daniel Martins-de-Souza[2,3], Ingrid Velásquez[4], Gabriel Reis Alves Carneiro[5], Andrea Schmitt[6], Peter Falkai[6], Gilberto B Domont[1*] and Fabio CS Nogueira[1,5*]

[1]Proteomics Unit, Department of Biochemistry, Institute of Chemistry, Federal University of Rio de Janeiro.

[2]Laboratory of Neuroproteomics, Department of Biochemistry, Institute of Biology, University of Campinas (UNICAMP).

[3]UNICAMP's Neurobiology Center, Campinas, Brazil.

[4]University of Carabobo, Venezuela.

[5]Laboratory of Proteomics, LADETEC, Institute of Chemistry, Federal University of Rio de Janeiro.

[6]Department of Psychiatry and Psychotherapy, Ludwig Maximilian University of Munich (LMU), Munich, Germany.

*Corresponding authors

Gilberto B Domont, gilberto@iq.ufrj.br

Fabio CS Nogueira, fabiocsn@iq.ufrj.br

## ABSTRACT

Schizophrenia is a chronic disease characterized by the impairment of mental functions with a marked social dysfunction. A proteomic approach using iTRAQ labeling and selected reaction monitoring, applied to the characterization of mitochondria (MIT), crude nuclear fraction (NUC) and cytoplasm (CYT), can allow the observation of dynamic changes in cell compartments providing valuable insights concerning schizophrenia physiopathology. Mass spectrometry analyses of the orbitofrontal cortex from 12 schizophrenia patients and 8 healthy controls identified 939 protein groups in MIT fraction, 2021 in NUC and 2433 in CYT. We found 358 groups of proteins dysregulated among all enriched cellular fractions. Through the quantitative proteomic analysis, we detect as the main biological pathways those related to calcium and glutamate imbalance, cell signaling disruption of CREB activation, axon guidance and

proteins involved in the activation of NF-kB signaling along with the increase of complement proteins C3. Based on our data analysis, we suggest the activation of NF-kB as a possible pathway that links the deregulation of glutamate, calcium, apoptosis and the activation of the immune system in schizophrenia patients. All MS data are available in the ProteomeXchange Repository under the identifier PXD014284 and PXD014350.
**Keywords:** Schizophrenia, cellular fractions, proteomics, quantification.

## 1. INTRODUCTION

Schizophrenia is a chronic disease characterized by the impairment of mental functions with a marked social dysfunction. Over the years several hypotheses have emerged about its etiology and physiopathology but it is widely accepted that factors such as genetic susceptibility and environmental influences can cause the onset of the disease[1]. Diagnosis and classification depend mainly upon a collection of clinical features through the observation of positive symptoms including delusions, hallucinations, speech or disorganized behavior, as well as negative symptoms as affective bottling, anhedonia, alogia, avolition, social withdrawal and impaired cognitive capacity[2]. Negative and cognitive symptoms currently remain without totally effective therapeutic options, persisting in the chronic phase[3].

One of the main brain areas related to cognitive and behavioral disturbances is the frontal cortex. The dysfunction of this brain region is associated with mental disorders like psychosis, depression, and anxiety[4]. Particularly the orbitofrontal cortex (OFC), a subdivision of prefrontal cortex, is involved in the emotional and executive processing, reward-guided behavior and decision-making duet to its connection with neuroanatomical structures as the hippocampus, ventral striatum, amygdala, hypothalamus, anterior cingulate and other medial temporal areas[5]. Clinical findings have linked social functioning impairment with anatomic structural abnormalities in the OFC in first-episode schizophrenia patients[6]. In the same way, it was showed the relationship between structural brain abnormalities in the OFC and the severity of negative symptoms[7,8] suggesting the key role of OFC in the abnormal emotional responses and social disability.

According to the Schizophrenia Working Group of the Psychiatric Consortium of Genomic (2014)[9], single nucleotide polymorphisms related to schizophrenia gene risk are associated with several genes involving dopamine receptor, glutamate neurotransmission, and immunity. Otherwise, transcriptomic data show that pathways linked with

mitochondrial function and energy production, tight junction signaling, protein translation, neurodevelopment, and immune system seem to be very important in the pathophysiology of schizophrenia[10, 11, 12].

Several studies have been carried out the proteomic characterization of post-mortem brain tissue of different areas from patients with schizophrenia, showing that the dysregulation of synaptic function as the NMDA receptors hypofunction, calcium homeostasis, imbalance of mitochondrial energy metabolism and oxidative stress, dysregulation in proteins of cytoskeleton and immune system are the main pathways reported so far[13]. However, only a few of these proteomic studies have deepened into the subcellular level[14,15,16]. The traditional proteomic approach lacks the important spatial information of the data; protein function is related to its environment, and the pathophysiological process can involve changes in protein subcellular localization[17].

We analyzed OFC post-mortem brain tissue from patients classified as residual schizophrenia according to the DMS-IV manual. In this classification, the patients do not manifest prominent positive psychotic symptoms but prevail characteristic disturbance of negative symptoms[18]. Through the comparison of patient´s samples against a pool of control subjects without any history of psychiatric illness we generated an organellar proteome map from different subcellular fractions such as mitochondria (MIT), crude nuclear fraction (NUC) and cytoplasm (CYT) with the aim to monitor the subproteome changes using iTRAQ labelling for relative quantification and Selected Reaction Monitoring (SRM) for targeted quantification. Subcellular proteome maps allowed to observe dynamic changes in cell compartments providing valuable insights concerning schizophrenia physiopathology in the chronic phase of the disease.

## 2. EXPERIMENTAL PROCEDURES

### 2.1. Brain samples

The OFC postmortem tissues were collected from 12 schizophrenia patients at the State Mental Hospital in Wiesloch, Germany. Patients were diagnosed as residual schizophrenia (295.6) according to the Diagnostic and Statistical Manual of Mental Disorders (DSM-IV) criteria[18]. The OFC control samples were collected from eight individuals at the Institute of Neuropathology, Heidelberg University, in Heidelberg, Germany (Table S-1). It was selected control subjects without any medical records of mental clinical diseases, antidepressants or antipsychotics treatment during their lifetime

and no history of alcohol or drug abuse. Other neuropathologies were ruled out by histopathological analysis, considering only brains with Braak staging less than II. All assessments, postmortem evaluations and procedures were approved by the ethics committee of the Faculty of Medicine, Heidelberg University, Heidelberg, Germany.

### 2.2. Subcellular enrichment

For nuclear enrichment, fifty milligrams of OFC tissue were homogenized in 10 volumes of Buffer A pH 7.4 (0.32M sucrose, 4mM HEPES and protease cocktail inhibitor tablets (Roche)) and phosphatase inhibitor cocktail I and II (Sigma). The homogenate was centrifuged at 1.000g for 10 min, 4ºC obtaining the P1: crude nuclei. In the case of the mitochondria and cytoplasm enrichment, thirty milligrams of intact OFC brain tissue was incubated for 15 min on ice with 180µl of 250-STM buffer (250 mM Sucrose, 50 mM Tris-HCl pH 7,4, 5 mM $MgCl_2$, Mini protease inhibitor and phosphatase inhibitor (Roche)). The tissue homogenization was made two times with a pestle for 1-2 minutes incubating for 10 min. The sample was centrifugated at 800g for 15 min 4°C, obtaining the supernatant Cyt 1 (cytoplasm + mitochondria). The pellet was resuspended in 640µl 250-STM buffer, centrifuging at 800g, 15 min, 4°C until the supernatant was clear. All supernatants were combined and centrifugated at 6.000g, 15 min, 4°C. The last supernatant was collected as CYT fraction and saved to -80°C until its use and the pellet (PM) was used for mitochondria enrichment.

PM was resuspended in 250 µl of 250-STM buffer and centrifuged at 6.000g, 15 min, 4°C. The pellet was resuspended in 250µl Hepes buffer (10 mM Hepes, (pH 7,9 / Mini protease inhibitor and phosphatase inhibitor (Roche) and incubated at 4°C for 30 min (Eppendorf ThermoMixer®, cold room/ mixing). The enriched mitochondria were loaded on a sucrose gradient containing 1,75ml of 50% sucrose, 1,75 ml of 36% sucrose and 0,75 ml of 20% sucrose centrifuging at 25.000rpm, 4°C, 60 min. The MIT fraction was transferred to a new tube, filling in with Hepes buffer until 2 ml and centrifuged at 17.200g, 20 min, 4°C. This procedure was repeated four times. Finally, the pellet was saved to -80°C until use.

### 2.3. Protein extraction and western blot analysis

Protein extraction was made according to Saia-Cereda and collaborators protocol (2016)[15], determining the protein concentration by the Bradford assay (*BioRad; Munich,*

*Germany*). For SDS-PAGE electrophoresis and the Western blot analysis we proceeded as previously described[16], evaluating the subcellular enrichment efficiency using antibodies against collapsin 2 for cytosolic proteins, ATP synthase subunit alpha (ATP5A1) for mitochondrial proteins, postsynaptic density protein 95 (PSD95) for synaptosomal proteins, and histone deacetylase 1 (HDAC1) for nuclear proteins.

### 2.4. Protein digestion

Enzymatic digestion for iTRAQ labeling experiment used 10 µg of protein from MIT (n=6), 25 µg of NUC (n=12), 50 µg of CYT (n=11) and control pool (20 µg MIT, 100 µg NUC, and 200 µg CYT, all with n=8). The samples were reduced with 5 mM TCEP for 1 hour at 30 ºC, alkylated with 10 mM iodoacetamide for 30 minutes at room temperature followed by dilution (1:10) with 50 mM triethylammonium bicarbonate (TEAB) pH 8 and digestion with trypsin (1:50) for 18 hours at 35 º C. The samples were cleaning in $C_{18}$ MacroSpin Columns (*Harvard Apparatus*) The peptides were dried in Speed Vac and resuspended in 30 µl of TEAB 20 mM for Qubit® assay quantification. For SRM experiments were digested 8 µg of proteins from all subcellular fractions (MIT n=12, NUC n=8, and CYT n=12) and 8 µg of control pool (n=8 for MIT, NUC, and CYT) following the procedure above.

### 2.5. Isobaric tag labeling with iTRAQ and strong cation exchange (SCX)

The peptides from each subcellular fraction were labeled according to Núñez and collaborators protocol (2017). The organization of 4-plex iTRAQ in all subcellular fractions was made up as follows: three channels (114, 115 and 116) were labeled with patients' samples and one channel (117) containing the pool of 8 control samples. Labeled peptides were dried to a volume of 20 µl. For SCX chromatography (MacroSpin Columns - *Harvard Apparatus*) the samples were completed to a final volume of 100 µl with a solution of $KH_2PO_4$ 5 mM / ACN 25% pH 3. Peptides were eluted by one step with 500 mM KCl for MIT and NUC fractions and 75, 150, 250 and 500 mM KCl for CYT fraction. Samples were desalted in $C_{18}$ MacroSpin columns (*Harvard apparatus*), dried and suspended in 0.1% formic acid for quantification (*Qubit*® protein assay Kit – Thermo Scientific).

### 2.6. Mass spectrometry analyses

Peptides (2 µg) were analyzed in technical triplicate by nLC Proxeon EASY-II system (*Thermo Scientific*). The chromatographic condition was as follow: flow-rate of 250 nL/min, three hours of gradient beginning with 5% to 40% B for 167 minutes, 40% to 95% B for 5 min, 95% B for 8 minutes, using as solvent A a solution of 95% $H_2O$ / 5% ACN / 0.1% formic acid and solvent B 95% ACN / 5% $H_2O$ / 0.1% formic acid. The analytical column length was 15 cm and an internal diameter of 75 µm (3 µm spheres-Reprosil Pur C18, Dr. Maish) and the trap-column length was 3 cm with an internal diameter of 200 µm (5 µm spheres-Reprosil Pur C18, Dr. Maish). Data acquisition was carried out under a stream atmosphere provided by 5% ammonium hydroxide[19].

The chromatographic system was coupled on-line to an LTQ Orbitrap Velos (*Thermo Scientific*) mass spectrometer. A dynamic exclusion list of 90 s, spray voltage at 2.5 kV and no auxiliary gas flow were the settings used for data-dependent acquisition mode. For Full MS scan was used a scan range of m/z 375-2000 and a resolution of 60,000 (at m/z 400) in the Orbitrap analyzer. We selected the ten most intense ions for fragmentation, excluding unassigned and 1+ charge state, acquiring the $MS^2$ spectra in the Orbitrap (resolution of 7,500 at m/z 400) with higher-energy collision dissociation (HCD) using normalized collision energy of 40.

**2.7. Mass spectra analysis**

Raw data was analyzed using Proteome Discoverer 2.1 software against the human database from UniProt (48883 protein entreis) using a target-decoy strategy (maximum delta CN of 0.05) and concatenated calculation of target false discovery rate (FDR) of 0.01. The search space was full-tryptic considering two missed cleavages for trypsin. The precursor mass tolerance and fragment mass tolerance were 10 ppm and 0.1 Da respectively. As fixed modification was included the carbamidomethylation of cysteine. Methionine oxidation, protein N-terminal acetylation and iTRAQ modifications (K, Y, and N-terminal) were considered as dynamic modifications. The peptide filter was set up for high confidence counting only peptides rank 1 with a minimum length of 6 amino acids using as peptide validation settings an automatic control level peptide error with a strict target FDR of 0.01 (contatenated). The confidence threshold in FDR protein validator was 0.01, grouping the proteins by maximum parsimony.

iTRAQ quantification was made with unique peptide using patients' value as nominator and pool of controls as the denominator for fold-change calculation. Additional

filters as a correction for the impurity reporter and a filter to do not report quantitative values for a single-peak in the precursor isotope pattern were applied.

### 2.8. Statistical evaluation of the data

Data analyses were performed in the *InfernoRDN* program[20] using unique peptides. For data normalization was applied to the Central Tendency and the absolute deviation of the adjusted median. Grubbs test, with a minimum of three peptides and p-value <0.05, was used as a parameter to group the peptides in their corresponding protein. Robust estimators such as the median and median absolute deviation were used to calculate the z-score and the p-value associated with a 95% confidence level, determining the statistically significant variations in the relative abundance of proteins. Also, *InfernoRDN* was used for the principal component analysis (PCA) of the different subcellular fractions.

### 2.9. Biological and functional analysis

Subcellular localization protein assignment was made using UniProt[21]. Comparative analyses of data were performed in Venny 2.1 program[22]. The biological function was analyzed by Reactome Pathways[23]. For protein-protein interaction analyses and evaluations of functional network enrichment in the deregulated proteins were used the STRING 10.5[24] (considering high-confidence interactions) and KEGG program[25].

### 2.10. SRM Analysis

The SRM analysis was performed in an EASYII-nano-LC (ThermoScientific) in a C18 column PicoChip 75µm x 105mm (New Objective) and C18 trap column Acclaim PepMap 75µm x 2 cm (ThermoScientific). As Solvent A was used a solution of 95% $H_2O$ / 5% ACN / 0.1% formic acid and solvent B 95% ACN / 5% $H_2O$ / 0.1% formic acid in a flow-rate 320 nL/min during 60 min.

The data were acquired in a positive mode using the SRM (Selected Reaction Monitoring) mode in the TSQ Quantiva (Thermo Scientific) mass spectrometer. The first and third quadrupoles were set up with a resolution of 0.7 (FWHM) using a cycle time of 2 s. The precursor ions fragmentation was carried out with Argon gas with a CID gas pressure of 1.5 mTorr using normalized collision energy for each peptide in a range of 10-30. Regarding the ion source parameters, the spray voltage and the ion transfer tube

temperature used was 2,6kV and 280ºC, respectively, and the sweep gas was set up as 0 (Arb). The data analysis of SRM results was performed with Skyline v. 4.2 software using a public NIST library of peptide ion fragmentation spectra (Ion Trap: Human. SpectraST format with short peptides (<7AA) excluded. File Name: NIST_human_IT_2012-05-30_7AA.splib.zip). Available in: https://db.systemsbiology.net/sbeams/cgi/PeptideAtlas/buildDetails?atlas_build_id=479 ). For data normalization, we use as global standard the heavy peptide sequence AVLDLFEETSNIGSK. For proteins with more than one monitored peptide, the sum of normalized areas of all peptides were used for the statistical analyses. The statistically significant variations were calculated applying a completely randomized ANOVA test followed by Tukey HSD all-pairwise comparisons considering an alpha value of 0.05 using the Statistix 8.0 software.

## 3. RESULTS AND DISCUSSION

### 3.1. Proteins identified by mass spectrometry

In the mass spectrometry analyses we identified 939 protein groups from MIT fraction, 2021 proteins groups in NUC and 2432 protein groups in CYT (Table S-2), getting the identification of 3358 protein groups among all fractions (Figure 1). The estimated FDR values were reported in the Table S-2. Venny diagram reveals that the proteins identified in all fractions (17.8%) are mainly related to metabolism and axon growth. Five percent of proteins were identified only in MIT and they are involved in electron transport, citric acid cycle, and ATP synthesis. The percentage of proteins found only in NUC and CYT represents 18,7 % and 33,1% respectively. In NUC the biological function of these proteins is related to mRNA splicing, on the other hand, in CYT fraction proteins are involved in polyamines metabolism and NF-κB activation (Figure 1B; Table S-3). In figure 1C, the PCA shows three well-defined different subpopulations corresponding to the patient data distribution for each fraction.

After data normalization, we applied the Grubbs test with a minimum of three peptides and p-value <0.05 per protein, in order to obtain the highest quality data for protein quantification. iTRAQ labeling robustly quantified a total of 1727 proteins, in which 523 for MIT fraction, 1109 for NUC and 1341 for CYT (Figure 1D; Table S-4).

### 3.2. Dysregulated proteins and their functional analysis

For the selection of dysregulated proteins, in addition to the use of rigorous statistical criteria, we also consider the same quantitative behavior for up- and down-regulated proteins in at least 50% of patients. These criteria drastically reduce the number of proteins considered as dysregulated to a total of 358 in all fractions (Figure 1D; Table S-5). Proteins as γCaMKII, UCH-L1, MAPK2, C3, GS, and NF-kB family were selected for quantification by SRM analysis (Table S-6).

### 3.2.1. Mitochondrial fraction

Mitochondrial dysfunction and structural changes have been widely reported in schizophrenia patients[26,27,28]. According to a recent review[29] in post-mortem brain tissue, mitochondrial abnormalities in these patients vary according to the brain area, cell type and also to treatment response. Twenty-three proteins were found dysregulated in MIT fraction (Table S-5). We detected five proteins down-regulated such as UCH-L1, CLH-17, PGAM-B, Guanine nucleotide-binding protein G(I)/G(S)/G(T) subunit beta-1 and PPIase A (Table S-5). Some of these proteins have participation in apoptosis processes. Additionally, we found 18 up-regulated proteins, mainly involved in the biological processes such as oxidative phosphorylation, the terminal pathway of complement and cristae formation (Figure 2; Table S-7).

In our study, we found up-regulated proteins involved in oxidative phosphorylation (OXPHOS) as cytochrome c oxidase 2 (MT-CO2), cytochrome b-c1 (complex III) and ATP1-ATP synthase. In a previous study, proteins as MT-CO2 was found decreased in the Substantia Nigra/Ventral Tegmental Area in schizophrenia patients[30]. However, the increase of these proteins in our results must be analyzed in accordance with the biological context. In previous work by our group, in an analysis of the synaptosome fraction of schizophrenic patients from the same brain area[16], we observed the deregulation of calcium metabolism pathway concomitantly with the activation of an apoptotic process. Indeed, we found the Protein NipSnap homolog 2 (NipSnap2) increased in MIT fraction. It was demonstrated that NipSnap2 acts as a positive regulator of L-type $Ca^{2+}$ channels and its overexpression increase the intracellular $Ca^{2+}$ influx impacting the CREB phosphorylation[31] and mitophagy signaling[32]. Also, it is well known that $Ca^{2+}$ is an important cell death regulator and it has been proposed that $Ca^{2+}$ influx through cell channels can be apoptogenic[33]. In this sense, it was shown that MT-CO2 and ATP1-ATP synthase complex are up-regulated during apoptosis[34] and

recently the complex III is apparently involved in triggering apoptosis in animal cells; under oxidative stress condition complex III can trigger the intrinsic apoptosis pathway[35].

Additionally, the up-regulation of proteins such as voltage-dependent anion-selective channel protein 1 (VDAC1) and glyceraldehyde-3-phosphate dehydrogenase (GAPDH) are consistent with these observations, being dysregulated in previous studies as well[27,36]. VDAC1 overexpression mediated the mitochondrial apoptosis and its oligomerization seems to be important for the release of the pro-apoptotic proteins from the mitochondrial intermembrane space to the cytosol[37]. In the same way, it was reported that GAPDH accumulates in mitochondria during apoptosis and interacts with VDAC1 leading the increase of $Ca^{2+}$ uptake, mitochondrial swelling and the permeabilization of the inner mitochondrial membrane with the release of cytochrome c (Cyt c) and apoptosis-inducing factor (AIF)[38]. These data match with what it was previously reported by our group where Cyt c was found up-regulated in the synaptosome fraction[16]. VDAC1 is also the point of interaction that connects specialized endoplasmic reticulum (ER) microdomains known as mitochondria-associated membranes with the mitochondria; these hot spots allow the crosstalk between the ER and mitochondria to maintain the $Ca^{2+}$ homeostasis and mitochondrial metabolism balance[39]. In this context, calnexin (CNX) a molecular chaperone protein located in the mitochondria-associated membrane (MAMs) was found increased in the MIT fraction. This evidence indicates that CNX overexpression can induce apoptosis without exogenous ER stress conditions, but usually, it is involved in the early steps of apoptotic death by overwhelming ER stress[40].

When an apoptotic signal is activated the balance between pro- and anti-apoptotic stimulus determines the cell death. In response to the apoptotic signals, we found the increase of the terminal pathway of complement, represented by clusterin, a glycoprotein that inhibits Bax oligomerization and subsequently the release of Cyt c and the activation of the caspase[41]. Also, the cristae formation pathway is dysregulated in schizophrenia patients. One of the most noticeable alterations in the apoptotic processes is the structural changes of mitochondria and it has been suggested that mitochondrial cristae remodeling can impact Cyt c release and mitochondrial storage[42]. In that sense, scaffolding proteins involved in maintaining crista architecture, membrane organization and membrane contact sites formation as Mic19 and its paralog Mic25[43,44,45] are up-regulated in MIT fraction.

### 3.3. Crude Nuclear fraction

In NUC fraction we found 164 proteins with significant variation in their relative abundance (Table S-5). Forty less abundant proteins are related with Transmission across Chemical Synapses including cAMP and $Ca^{2+}$ responsive-element-binding protein (CREB) phosphorylation through the activation of Calcium/calmodulin-dependent protein kinase II (CaMKII). On the other hand, 124 proteins increased the abundance in this subcellular fraction, and many of these are involved in chemical synapses transmission and respiratory electron transport (Table S-7).

3.3.1- Proteins located in the cell nucleus

3.3.1.1. CREB signaling activation

Cognitive impairments are widely reported in schizophrenia patients as one of the main symptoms of the illness. We found down-regulated pathways involving the chemical synaptic transmission including CREB phosphorylation through the activation of CaMKII. First, we would like to highlight the αCaMKII dysregulation in the NUC fraction. αCaMKII is critical for memory formation and neuronal plasticity; its inhibition or knocking out affect the long-term potentiation (LTP) impairing learning and memory process[46]. αCaMKII not only participates in AMPA receptors functioning, but also it is translocated to the nucleus after cellular calcium influx for CREB phosphorylation and gene expression for the LTP maintenance[46]. The genetic deletion of αCaMKII cause behavioral changes similar to the cognitive symptoms of schizophrenia. A αCaMKII null mutation in mouse models entails a significant working memory deficit[47] and αCaMKII heterozygous knock-out animals displayed significantly increase of dopamine D2 receptors as well[48]. Moreover, a sub-chronic dose of the non-selective NMDAR antagonist ketamine induces NMDAR hypofunction with a αCaMKII loss decreasing the insulin-like growth factor receptor 1 signaling[49].

As part of this same pathway, we also found decreased calmodulin (CaM) in NUC. CaM was also identified and quantified in the CYT fraction but no significant differences were observed between schizophrenia patients and controls. When the L-type $Ca^{2+}$-channels are open, the calcium influx promotes the CaM translocation into the nucleus[50] for CREB activation. Nuclear translocation of CaM activates the Calcium/calmodulin-dependent protein kinase kinase (CaMKK) and Calcium/calmodulin-dependent protein kinase IV (CaMKIV) trigging CREB phosphorylation and downstream *c-fos* expression

proportionally to nuclear $Ca^{2+}$/CaM increase[51]. Also, it was demonstrated that *in vivo* CaM nuclear signaling phosphorylated the S133 of CREB and the use of a specific CaM nuclear inhibitor affects the memory consolidation[52].

On the other hand, we find increased pathways related to chemical synapses in the NUC fraction. This is represented principally with the increase of proteins as Calcium/calmodulin-dependent protein kinase type II gamma (γCaMKII). γCaMKII is a shuttle protein that binds $Ca^{2+}$/CaM. After the cytosolic increase of $Ca^{2+}$, γCaMKII translocate CaM from the cytoplasm to the nucleus[46]. This protein was reported previously up-regulated (together with CaM) in a nuclear fraction from corpus callosum and anterior temporal lobe of schizophrenia patients[15], also it was shown that γCaMKII has an abnormal regulation in the prefrontal cortex by the miR-219 in the dizocilpine murine model[53]. γCaMKII unique peptides were mapped and quantified using the SRM technique in the NUC and CYT fractions (where previously it could not be identified) demonstrating that γCaMKII apparently is mainly located in NUC since it was found increased in that fraction and no significant change in CYT. However, how can be increased the nuclear γCaMKII in our results if the nuclear CaM remains decreased? Previously, studies demonstrated that γCaMKII needs to be phosphorylated in Thr287 for effective CaM nuclear delivery[54,55] and for this process, it was shown that βCaMKII kinase function is responsible for pThr287[54]. In accordance with these observations, we found βCaMKII down-regulated in CYT fraction. Ma and colleagues (2014) elegantly demonstrated that without βCaMKII phosphorylation at T287, the nuclear translocation of the γCaMKII in not affected but nuclear delivery of CaM and CREB activation is impaired[54] (Figure 3).

The crude nuclear fraction obtained during the sample processing, in addition to enriching nuclear proteins, brings common contaminants such as mitochondria (especially those located in the perinuclear region), sheets of the plasma membrane and also, possibly, minor contaminants such as lysosomes, peroxisomes, Golgi membranes, and various membrane vesicles[56]. The methodology implemented restricts the interpretation of the biological function of proteins that can share different subcellular locations besides the nucleus, in this data set, we detect as the main contaminants of NUC fraction, proteins whose more frequent subcellular location has been reported in mitochondrion and cellular membrane, nevertheless, some of these proteins are interesting to mention due to their biological importance.

3.3.2. Mitochondrial proteins present in the crude nuclear fraction

We quantified proteins in the crude nuclear fraction whose subcellular location has been reported only in the mitochondrion and for which in the MIT fraction we have not identified or observed any significant variation in the relative abundance compared to the control group. What could, then, explain that these proteins do not significantly change their abundance in the MIT fraction and, at the same time, are dysregulated in this crude nuclear fraction? One possible answer is that these proteins have a nuclear function not yet described or, the most plausible explanation is that these proteins could reflect the activity of the perinuclear mitochondria, due to the technical limitations mentioned above for this type of enrichment for nuclear proteins. Since a long time ago, the heterogeneity of mitochondria in a single cell has been reported[57]. In the same cell the mitochondria can be morphologically heterogeneous in terms of ultrastructure, cristae density, and shape, having different respiratory status and functional properties as divergences in $Ca^{2+}$ and reactive oxygen species (ROS) levels, protein composition, mitochondrial membrane potential, respond differently to apoptotic and mitophagy signals and also, they can have a different fission and fusion dynamic[57,58,59,60,61].

Among these mitochondrial proteins are dysregulated those belonging to ATP synthase complex and the ATPase inhibitor (IF1) which is increased in schizophrenia patients. IF1 overexpression has the capacity to limit the cell death avoiding the ATP depletion from the mitochondrial matrix induced by the reverse pumping of F1Fo-ATP synthase during reduced membrane potential conditions[62]. IF1 also controls the mitochondrial cristae morphogenesis and structure in a synergic to dynamin-related protein optic atrophy 1 (OPA1) up-regulated in this fraction as well[63]. OPA1 oligomers are necessaries for mitochondrial cristae formation and seem that IF1 through the regulation of OPA1 can preserve the mitochondrial structure during apoptosis[63].

The NADH dehydrogenase 1 alpha subcomplex subunit 9 and NADH dehydrogenase 1 alpha subcomplex subunit 5 were also found down-regulated while NADH dehydrogenase iron-sulfur protein 4 and NADH dehydrogenase 1 beta subcomplex subunit 11 are up-regulated in our data set. Complex I subunits were reported down-regulated in post-mortem brain tissues from different brain areas in schizophrenia patients[13,64,65] and it was demonstrated that antipsychotic treatment and early onset of illness have a strong correlation with Complex I decline[64]. On the other hand, the mRNA expression of certain Complex I and Complex III subunits was significantly higher in

blood samples of schizophrenia group, having a positive correlation with the first-episode schizophrenia subgroup[66]. It is still not fully elucidated the biological meaning about the discrepancy in the abundance of the different complex I subunits, nevertheless, impairments in mitochondrial metabolism have been associated with cognitive and behavioral abnormalities during the clinical course of schizophrenia[66].

Another set of important proteins that we detect in this fraction were those related to the glutamate metabolism such as glutaminase (GA) and glutamine synthetase (GS), increased in their abundance, and glutamate dehydrogenase (GLDH) and aspartate aminotransferase (ASAT) found as decreased (Figure 4). Almost all of them are located in the astrocytes, where the glutamate is taken up from the synaptic cleft and converted to glutamine by GS, or in α-ketoglutarate by GLDH or undergoes transamination by ASAT[67]. In this case, we can interpret from our data that glutamine production can be dysregulated in these patients. On the other hand, once the glutamine is produced in the astrocytes it is transported to the neurons where it is converted back into glutamate by the GA[68] so we can infer that maybe the amount of glutamate is higher than in the control group.

Over the years, the deregulation of glutamate has been formulated as one of the main hypotheses in the pathophysiology of schizophrenia in patients. High levels of glutamate plus glutamine have been reported in unmedicated patients when they are compared with healthy subjects[69]. The GA and GS transcripts have been reported as up-regulated in schizophrenia thalamus suggesting the enhanced glutamatergic neurotransmission[70]. Moreover, GS was found decreased in the prefrontal cortex and increased in the anterior cingulate and cerebellar cortex whereas no significant differences were observed in the posterior cingulate cortex[71]. Despite this, a study points out that there are no significant differences between the GS activity in the prefrontal cortex of schizophrenia patients and controls[72]. On the other hand, the level of platelet GLDH before antipsychotic treatment has been reported as significantly lower in schizophrenia patients[73] and significantly higher in post-mortem brain tissues from the pre-frontal cortex of chronic patients[72]. Nevertheless, in a study performed by Lander and colleges[74] the gene expression profile of Glud-1 was found down-regulated in the CA1 region of schizophrenia patients, proving that Glud-1 deficient mouse had an elevated excitatory/ inhibitory balance in CA1 region with similar behavioral abnormalities to the schizophrenia symptoms. It is important to highlight that enzymes as GLDH has been

previously reported in the rat cell nucleus[75] and also expressed in the nuclear membrane of human cortex in subpopulation of astrocytes and oligodendrocytes, but the exact function of nuclear GLDH remains unclear; it was suggested that maybe the nuclear α-ketoglutarate acts as co-factor of nuclear dioxygenases that participates in DNA and histone deacetylation[76].

3.3.2. Membrane proteins present in the crude nuclear fraction

The first cluster of proteins dysregulated that we would like to highlight are those related to glutamate pathways, such as excitatory amino acid transporter 1(EAAT1) and 2 (EAAT2), whose main function is the regulation of total glutamate uptake (Figure 4). EAAT1 and EAAT2 are mainly localized in the plasma membrane of astrocytes, but also in other cells as oligodendrocytes, microglia; and recently EAAT2 was also identified in neurons[77]. EAAT2 is the main transporter, responsible for about 90% of the glutamate clearance in the synaptic cleft[78].

It is widely reported the abnormal amount of transcript and protein level of EAATs in the different brain areas of schizophrenia patients. EAAT1 mutant mice exhibit a similar phenotype of schizophrenia symptoms[79] and it was shown that an acute glutamate exposure downregulates EAAT1 expression and plasma membrane availability[80]. Additionally, it was detected in the dorsolateral prefrontal cortex of schizophrenia patients a decrease in EAAT1 protein expression without any variation in the amount of EAAT2 transcript or protein level[81]. However, in another study the mRNA levels of EAAT2 in prefrontal cortex of medication-free patients was increased compared to controls[82]; in fact, data reveals that in the thalamus, the astrocytes have a decrease in the mRNA levels of EAAT1 whereas the in excitatory neurons had a compensatory increment in the EAAT2 mRNA expression suggesting an impairment in the clearance of glutamate capacity by astrocytes and decoupled glutamate metabolism in the tripartite synapse[83]. Finally, EAATs are associated with proteins as sodium/potassium-transporting ATPase ($Na^+/K^+$-ATPase) also up-regulated in schizophrenia patients (Figure 4). $Na^+/K^+$-ATPase produces an electrochemical gradient for glutamate uptake and through its interaction with EAAT2 modulates the localization, trafficking, and activity of these transporter complexes[84,85]. In ketamine rat models, $Na^+/K^+$-ATPase was increased in the prefrontal cortex, suggesting that it could have an important role in the physiopathology of glutamate neurotransmission system[86].

The second group of proteins that we would like to mention is involved in the complement system pathway and its relation to certain nuclear proteins quantified in the NUC fraction. First, we quantified as up-regulated the CD59 glycoprotein, an important cell membrane whose main function is the inhibition of C9 complement molecule in order to prevent the pore membrane attack complex (MAC)[87]. In Alzheimer disease was observed that CD59 activation is not efficient to suppress the complement pathway[88]. In parallel, we were able to detect the increase of several nuclear proteins related to NF-kB activation (Figure 5A), such as 1) RhoB[89] which can also have elevated the caspase 3 in the corticohippocampal neurons[90], 2) HMGB1, involved in the excitoneurotoxicity mediated by NF-kB[91] is released from neurons to astrocytes activating the nuclear factor-kB[92,93]; it is important to mention that HMGB1 activates the canonical NF-kB pathway via ERK-dependent mechanism[94], in this sense, we have detected by SRM the protein ERK-2 which is increased in NUC fraction, an indirect evidence of ERK activation[95], 3) Ubiquitin-conjugating enzyme E2N (UBE2N), involved in the lysine 63-linked polyubiquitin of NF-kB, an important mechanism for the signal transduction of this pathway[96,97,98]. Also, we found the nuclear Protein kinase beta involved in NF-kB regulation down-regulated[99,100].

A microarray profiled from the superior temporal gyrus of patients with schizophrenia suggest that NF-kB signaling is down-regulated in this brain area[101], but a recent study of Volk and colleagues[102] extensively map the expression of genes related to NF-kB signaling through the canonical and non-canonical pathways in the prefrontal cortex of schizophrenia patients, concluding that both pathways are increased and they are not affected by the antipsychotic treatment. Recently, it has been described an activation in astrocytes of the NF-kB signaling pathway, one of the main sources of NF-kB that promote the production of C3 which stimulates C3R neuronal receptors, generating a calcium imbalance and morphological change in dendrites[103].

Based on this information and the importance of the complement pathway in schizophrenia disease, we decided to implement a targeted approach to quantify the complement C3 and members of the NF-kB family using SRM (Table S-6). We observed that C3 is increased in schizophrenia patients compared to the control only in the NUC fraction, which probably suggests its location in the plasma membrane and the activation of complement pathway (Figures 5B and 5C). The NF-kB family members such as NF-kB1 and NF-kB2 were also increased in NUC fraction, suggesting an important role of

this pathway as a possible mechanism for C3 activation. Complement proteins are required for the central nervous system to carry out the elimination of inappropriate synapses[104]. The expression of C3 fragments on the cell surface also allows the recognition of this signal by microglia CR3 receptors promoting the engulfment of synaptic elements[105].This process could participate in the active elimination of long-term depression synapses when apoptotic mechanism as caspase-3 cascade is activated in dendrites without causing cell death[106,104].

Over the years the complement system has been indicated as an important element in the schizophrenia pathogenesis. Recently, one of the most extensive genetic studies links the human major histocompatibility complex as one of the most significant loci related to schizophrenia[9]. In 2016, Sekar and colleagues[107] have reported elevated expression of the C4A transcript in schizophrenia patients, reinforcing the theory that C4 leads the C3 activation and the synapsis elimination.

### 3.4. Cytoplasmatic fraction

In the CYT fraction, we quantified 216 dysregulated proteins (Table S-5). This fraction stands out because most of the proteins, that fulfilled our selection criteria, are not only down-regulated but counter-regulated in relation to the other fractions, that is, the same protein is mostly up-regulated in NUC or/and in MIT fraction. The biological functions associated with these proteins are the axon guidance process and eukaryotic translation elongation (Table S-7).

One of the main proteins involved in axon guidance, neuronal outgrowth, and synaptic plasticity is the neuromodulin (GAP-43), decreased in the schizophrenia cohort. GAP-43 down-regulation inhibits the initiation of axonal regrowth after axotomy[108]. In schizophrenia, subjects were observed a significant reduction of GAP-43 in the dentate gyrus[109]. Moreover, the astrocytic GAP43 knockdown induces the over-expression of EAAT2 what causes the excessive extracellular glutamate uptake activating the astrocyte-induced neurotoxicity and microglial activation[110].

In the same way, discs large homolog 1 (DLG1) is also decreased in CYT fraction. DLG1 is located in glia cells and neurons as part of the postsynaptic density-95/discs large/zone occludens-1 (PDZ)[111,112]. PDZ is responsible for membrane organization and stability. EAAT2 through the interaction with DLG1 maintains its expression on the cell surface[112]. In post-mortem brain tissue from PC, protein abundance of DLG1 was

reduced[113] also; a real-time RT-PCR revealed that DLG1mRNA levels are significantly decreased in patients with early-onset schizophrenia[114]. The dynamic in DLG1 regulation can impact the glutamatergic signaling through the interaction with EAAT2 isoforms[112]. Another protein from PDZ that it is also down-regulated in our data is the PSD-95. The reduction in its expression in the dorsolateral prefrontal cortex of schizophrenia patients is associated with abnormal traffic of AMPAR and an atypical localization of GluN2B NMDAR subunit[115]. It was suggested that PSD-95 decrease can compromise the synaptic spine cytoarchitecture and downstream signaling pathway of PSD-95[116].

Several proteins belonging to the ubiquitin-proteasome system (UPS) were found dysregulated. UPS is the main system for protein degradation but acts in receptors recycling, vesicle trafficking and vacuolar degradation[117]. The decrease of UPS system in the superior temporal gyrus and dentate granule neurons of individuals with schizophrenia results in impairment of AMPAR homeostasis, an abnormal structure in dendritic spine and accumulation of aberrant proteins in the ER[118,119]. An inefficient UPS can make the neurons more vulnerable to reactive oxygen species contributing to the mitochondrial impairments reported in schizophrenia[118].

The eukaryotic translation elongation pathway is another important cluster of proteins to mention. We found decreased principally the ribosomal proteins (RP), from the 60S and 40S ribosomal subunits (RS), responsible for catalyzing, during the protein synthesis process, the peptide bond formation and for binding, decoding and pairing the mRNAs codons and aminoacylated tRNAs respectively[120]. New protein synthesis is essential for structural remodeling and functional change behind the long-term potentiation and depression, to establish new synaptic connections and/or strength the pre-existing synaptic communication; the molecular basis for memory formation and maintenance[121]. An integrated study of proteomics and transcriptomic analysis using human olfactory neurosphere-derived from schizophrenia patient, detect a significant reduction in 17 ribosomal proteins with a lower global protein synthesis rates compared with control, also it was noticed a dysregulation in the upstream signaling pathways that control the protein synthesis such as the eIF2 and mTOR signaling[122].

Nevertheless, in this study, our dataset reveals something else about the eukaryotic translation elongation cluster. When we look the quantification in the other fractions, specifically in NUC fraction, two of that RP are up-regulated in NUC, together with the Elongation factor 2 (eEF2) and Elongation factor 1-alpha 2 (eEF1A2) whereas the

Elongation factor 1-alpha 1 (eEF1A1) remains down-regulated in this fraction. For years, it has been investigated the role of extraribosomal function of RS in different physiological and pathological processes, especially during ribosomal stress, development, immune response, and tumorigenesis[123]. The main function of the dysregulated RP with extraribosomal function are described in Table 1.

Among all quantified RP we can highlight S19 and L23. S19 inhibits the Macrophage migration inhibitory factor (MIF) and prevents its transcription and protein expression[124,125]. Interestingly, we found in CYT fraction a decrease abundancy of MIF. The overexpression of MIF protects against the apoptosis induced by oxidative stress and in vitro ischemia/reperfusion through the reduction of caspase 3 activation[126]. Indeed, in neutrophils, MIF prevents the apoptosis from delaying the cleavage of Bid, Bax and cytochrome c and Smac release from the mitochondria[127]. MIF-knockout is characterized by the increase in caspase 3 activity and down-regulation of MIF, under hypoxia condition, increment the neuronal loss through the NF-kB signaling[126].

On the other hand, L23 inhibits the transactivation of MIZ1, a protein responsible for the activation of genes that control cell arrest cycle in carcinoma cell lines[128,129]. Furthermore, in our NUC proteins set, we found to increase the Far upstream element-binding protein 1, a regulator that induces the overexpression of MYC[130,131], a key protein with opposite biological functions, depending on the cellular context, as cell proliferation, and apoptosis[132]. Specifically, in neurons, MYC overexpression promotes the activation of the cell cycle leading to neuronal cell death[133,134] and participates in the apoptotic response mediated by NF-kB signaling in response to neuronal excitotoxicity[135]. Among all its functions, MYC also regulates the expression of the target gene of L23[129] and it can inhibit MIZ1 as well as L23[136]. In myelodysplastic syndrome, the RPL23/Miz-1/c-Myc circuit provides a regulatory feedback to lead apoptotic resistance[137]; nevertheless, it was reported that in fibroblast models, MIZ1 inactivation is essential for MYC apoptotic function not for cell cycle progression and transformation[138]. However, in the context of nervous system cells (NSC), it has been described as different functions for MIZ1 such as the regulation of genes responsible for vesicular transport and autophagy[139]. Until the moment, the function of L23-MIZ1 in the cells of the nervous system has not been described, but it is possible that L23 could exert a regulation of the MIZ1 function on the transcription of this type of genes in the NSC. Although, despite the lack of evidence in this sense, it is curious that in our data, we observed the decreased of proteins such as

TBC1 domain family member 24 and VAMP-associated protein which have similar functions to those observed by Wolf and collaborators[139], but the biological functions of L23-MIZ1-Myc remains to be elucidated in schizophrenia physiopathology.

Finally, the different elongation factors that we quantify, eEF1A1 and eEF1A2, act as a proapoptotic and anti-apoptotic factor[140]. The overexpression of eEF1A confers significant resistance to apoptosis triggered by ER stress[141] and one of the main proposed mechanisms through which they exert the anti-apoptotic effect is through the regulation of the protein p53[142]; moreover, data indicate that eEF2 induces a decrease in protein translation as a protective mechanism against glutamate excitotoxicity[143].

## 4. CONCLUSION

OFC is a brain area that plays a key role in sensory integration and feedback processing. Changes in OFC volume gray matter is associated with the severity of negative as well as cognitive deficits in schizophrenia. In a previous study of this same brain area, we perform the proteomic characterization of the synaptosome fraction, finding as one of the main dysregulated routes the calcium signaling pathway together with proteins involved in ER stress and activation of the apoptosis process[16].

In accordance with our previous results, one of our first conclusions is that proteins related to calcium metabolism are important in the physiopathology of schizophrenia, at least in the OFC and other brain areas[144]. In the first place, contributing to the activation of an apoptotic process as we saw it reflected in the increase of pro-apoptotic proteins in MIT as VDAC1, MT-CO2, and ATP1-ATP synthase complex and for its participation in the cell signaling disruption of CREB activation, an important element in LTP maintenance reported in the NUC fraction. The decreased abundance of nuclear αCaMKII and in what seems to be the dysregulation of the nuclear shuttle of $Ca^{2+}$/CaM by γCaMKII when the cytoplasmatic βCaMKII is down-regulated[54] can be a mechanism for the imbalance in CREB activation and cognitive disability in schizophrenia patients.

Second, the dysregulation of glutamate metabolism apparently happens in the regulation of its synthesis and clearance from the synaptic cleft, simultaneously with impairment of the cytoplasmatic membrane traffic, which impact in EAATs regulation. Evidence indicates that glutamate dysregulation can lead to synaptic damage and neuron death, with a marker behavioral and cognitive dysfunction[145]. Also, glutamate can

activate NF-kB pathway[146]. One of the most important findings of this study is the overexpression of proteins intimately related to the activation of NF-kB. In NUC fraction, we found RhoB, HMGB1, Ubiquitin-conjugating enzyme E2N; in the same way, we also found in NUC and CYT fraction, proteins involved in the regulation of NF-kB signaling as Protein kinase beta and L23 respectively, as well as proteins that under influence of NF-kB pathway can induce neuronal loss, for instance, MIF down-regulation and Myc activation.

Finally, the abnormality in the cytoarchitecture of schizophrenia patients' brains has been widely reported and this evidence indicates that the loss of volume in the OFC is not a consequence of the antipsychotic drug treatment[147]. As we mentioned earlier, in astrocytes the NF-kB signaling pathway activation can promote the astrocytic production of C3, stimulating the C3R neuronal receptors which entail a calcium imbalance and changes in neural morphology[103]. Our data reveal the increase of the complement system C3 in the OFC. The expression of C3 can promote and excessive synaptic pruning by microglia engulfment constituting one of the possible main mechanisms of gray matter loss in schizophrenia patients. Based on our data analysis, we suggest the activation of NF-kB as a possible pathway that links the deregulation of glutamate, calcium, apoptosis and the activation of the immune system in schizophrenia patients.

Authors recognize that the protein-level FDR is an estimate based on several imperfect assumptions, and present the FDR with appropriate precision and acknowledge that not all proteins surviving the threshold are "confidently identified".

**ACNOWLEDGEMENTS**

DMS is supported by São Paulo Research Foundation (FAPESP), grants 2013/08711-3 and 2014/10068-4 and the Brazilian National Council for Scientific and Technological Development (CNPq) grant 460289/2014-4. EV thanks CNPq for her PhD scholarship; FCSN for grant E-26/202.650/2018 from the Rio de Janeiro State Foundation for Science Support (FAPERJ); and GBD for CNPq grant 306316/2015-3.

**REFERENCES**


(1) Patel, K. R.; Cherian, J.; Gohil, K.; Atkinson, D. Schizophrenia: Overview and Treatment Options. *P T* **2014**, *39* (9), 638–645.

(2) Stępnicki, P.; Kondej, M.; Kaczor, A. A. Current Concepts and Treatments of Schizophrenia. *Molecules* **2018**, *23* (8), 2087. https://doi.org/10.3390/molecules23082087.

(3) Möller, H.-J. The Relevance of Negative Symptoms in Schizophrenia and How to Treat Them with Psychopharmaceuticals? *Psychiatr. Danub.* **2016**, *28* (4), 435–440.

(4) Gao, W.-J.; Wang, H.-X.; A., M.; Li, Y.-C. The Unique Properties of the Prefrontal Cortex and Mental Illness. *When Things Go Wrong - Dis. Disord. Hum. Brain* **2012**. https://doi.org/10.5772/35868.

(5) Jackowski, A. P.; Araújo Filho, G. M. de; Almeida, A. G. De; Araújo, C. M. De; Reis, M.; Nery, F.; Batista, I. R.; Silva, I.; Lacerda, A. L. T. The Involvement of the Orbitofrontal Cortex in Psychiatric Disorders: An Update of Neuroimaging Findings. *Rev. Bras. Psiquiatr.* **2012**, *34* (2), 207–212. https://doi.org/10.1016/j.rbp.2012.11.003.

(6) Takayanagi, Y.; Takahashi, T.; Orikabe, L.; Masuda, N.; Mozue, Y.; Nakamura, K.; Kawasaki, Y.; Itokawa, M.; Sato, Y.; Yamasue, H.; et al. Volume Reduction and Altered Sulco-Gyral Pattern of the Orbitofrontal Cortex in First-Episode Schizophrenia. *Schizophr. Res.* **2010**, *121* (1–3), 55–65. https://doi.org/10.1016/j.schres.2010.05.006.

(7) Kanahara, N.; Sekine, Y.; Haraguchi, T.; Uchida, Y.; Hashimoto, K.; Shimizu, E.; Iyo, M. Orbitofrontal Cortex Abnormality and Deficit Schizophrenia. *Schizophr. Res.* **2013**, *143* (2–3), 246–252. https://doi.org/10.1016/j.schres.2012.11.015.

(8) Ohtani, T.; Bouix, S.; Hosokawa, T.; Saito, Y.; Eckbo, R.; Ballinger, T.; Rausch, A.; Melonakos, E.; Kubicki, M. Abnormalities in White Matter Connections between Orbitofrontal Cortex and Anterior Cingulate Cortex and Their Associations with Negative Symptoms in Schizophrenia: A DTI Study. *Schizophr. Res.* **2014**, *157* (1–3), 190–197. https://doi.org/10.1016/j.schres.2014.05.016.

(9) Ripke, S.; Neale, B. M.; Corvin, A.; Walters, J. T. R.; Farh, K.-H.; Holmans, P. A.; Lee, P.; Bulik-Sullivan, B.; Collier, D. A.; Huang, H.; et al. Biological Insights from 108 Schizophrenia-Associated Genetic Loci. *Nature* **2014**, *511* (7510), 421–427. https://doi.org/10.1038/nature13595.

(10) Enwright, J. F.; Huo, Z.; Arion, D.; Corradi, J. P.; Tseng, G.; Lewis, D. A. Transcriptome Alterations of Prefrontal Cortical Parvalbumin Neurons in Schizophrenia. *Mol. Psychiatry* **2018**, *23* (7), 1606–1613. https://doi.org/10.1038/mp.2017.216.

(11) Arion, D.; Huo, Z.; Enwright, J. F.; Corradi, J. P.; Tseng, G.; Lewis, D. A. Transcriptome Alterations in Prefrontal Pyramidal Cells Distinguish Schizophrenia From Bipolar and Major Depressive Disorders. *Biol. Psychiatry* **2017**, *82* (8), 594–600. https://doi.org/10.1016/j.biopsych.2017.03.018.

(12) Sanders, A. R.; Drigalenko, E. I.; Duan, J.; Moy, W.; Freda, J.; Göring, H. H. H.; Gejman, P. V.; Levinson, D. F.; Shi, J.; Buccola, N. G.; et al. Transcriptome Sequencing Study Implicates Immune-Related Genes Differentially Expressed in Schizophrenia: New Data and a Meta-Analysis. *Transl. Psychiatry* **2017**, *7* (4), 1–10. https://doi.org/10.1038/tp.2017.47.

(13) Nascimento, J. M.; Martins-de-Souza, D. The Proteome of Schizophrenia. *npj Schizophr.* **2015**, *1* (1), 14003. https://doi.org/10.1038/npjschz.2014.3.

(14) Shan, D.; Mount, D.; Moore, S.; Haroutunian, V.; Meador-Woodruff, J. H.; McCullumsmith, R. E.

Abnormal Partitioning of Hexokinase 1 Suggests Disruption of a Glutamate Transport Protein Complex in Schizophrenia. *Schizophr. Res.* **2014**, *154* (1–3), 1–13. https://doi.org/10.1016/j.schres.2014.01.028.

(15) Saia-Cereda, V. M.; Santana, A. G.; Schmitt, A.; Falkai, P.; Martins-de-Souza, D. The Nuclear Proteome of White and Gray Matter from Schizophrenia Postmortem Brains. *Mol. Neuropsychiatry* **2017**, *3* (1), 37–52. https://doi.org/10.1159/000477299.

(16) Velásquez, E.; Nogueira, F. C. S.; Velásquez, I.; Schmitt, A.; Falkai, P.; Domont, G. B.; Martins-De-Souza, D. Synaptosomal Proteome of the Orbitofrontal Cortex from Schizophrenia Patients Using Quantitative Label-Free and ITRAQ-Based Shotgun Proteomics. *J. Proteome Res.* **2017**, *16* (12), 4481–4494. https://doi.org/10.1021/acs.jproteome.7b00422.

(17) Itzhak, D. N.; Tyanova, S.; Cox, J.; Borner, G. H. H. Global, Quantitative and Dynamic Mapping of Protein Subcellular Localization. *Elife* **2016**, *5* (JUN2016), 1–36. https://doi.org/10.7554/eLife.16950.

(18) Eroglu S., Toprak S., Urgan O, MD, Ozge E. Onur, MD, Arzu Denizbasi, MD, Haldun Akoglu, MD, Cigdem Ozpolat, MD, Ebru Akoglu, M. *DSM-IV Diagnostic and Statistical Manual of Mental Disorder*; 1994; Vol. 33. https://doi.org/10.1073/pnas.0703993104.

(19) Larsen, M. R.; Thingholm, T. E.; Jensen, O. N.; Roepstorff, P.; Jørgensen, T. J. D. Highly Selective Enrichment of Phosphorylated Peptides from Peptide Mixtures Using Titanium Dioxide Microcolumns *. **2005**, 873–886. https://doi.org/10.1074/mcp.T500007-MCP200.

(20) Polpitiya, A. D.; Qian, W. J.; Jaitly, N.; Petyuk, V. A.; Adkins, J. N.; Camp, D. G.; Anderson, G. A.; Smith, R. D. DAnTE: A Statistical Tool for Quantitative Analysis of -Omics Data. *Bioinformatics* **2008**, *24* (13), 1556–1558. https://doi.org/10.1093/bioinformatics/btn217.

(21) Bateman, A.; Martin, M. J.; O'Donovan, C.; Magrane, M.; Alpi, E.; Antunes, R.; Bely, B.; Bingley, M.; Bonilla, C.; Britto, R.; et al. UniProt: The Universal Protein Knowledgebase. *Nucleic Acids Res.* **2017**, *45* (D1), D158–D169. https://doi.org/10.1093/nar/gkw1099.

(22) Oliveros, J. C. NoVENNY. An interactive tool for comparing lists with Venn Diagrams Title http://bioinfogp.cnb.csic.es/tools/venny/index.html.

(23) Fabregat, A.; Sidiropoulos, K.; Garapati, P.; Gillespie, M.; Hausmann, K.; Haw, R.; Jassal, B.; Jupe, S.; Korninger, F.; McKay, S.; et al. The Reactome Pathway Knowledgebase. *Nucleic Acids Res.* **2016**, *44* (D1), D481–D487. https://doi.org/10.1093/nar/gkv1351.

(24) Szklarczyk, D.; Franceschini, A.; Wyder, S.; Forslund, K.; Heller, D.; Huerta-Cepas, J.; Simonovic, M.; Roth, A.; Santos, A.; Tsafou, K. P.; et al. STRING V10: Protein-Protein Interaction Networks, Integrated over the Tree of Life. *Nucleic Acids Res.* **2015**, *43* (D1), D447–D452. https://doi.org/10.1093/nar/gku1003.

(25) Ogata, H.; Goto, S.; Sato, K.; Fujibuchi, W.; Bono, H.; Kanehisa, M. KEGG: Kyoto Encyclopedia of Genes and Genomes. *Nucleic Acids Res.* **1999**, *27* (1), 29–34. https://doi.org/10.1093/nar/27.1.29.

(26) Iwamoto, K.; Bundo, M.; Kato, T. Altered Expression of Mitochondria-Related Genes in Postmortem Brains of Patients with Bipolar Disorder or Schizophrenia, as Revealed by Large-Scale DNA Microarray Analysis. *Hum. Mol. Genet.* **2005**, *14* (2), 241–253. https://doi.org/10.1093/hmg/ddi022.

(27) English, J. A.; Pennington, K.; Dunn, M. J.; Cotter, D. R. The Neuroproteomics of Schizophrenia. *Biol. Psychiatry* **2011**, *69* (2), 163–172. https://doi.org/10.1016/j.biopsych.2010.06.031.

(28) Robicsek, O.; Ene, H. M.; Karry, R.; Ytzhaki, O.; Asor, E.; McPhie, D.; Cohen, B. M.; Ben-Yehuda, R.; Weiner, I.; Ben-Shachar, D. Isolated Mitochondria Transfer Improves Neuronal Differentiation of

Schizophrenia-Derived Induced Pluripotent Stem Cells and Rescues Deficits in a Rat Model of the Disorder. *Schizophr. Bull.* **2018**, *44* (2), 432–442. https://doi.org/10.1093/schbul/sbx077.

(29) Roberts, R. C. Postmortem Studies on Mitochondria in Schizophrenia. *Schizophr. Res.* **2017**, *187*, 17–25. https://doi.org/10.1016/j.schres.2017.01.056.

(30) Rice, M. W.; Smith, K. L.; Roberts, R. C.; Perez-Costas, E.; Melendez-Ferro, M. Assessment of Cytochrome C Oxidase Dysfunction in the Substantia Nigra/Ventral Tegmental Area in Schizophrenia. *PLoS One* **2014**, *9* (6). https://doi.org/10.1371/journal.pone.0100054.

(31) Brittain, J. M.; Wang, Y.; Wilson, S. M.; Khanna, R. Regulation of CREB Signaling through L-Type Ca 2+ Channels by Nipsnap-2. *Channels* **2012**, *6* (2). https://doi.org/10.4161/chan.19415.

(32) Princely Abudu, Y.; Pankiv, S.; Mathai, B. J.; Håkon Lystad, A.; Bindesbøll, C.; Brenne, H. B.; Yoke Wui Ng, M.; Thiede, B.; Yamamoto, A.; Mutugi Nthiga, T.; et al. NIPSNAP1 and NIPSNAP2 Act as "Eat Me" Signals for Mitophagy. *Dev. Cell* **2019**, *49* (4), 509-525.e12. https://doi.org/10.1016/j.devcel.2019.03.013.

(33) Pinton, P.; Rizzuto, R. Bcl-2 and Ca2+ Homeostasis in the Endoplasmic Reticulum. *Cell Death Differ.* **2006**, *13* (8), 1409–1418. https://doi.org/10.1038/sj.cdd.4401960.

(34) Singh, S.; Khar, A. Differential Gene Expression during Apoptosis Induced by a Serum Factor: Role of Mitochondrial F0-F1 ATP Synthase Complex. *Apoptosis* **2005**, *10* (6), 1469–1482. https://doi.org/10.1007/s10495-005-1394-1.

(35) Dibrova, D. V.; Cherepanov, D. A.; Galperin, M. Y.; Skulachev, V. P.; Mulkidjanian, A. Y. Evolution of Cytochrome Bc Complexes: From Membrane-Anchored Dehydrogenases of Ancient Bacteria to Triggers of Apoptosis in Vertebrates. *Biochim. Biophys. Acta - Bioenerg.* **2013**, *1827* (11–12), 1407–1427. https://doi.org/10.1016/j.bbabio.2013.07.006.

(36) Herberth, M.; Koethe, D.; Cheng, T. M. K.; Krzyszton, N. D.; Schoeffmann, S.; Guest, P. C.; Rahmoune, H.; Harris, L. W.; Kranaster, L.; Leweke, F. M.; et al. Impaired Glycolytic Response in Peripheral Blood Mononuclear Cells of First-Onset Antipsychotic-Naive Schizophrenia Patients. *Mol. Psychiatry* **2011**, *16* (8), 848–859. https://doi.org/10.1038/mp.2010.71.

(37) Shoshan-Barmatz, V.; N. Maldonado, E.; Krelin, Y. VDAC1 at the Crossroads of Cell Metabolism, Apoptosis and Cell Stress. *Cell Stress* **2017**, *1* (1), 11–36. https://doi.org/10.15698/cst2017.10.104.

(38) Tarze, A.; Deniaud, A.; Le Bras, M.; Maillier, E.; Molle, D.; Larochette, N.; Zamzami, N.; Jan, G.; Kroemer, G.; Brenner, C. GAPDH, a Novel Regulator of the pro-Apoptotic Mitochondrial Membrane Permeabilization. *Oncogene* **2007**, *26* (18), 2606–2620. https://doi.org/10.1038/sj.onc.1210074.

(39) Krols, M.; Bultynck, G.; Janssens, S. ER-Mitochondria Contact Sites: A New Regulator of Cellular Calcium Flux Comes into Play. *J. Cell Biol.* **2016**, *214* (4), 367–370. https://doi.org/10.1083/jcb.201607124.

(40) Renée Guérin, Geneviève Arseneault, Stéphane Dumont, and L. A. R. Calnexin Is Involved in Apoptosis Induced by Endoplasmic Reticulum Stress in the Fission Yeast. *Mol. Biol. Cell Vol. 19*, 4404–4420. https://doi.org/doi: 10.1091/mbc.E08-02-0188.

(41) Zhang, H.; Kim, J. K.; Edwards, C. A.; Xu, Z.; Taichman, R.; Wang, C. Y. Clusterin Inhibits Apoptosis by Interacting with Activated Bax. *Nat. Cell Biol.* **2005**, *7* (9), 909–915. https://doi.org/10.1038/ncb1291.

(42) Frezza, C.; Cipolat, S.; Martins de Brito, O.; Micaroni, M.; Beznoussenko, G. V.; Rudka, T.; Bartoli, D.; Polishuck, R. S.; Danial, N. N.; De Strooper, B.; et al. OPA1 Controls Apoptotic Cristae Remodeling

Independently from Mitochondrial Fusion. *Cell* **2006**, *126* (1), 177–189. https://doi.org/10.1016/j.cell.2006.06.025.

(43) Darshi, M.; Mendiola, V. L.; Mackey, M. R.; Murphy, A. N.; Koller, A.; Perkins, G. A.; Ellisman, M. H.; Taylor, S. S. ChChd3, an Inner Mitochondrial Membrane Protein, Is Essential for Maintaining Crista Integrity and Mitochondrial Function. *J. Biol. Chem.* **2011**, *286* (4), 2918–2932. https://doi.org/10.1074/jbc.M110.171975.

(44) An, J.; Shi, J.; He, Q.; Lui, K.; Liu, Y.; Huang, Y.; Sheikh, M. S. CHCM1/CHCHD6, Novel Mitochondrial Protein Linked to Regulation of Mitofilin and Mitochondrial Cristae Morphology. *J. Biol. Chem.* **2012**, *287* (10), 7411–7426. https://doi.org/10.1074/jbc.M111.277103.

(45) Friedman, J. R.; Mourier, A.; Yamada, J.; Michael McCaffery, J.; Nunnari, J. MICOS Coordinates with Respiratory Complexes and Lipids to Establish Mitochondrial Inner Membrane Architecture. *Elife* **2015**, *2015* (4), 1–61. https://doi.org/10.7554/eLife.07739.

(46) Li, B.; Tsien, R. W.; Ma, H. Distinct Roles of Multiple Isoforms of CaMKII in Signaling to the Nucleus. *Biochim. Biophys. Acta* **2016**, *1853* (9), 1953–1957. https://doi.org/10.1016/j.bbamcr.2015.02.008.Distinct.

(47) Yamasaki, N.; Maekawa, M.; Kobayashi, K.; Kajii, Y.; Maeda, J.; Soma, M.; Takao, K.; Tanda, K.; Ohira, K.; Toyama, K.; et al. Alpha-CaMKII Deficiency Causes Immature Dentate Gyrus, a Novel Candidate Endophenotype of Psychiatric Disorders. *Mol. Brain* **2008**, *1*, 6. https://doi.org/10.1186/1756-6606-1-6.

(48) Novak, G.; Seeman, P. Hyperactive Mice Show Elevated D2High Receptors, A Model for Schizophrenia: Calcium/Calmodulin-Dependent Kinase II Alpha Knockouts. *Synapse* **2010**, *64* (10), 794–800. https://doi.org/10.1002/syn.20786.

(49) Ogundele, O. M.; Lee, C. C. CaMKIIα Expression in a Mouse Model of NMDAR Hypofunction Schizophrenia: Putative Roles for IGF-1R and TLR4. *Brain Res. Bull.* **2018**, *137* (November 2017), 53–70. https://doi.org/10.1016/j.brainresbull.2017.11.007.

(50) Mermelstein, P. G.; Deisseroth, K.; Dasgupta, N.; Isaksen, A. L.; Tsien, R. W. Calmodulin Priming: Nuclear Translocation of a Calmodulin Complex and the Memory of Prior Neuronal Activity. *Proc. Natl. Acad. Sci.* **2001**, *98* (26), 15342–15347. https://doi.org/10.1073/pnas.211563998.

(51) Samuel M. Cohen, Boxing Li, Richard W. Tsien, and H. M. Evolutionary and Functional Perspectives on Signaling from Neuronal Surface to Nucleus. *Biochem Biophys Res Commun 460(1)*, 88–99. https://doi.org/doi: 10.1016/j.bbrc.2015.02.146.

(52) Limback-Stokin, K. Nuclear Calcium/Calmodulin Regulates Memory Consolidation. *J. Neurosci.* **2004**, *24* (48), 10858–10867. https://doi.org/10.1523/JNEUROSCI.1022-04.2004.

(53) Coyle, J. T. MicroRNAs Suggest a New Mechanism for Altered Brain Gene Expression in Schizophrenia. *PNAS* **2009**, *106* (9), 2975–2976. https://doi.org/10.1073/pnas.0813321106.

(54) Ma, H.; Groth, R. D.; Cohen, S. M.; Emery, J. F.; Li, B.; Hoedt, E.; Zhang, G.; Neubert, T. A.; Tsien, R. W. ΓcaMKII Shuttles Ca 2+ /CaM to the Nucleus to Trigger CREB Phosphorylation and Gene Expression. *Cell* **2014**, *159* (2), 281–294. https://doi.org/10.1016/j.cell.2014.09.019.

(55) Cohen, S. M.; Suutari, B.; He, X.; Wang, Y.; Sanchez, S.; Tirko, N. N.; Mandelberg, N. J.; Mullins, C.; Zhou, G.; Wang, S.; et al. Calmodulin Shuttling Mediates Cytonuclear Signaling to Trigger Experience-Dependent Transcription and Memory. *Nat. Commun.* **2018**, *9* (1), 1–12. https://doi.org/10.1038/s41467-018-04705-8.

(56) Graham, J. M. Preparation of Crude Subcellular Fractions by Differential Centrifugation. *ScientificWorldJournal.* **2002**, *2*, 1638–1642. https://doi.org/10.1100/tsw.2002.851.

(57) Collins, T. J. Mitochondria Are Morphologically Heterogeneous within Cells. *J. Exp. Biol.* **2003**, *206* (12), 1993–2000. https://doi.org/10.1242/jeb.00244.

(58) Kuznetsov, A. V.; Troppmair, J.; Sucher, R.; Hermann, M.; Saks, V.; Margreiter, R. Mitochondrial Subpopulations and Heterogeneity Revealed by Confocal Imaging: Possible Physiological Role? *Biochim. Biophys. Acta - Bioenerg.* **2006**, *1757* (5–6), 686–691. https://doi.org/10.1016/j.bbabio.2006.03.014.

(59) Brown, M. R.; Sullivan, P. G.; Geddes, J. W. Synaptic Mitochondria Are More Susceptible to Ca2+ Overload than Nonsynaptic Mitochondria. *J. Biol. Chem.* **2006**, *281* (17), 11658–11668. https://doi.org/10.1074/jbc.M510303200.

(60) Kuznetsov, A. V.; Margreiter, R. Heterogeneity of Mitochondria and Mitochondrial Function within Cells as Another Level of Mitochondrial Complexity. *Int. J. Mol. Sci.* **2009**, *10* (4), 1911–1929. https://doi.org/10.3390/ijms10041911.

(61) Woods, D. C. Review Article Mitochondrial Heterogeneity : Evaluating Mitochondrial Subpopulation Dynamics in Stem Cells. **2017**, *2017*. https://doi.org/10.1155/2017/7068567.

(62) Campanella, M.; Parker, N.; Tan, C. H.; Hall, A. M.; Duchen, M. R. IF1: Setting the Pace of the F1Fo-ATP Synthase. *Trends Biochem. Sci.* **2009**, *34* (7), 343–350. https://doi.org/10.1016/j.tibs.2009.03.006.

(63) Faccenda, D.; Nakamura, J.; Gorini, G.; Dhoot, G. K.; Piacentini, M.; Yoshida, M.; Campanella, M. Control of Mitochondrial Remodeling by the ATPase Inhibitory Factor 1 Unveils a Pro-Survival Relay via OPA1. *Cell Rep.* **2017**, *18* (8), 1869–1883. https://doi.org/10.1016/j.celrep.2017.01.070.

(64) Rollins, B. L.; Morgan, L.; Hjelm, B. E.; Sequeira, A.; Schatzberg, A. F.; Barchas, J. D.; Lee, F. S.; Myers, R. M.; Watson, S. J.; Akil, H.; et al. Mitochondrial Complex I Deficiency in Schizophrenia and Bipolar Disorder and Medication Influence. *Mol. Neuropsychiatry* **2017**, *3* (3), 157–169. https://doi.org/10.1159/000484348.

(65) Holper, L.; Ben-Shachar, D.; Mann, J. Multivariate Meta-Analyses of Mitochondrial Complex I and IV in Major Depressive Disorder, Bipolar Disorder, Schizophrenia, Alzheimer Disease, and Parkinson Disease. *Neuropsychopharmacology* **2019**, *44* (5), 837–849. https://doi.org/10.1038/s41386-018-0090-0.

(66) Akarsu, S.; Torun, D.; Bolu, A.; Erdem, M.; Kozan, S.; Ak, M.; Akar, H.; Uzun, Ö. Mitochondrial Complex I and III Gene MRNA Levels in Schizophrenia, and Their Relationship with Clinical Features. *J. Mol. psychiatry* **2014**, *2* (1), 6. https://doi.org/10.1186/s40303-014-0006-9.

(67) Farinelli, S. E.; Nicklas, W. J. Glutamate Metabolism in Rat Cortical Astrocyte Cultures. *J. Neurochem.* **1992**, *58* (5), 1905–1915. https://doi.org/10.1111/j.1471-4159.1992.tb10068.x.

(68) Hassel, B.; Bachelard, H. Trafficking of Amino Acids Between Neurons and Glia I n Vivo . Effects of Inhibition of Glial Metabolism by Fluoroacetate Journal of Cerebral Blood Flow & Metabolism - Trafficking of Arnino Acids Between ... Page 2 of 6. **2007**, No. 1997, 1230–1238.

(69) Poels, E. M. P.; Kegeles, L. S.; Kantrowitz, J. T.; Slifstein, M.; Javitt, D. C.; Lieberman, J. A.; Abi-Dargham, A.; Girgis, R. R. Imaging Glutamate in Schizophrenia: Review of Findings and Implications for Drug Discovery. *Mol. Psychiatry* **2014**, *19* (1), 20–29. https://doi.org/10.1038/mp.2013.136.

(70) Bruneau, E. G.; McCullumsmith, R. E.; Haroutunian, V.; Davis, K. L.; Meador-Woodruff, J. H. Increased Expression of Glutaminase and Glutamine Synthetase MRNA in the Thalamus in Schizophrenia.

*Schizophr. Res.* **2005**, *75* (1), 27–34. https://doi.org/10.1016/j.schres.2004.12.012.

(71) Boksha, I. S.; Tereshkina, E. B.; Savushkina, O. K.; Prokhorova, T. A.; Vorobyeva, E. A.; Burbaeva, G. S. Comparative Studies of Glutamine Synthetase Levels in the Brains of Patients with Schizophrenia and Mentally Healthy People. *Neurochem. J.* **2018**, *12* (1), 95–101. https://doi.org/10.1134/s1819712418010026.

(72) Burbaeva, G. S.; Boksha, I. S.; Turishcheva, M. S.; Vorobyeva, E. A.; Savushkina, O. K.; Tereshkina, E. B. Glutamine Synthetase and Glutamate Dehydrogenase in the Prefrontal Cortex of Patients with Schizophrenia. *Prog. Neuro-Psychopharmacology Biol. Psychiatry* **2003**, *27* (4), 675–680. https://doi.org/10.1016/S0278-5846(03)00078-2.

(73) Prokhorova, T. A.; Boksha, I. S.; Savushkina, O. K.; Tereshkina, E. B.; Vorobyeva, E. A.; Pomytkin, A. N.; Kaleda, V. G.; Burbaeva, G. S. Glutamate Dehydrogenase Activity in Platelets of Patients with Endogenous Psychosis. *Zhurnal Nevrol. i psikhiatrii im. S.S. Korsakova* **2016**, *116* (3), 44. https://doi.org/10.17116/jnevro20161163144-48.

(74) Lander, S. S.; Khan, U.; Lewandowski, N.; Chakraborty, D.; Provenzano, F. A.; Mingote, S.; Chornyy, S.; Frigerio, F.; Maechler, P.; Kaphzan, H.; et al. Glutamate Dehydrogenase-Deficient Mice Display Schizophrenia-Like Behavioral Abnormalities and CA1-Specific Hippocampal Dysfunction. *Schizophr. Bull.* **2019**, *45* (1), 127–137. https://doi.org/10.1093/schbul/sby011.

(75) di Prisco, G.; Banay-Schwartz, M.; Strecker, H. J. Glutamate Dehydrogenase in Nuclear and Mitochondrial Fractions of Rat Liver. *Biochem. Biophys. Res. Commun.* **1968**, *33* (4), 606–612. https://doi.org/10.1016/0006-291X(68)90339-2.

(76) Spanaki, C.; Kotzamani, D.; Plaitakis, A. Widening Spectrum of Cellular and Subcellular Expression of Human GLUD1 and GLUD2 Glutamate Dehydrogenases Suggests Novel Functions. *Neurochem. Res.* **2017**, *42* (1), 92–107. https://doi.org/10.1007/s11064-016-1986-x.

(77) Desilva, T. M.; Borenstein, N. S.; Volpe, J. J.; Kinney, H. C.; Rosenberg, P. A. Expression of EAAT2 in Neurons and Protoplasmic Astrocytes during Human Cortical Development. *J. Comp. Neurol.* **2012**, *520* (17), 3912–3932. https://doi.org/10.1002/cne.23130.

(78) Parkin, G. M.; Udawela, M.; Gibbons, A.; Dean, B. Glutamate Transporters, EAAT1 and EAAT2, Are Potentially Important in the Pathophysiology and Treatment of Schizophrenia and Affective Disorders. *World J. Psychiatry* **2018**, *8* (2), 51–63. https://doi.org/10.5498/wjp.v8.i2.51.

(79) Rose-Marie Karlsson1, 2; , Kohichi Tanaka3, Lisa M Saksida4, 5, Timothy J Bussey4, 5, M.; Heilig1, 2, and A. H. Assessment of Glutamate Transporter GLAST (EAAT1)-Deficient Mice for Phenotypes Relevant to the Negative and Executive/ Cognitive Symptoms of Schizophrenia. *Neuropsychopharmacology* **2009**, *34(6)*, 1578–1589. https://doi.org/doi:10.1038/npp.2008.215.

(80) Martínez, D.; García, L.; Aguilera, J.; Ortega, A. An Acute Glutamate Exposure Induces Long-Term down Regulation of GLAST/EAAT1 Uptake Activity in Cultured Bergmann Glia Cells. *Neurochem. Res.* **2014**, *39* (1), 142–149. https://doi.org/10.1007/s11064-013-1198-6.

(81) Deborah Bauer, Daya Gupta, Vahram Harotunian, J. H. M.-W. and; McCullumsmith, R. E. Abnormal Expression of Glutamate Transporter and Transporter Interacting Molecules in Prefrontal Cortex in Elderly Patients with Schizophrenia. *Schizophr Res* **2008**, *104(1-3)*, 108–120. https://doi.org/doi:10.1016/j.schres.2008.06.012.

(82) Matute, C.; Melone, M.; Vallejo-Illarramendi, A.; Conti, F. Increased Expression of the Astrocytic Glutamate Transporter GLT-1 in the Prefrontal Cortex of Schizophrenics. *Glia* **2005**, *49* (3), 451–455. https://doi.org/10.1002/glia.20119.

(83) McCullumsmith, R. E.; O'Donovan, S. M.; Drummond, J. B.; Benesh, F. S.; Simmons, M.; Roberts, R.; Lauriat, T.; Haroutunian, V.; Meador-Woodruff, J. H. Cell-Specific Abnormalities of Glutamate Transporters in Schizophrenia: Sick Astrocytes and Compensating Relay Neurons? *Mol. Psychiatry* **2016**, *21* (6), 823–830. https://doi.org/10.1038/mp.2015.148.

(84) Rose, E. M.; Koo, J. C. P.; Antflick, J. E.; Ahmed, S. M.; Angers, S.; Hampson, D. R. Glutamate Transporter Coupling to Na,K-ATPase. *J. Neurosci.* **2009**, *29* (25), 8143–8155. https://doi.org/10.1523/JNEUROSCI.1081-09.2009.

(85) O'Donovan, S. M.; Sullivan, C. R.; McCullumsmith, R. E. The Role of Glutamate Transporters in the Pathophysiology of Neuropsychiatric Disorders. *npj Schizophr.* **2017**, *3* (1). https://doi.org/10.1038/s41537-017-0037-1.

(86) Rd, D. L.; Db, F.; Fv, G.; Kolling, J.; Agk, F.; Luca, R. D. De; Fraga, D. D. B.; Ghedim, V.; Ferreira, A. G. K.; Aline, A.; et al. Na + , K + -ATPase Activity Is Increased in Rats Subjected to Chronic Administration of Ketamine. **2011**, No. c, 215–218. https://doi.org/10.1111/j.1601-5215.2011.00596.x.

(87) Farkas, I.; Baranyi, L.; Ishikawa, Y.; Okada, N.; Bohata, C.; Budai, D.; Fukuda, A.; Imai, M.; Okada, H. CD59 Blocks Not Only the Insertion of C9 into MAC but Inhibits Ion Channel Formation by Homologous C5b-8 as Well as C5b-9. *J. Physiol.* **2002**, *539* (2), 537–545. https://doi.org/10.1113/jphysiol.2001.013381.

(88) Yasojima, K.; McGeer, E. G.; McGeer, P. L. Complement Regulators C1 Inhibitor and CD59 Do Not Significantly Inhibit Complement Activation in Alzheimer Disease. *Brain Res.* **1999**, *833* (2), 297–301. https://doi.org/10.1016/S0006-8993(99)01514-0.

(89) Rodriguez, P. L.; Sahay, S.; Olabisi, O. O.; Whitehead, I. P. ROCK I-Mediated Activation of NF-KB by RhoB. *Cell. Signal.* **2007**, *19* (11), 2361–2369. https://doi.org/10.1016/j.cellsig.2007.07.021.

(90) Barberan, S.; , Kara McNair, Khalil Iqbal, Nicola C. Smith, G. C. P.; Trevor W. Stone, Stuart R. Cobb, and B. J. M. Altered Apoptotic Responses in Neurons Lacking RhoB GTPase. *Eur J Neurosci.* **2011**, *34(11)*, 1737–1746. https://doi.org/doi:10.1111/j.1460-9568.2011.07891.x.

(91) Sakamoto, K.; Okuwaki, T.; Ushikubo, H.; Mori, A.; Nakahara, T.; Ishii, K. Activation Inhibitors of Nuclear Factor Kappa B Protect Neurons against the NMDA-Induced Damage in the Rat Retina. *J. Pharmacol. Sci.* **2017**, *135* (2), 72–80. https://doi.org/10.1016/j.jphs.2017.09.031.

(92) Hulya Karatas, Sefik Evren Erdener, Yasemin Gursoy-Ozdemir, Sevda Lule, Emine Eren-Koçak, Zümrüt Duygu Sen, T. D. Spreading Depression Triggers Headache by Activating Neuronal Panx1 Channels. *Science (80-. ).* **2013**, *339* (6123), 1092–1095. https://doi.org/10.1126/science.1231897.

(93) Shi, Y.; Zhang, L.; Teng, J.; Miao, W. HMGB1 Mediates Microglia Activation via the TLR4 / NF- κ B Pathway in Coriaria Lactone Induced Epilepsy. **2018**, 5125–5131. https://doi.org/10.3892/mmr.2018.8485.

(94) Palumbo, R.; Galvez, B. G.; Pusterla, T.; De Marchis, F.; Cossu, G.; Marcu, K. B.; Bianchi, M. E. Cells Migrating to Sites of Tissue Damage in Response to the Danger Signal HMGB1 Require NF-KB Activation. *J. Cell Biol.* **2007**, *179* (1), 33–40. https://doi.org/10.1083/jcb.200704015.

(95) Chen, B.; Liu, J.; Ho, T.-T.; Ding, X.; Mo, Y.-Y. ERK-Mediated NF-KB Activation through ASIC1 in Response to Acidosis. *Oncogenesis* **2016**, *5* (12), e279–e279. https://doi.org/10.1038/oncsis.2016.81.

(96) Chen, Z. J.; Fuchs, S. Y. Ubiquitin-Dependent Activation of NF-KappaB: K63-Linked Ubiquitin Chains: A Link to Cancer? *Cancer Biol. Ther.* **2004**, *3* (3), 286–288. https://doi.org/10.4161/cbt.3.3.798.

(97) Chen, J. C. and Z. J. Regulation of NF- κ B by Ubiquitination. *Curr Opin Immunol.* **2014**, *25* (1), 4–12. https://doi.org/10.1016/j.coi.2012.12.005.Regulation.

(98) Chen, J.; Hao, L.; Li, C.; Ye, B.; Du, Y.; Zhang, H.; Long, B.; Zhu, P.; Liu, B.; Yang, L.; et al. The Endoplasmic Reticulum Adaptor Protein ERAdP Initiates NK Cell Activation via the Ubc13-Mediated NF-KB Pathway. *J. Immunol.* **2015**, *194* (3), 1292–1303. https://doi.org/10.4049/jimmunol.1402593.

(99) Saijo, K.; Mecklenbräuker, I.; Santana, A.; Leitger, M.; Schmedt, C.; Tarakhovsky, A. Protein Kinase C β Controls Nuclear Factor KB Activation in B Cells Through Selective Regulation of the IκB Kinase α. *J. Exp. Med.* **2002**, *195* (12), 1647–1652. https://doi.org/10.1084/jem.20020408.

(100) Kim, S. W.; Schifano, M.; Oleksyn, D.; Jordan, C. T.; Ryan, D.; Insel, R.; Zhao, J.; Chen, L. Protein Kinase C-Associated Kinase Regulates NF-KB Activation through Inducing IKK Activation. *Int. J. Oncol.* **2014**, *45* (4), 1707–1714. https://doi.org/10.3892/ijo.2014.2578.

(101) Roussos, P.; Katsel, P.; Davis, K. L.; Giakoumaki, S. G.; Siever, L. J.; Bitsios, P.; Haroutunian, V. Convergent Findings for Abnormalities of the NF-KB Signaling Pathway in Schizophrenia. *Neuropsychopharmacology* **2013**, *38* (3), 533–539. https://doi.org/10.1038/npp.2012.215.

(102) Volk, D. W.; Moroco, A. E.; Roman, K. M.; Edelson, J. R.; Lewis, D. A. The Role of the Nuclear Factor-KB Transcriptional Complex in Cortical Immune Activation in Schizophrenia. *Biol. Psychiatry* **2019**, *85* (1), 25–34. https://doi.org/10.1016/j.biopsych.2018.06.015.

(103) Lian, H.; Yang, L.; Cole, A.; Sun, L.; Chiang, A. C.; Fowler, S. W.; Shim, D. J.; Rodriguez-rivera, J.; Taglialatela, G.; Jankowsky, J. L. NFκB-Activated Astroglial Release of Complement C3 Compromises Neuronal Morphology and Function Associated with Alzheimer's Disease. *Neuron* **2016**, *85* (1), 101–115. https://doi.org/10.1016/j.neuron.2014.11.018.NF.

(104) Stephan, A. H.; Barres, B. A.; Stevens, B. The Complement System: An Unexpected Role in Synaptic Pruning During Development and Disease. *Annu. Rev. Neurosci.* **2012**, *35* (1), 369–389. https://doi.org/10.1146/annurev-neuro-061010-113810.

(105) Presumey, J.; Bialas, A. R.; Carroll, M. C. Complement System in Neural Synapse Elimination in Development and Disease. *Adv. Immunol.* **2017**, *135*, 53–79. https://doi.org/10.1016/bs.ai.2017.06.004.

(106) Zheng Li, Jihoon Jo, Jie-Min Jia, Shih-Ching Lo, Daniel J. Whitcomb, S.; Jiao, Kwangwook Cho, and M. S. Caspase-3 Activation via Mitochondria Is Required for Long-Term Depression and AMPA Receptor Internalization. *Cell* **2010**, *141* (5), 859–871. https://doi.org/10.1016/j.cell.2010.03.053.

(107) Sekar, A.; Bialas, A. R.; De Rivera, H.; Davis, A.; Hammond, T. R.; Kamitaki, N.; Tooley, K.; Presumey, J.; Baum, M.; Van Doren, V.; et al. Schizophrenia Risk from Complex Variation of Complement Component 4. *Nature* **2016**, *530* (7589), 177–183. https://doi.org/10.1038/nature16549.

(108) Holahan, M. GAP-43 in Synaptic Plasticity: Molecular Perspectives. *Res. Reports Biochem.* **2015**, 137. https://doi.org/10.2147/rrbc.s73846.

(109) Chambers, J. S.; Thomas, D.; Saland, L.; Neve, R. L.; Perrone-Bizzozero, N. I. Growth-Associated Protein 43 (GAP-43) and Synaptophysin Alterations in the Dentate Gyrus of Patients with Schizophrenia. *Prog. Neuro-Psychopharmacology Biol. Psychiatry* **2005**, *29* (2), 283–290. https://doi.org/10.1016/j.pnpbp.2004.11.013.

(110) Hung, C.-C.; Lin, C.-H.; Chang, H.; Wang, C.-Y.; Lin, S.-H.; Hsu, P.-C.; Sun, Y.-Y.; Lin, T.-N.; Shie, F.-S.; Kao, L.-S.; et al. Astrocytic GAP43 Induced by the TLR4/NF-KB/STAT3 Axis Attenuates Astrogliosis-Mediated Microglial Activation and Neurotoxicity. *J. Neurosci.* **2016**, *36* (6), 2027–2043. https://doi.org/10.1523/jneurosci.3457-15.2016.

(111) U. Thomas, S. Ebitsch, M. G.; Koh, Y. H.; , C.D. Hough, D. Woods, E. D.; Gundelfinger, and V. B. Synaptic Targeting and Localization of Discs-Large Is a Stepwise Process Controlled by Different Domains of the Protein. *Curr Biol* **2000**, *10* (18), 1108–1117. https://doi.org/https://doi.org/10.1016/S0960-9822(00)00696-5.

(112) Underhill, S. M.; Wheeler, D. S.; Amara, S. G. Differential Regulation of Two Isoforms of the Glial Glutamate Transporter EAAT2 by DLG1 and CaMKII. *J. Neurosci.* **2015**, *35* (13), 5260–5270. https://doi.org/10.1523/jneurosci.4365-14.2015.

(113) Makifuchi, T.; Nakamura, R.; Iritani, S.; Maeda, K.; Kakita, A.; Nawa, H.; Toyooka, K.; Shirakawa, O.; Niizato, K.; Watanabe, M.; et al. Selective Reduction of a PDZ Protein, SAP-97, in the Prefrontal Cortex of Patients with Chronic Schizophrenia. *J. Neurochem.* **2003**, *83* (4), 797–806. https://doi.org/10.1046/j.1471-4159.2002.01181.x.

(114) Uezato, A.; Yamamoto, N.; Iwayama, Y.; Hiraoka, S.; Hiraaki, E.; Umino, A.; Haramo, E.; Umino, M.; Yoshikawa, T.; Nishikawa, T. Reduced Cortical Expression of a Newly Identified Splicing Variant of the DLG1 Gene in Patients with Early-Onset Schizophrenia. *Transl. Psychiatry* **2015**, *5* (10), e654-8. https://doi.org/10.1038/tp.2015.154.

(115) Funk, A. J.; Mielnik, C. A.; Koene, R.; Newburn, E.; Ramsey, A. J.; Lipska, B. K.; McCullumsmith, R. E. Postsynaptic Density-95 Isoform Abnormalities in Schizophrenia. *Schizophr. Bull.* **2017**, *43* (4), 891–899. https://doi.org/10.1093/schbul/sbw173.

(116) Catts, V. S.; Derminio, D. S.; Hahn, C. G.; Weickert, C. S. Postsynaptic Density Levels of the NMDA Receptor NR1 Subunit and PSD-95 Protein in Prefrontal Cortex from People with Schizophrenia. *npj Schizophr.* **2015**, *1* (1), 26–30. https://doi.org/10.1038/npjschz.2015.37.

(117) Kleiger, G.; Mayor, T. Perilous Journey: A Tour of the Ubiquitin-Proteasome System. *Trends Cell Biol.* **2014**, *24* (6), 352–359. https://doi.org/10.1016/j.tcb.2013.12.003.

(118) Altar, C. A.; Jurata, L. W.; Charles, V.; Lemire, A.; Liu, P.; Bukhman, Y.; Young, T. A.; Bullard, J.; Yokoe, H.; Webster, M. J.; et al. Deficient Hippocampal Neuron Expression of Proteasome, Ubiquitin, and Mitochondrial Genes in Multiple Schizophrenia Cohorts. *Biol. Psychiatry* **2005**, *58* (2), 85–96. https://doi.org/10.1016/j.biopsych.2005.03.031.

(119) Rubio, M. D.; Wood, K.; Haroutunian, V.; Meador-Woodruff, J. H. Dysfunction of the Ubiquitin Proteasome and Ubiquitin-Like Systems in Schizophrenia. *Neuropsychopharmacology* **2013**, *38* (10), 1910–1920. https://doi.org/10.1038/npp.2013.84.

(120) Jennifer A Doudna, V. L. R. Structure and Function of the Eukaryotic Ribosome: The Next Frontier. *Cell* **2002**, *109* (2), 153–156. https://doi.org/https://doi.org/10.1016/S0092-8674(02)00725-0.

(121) Buffington, S. A.; Huang, W.; Costa-Mattioli, and M. Translational Control in Synaptic Plasticity and Cognitive Dysfunction. *Annu Rev Neurosci* **2014**, *37*, 17–38. https://doi.org/10.1146/annurev-neuro-071013-014100.

(122) English, J. A.; Fan, Y.; Föcking, M.; Lopez, L. M.; Hryniewiecka, M.; Wynne, K.; Dicker, P.; Matigian,

N.; Cagney, G.; Mackay-Sim, A.; et al. Reduced Protein Synthesis in Schizophrenia Patient-Derived Olfactory Cells. *Transl. Psychiatry* **2015**, *5* (April), e663. https://doi.org/10.1038/tp.2015.119.

(123) Xiang, Z.; Wen-Juan, L.; Jun-Ming, L.; Peng, L.; Hua, L. Ribosomal Proteins: Functions beyond the Ribosome. *J. Mol. Cell Biol.* **2015**, *7* (2), 92–104.

(124) Filip, A. M.; Klug, J.; Cayli, S.; Fröhlich, S.; Henke, T.; Lacher, P.; Eickhoff, R.; Bulau, P.; Linder, M.; Carlsson-Skwirut, C.; et al. Ribosomal Protein S19 Interacts with Macrophage Migration Inhibitory Factor and Attenuates Its Pro-Inflammatory Function. *J. Biol. Chem.* **2009**, *284* (12), 7977–7985. https://doi.org/10.1074/jbc.M808620200.

(125) Lv, J.; Huang, X. R.; Klug, J.; Fröhlich, S.; Lacher, P.; Xu, A.; Meinhardt, A.; Lan, H. Y. Ribosomal Protein S19 Is a Novel Therapeutic Agent in Inflammatory Kidney Disease. *Clin. Sci.* **2013**, *124* (10), 627–637. https://doi.org/10.1042/cs20120526.

(126) Zhang, S.; Zis, O.; Ly, P. T. T.; Wu, Y.; Zhang, S.; Zhang, M.; Cai, F.; Bucala, R.; Shyu, W. C.; Song, W. Down-Regulation of MIF by NFκB under Hypoxia Accelerated Neuronal Loss during Stroke. *FASEB J.* **2014**, *28* (10), 4394–4407. https://doi.org/10.1096/fj.14-253625.

(127) BAUMANN, R.; CASAULTA, C.; SIMON, D.; CONUS, S.; YOUSEFI, S.; SIMON, H.-U. Macrophage Migration Inhibitory Factor Delays Apoptosis in Neutrophils by Inhibiting the Mitochondria-Dependent Death Pathway. *FASEB J.* **2003**, *17* (15), 2221–2230. https://doi.org/10.1096/fj.03-0110com.

(128) Jin, A.; Itahana, K.; O'Keefe, K.; Zhang, Y. Inhibition of HDM2 and Activation of P53 by Ribosomal Protein L23. *Mol. Cell. Biol.* **2004**, *24* (17), 7669–7680. https://doi.org/10.1128/mcb.24.17.7669-7680.2004.

(129) Wanzel, M.; Russ, A. C.; Kleine-Kohlbrecher, D.; Colombo, E.; Pelicci, P. G.; Eilers, M. A Ribosomal Protein L23-Nucleophosmin Circuit Coordinates Miz1 Function with Cell Growth. *Nat. Cell Biol.* **2008**, *10* (9), 1051–1061. https://doi.org/10.1038/ncb1764.

(130) Yang, L.; Zhu, J. ya; Zhang, J. guo; Bao, B. jun; Guan, C. qi; Yang, X. jing; Liu, Y. hua; Huang, Y. jiao; Ni, R. zhou; Ji, L. li. Far Upstream Element-Binding Protein 1 (FUBP1) Is a Potential c-Myc Regulator in Esophageal Squamous Cell Carcinoma (ESCC) and Its Expression Promotes ESCC Progression. *Tumor Biol.* **2016**, *37* (3), 4115–4126. https://doi.org/10.1007/s13277-015-4263-8.

(131) Duan, J.; Bao, X.; Ma, X.; Zhang, Y.; Ni, D.; Wang, H.; Zhang, F.; Du, Q.; Fan, Y.; Chen, J.; et al. Upregulation of Far Upstream Element-Binding Protein 1 (FUBP1) Promotes Tumor Proliferation and Tumorigenesis of Clear Cell Renal Cell Carcinoma. *PLoS One* **2017**, *12* (1), 1–16. https://doi.org/10.1371/journal.pone.0169852.

(132) Dang, C. V. C-Myc Target Genes Involved in Cell Growth, Apoptosis, and Metabolism. *Mol. Cell. Biol.* **1999**, *19* (1), 1–11. https://doi.org/10.1128/mcb.19.1.1.

(133) Lee, H. G.; Casadesus, G.; Nunomura, A.; Zhu, X.; Castellani, R. J.; Richardson, S. L.; Perry, G.; Felsher, D. W.; Petersen, R. B.; Smith, M. A. The Neuronal Expression of MYC Causes a Neurodegenerative Phenotype in a Novel Transgenic Mouse. *Am. J. Pathol.* **2009**, *174* (3), 891–897. https://doi.org/10.2353/ajpath.2009.080583.

(134) Lee, H. P.; Kudo, W.; Zhu, X.; Smith, M. A.; Lee, H. gon. Early Induction of C-Myc Is Associated with Neuronal Cell Death. *Neurosci. Lett.* **2011**, *505* (2), 124–127. https://doi.org/10.1016/j.neulet.2011.10.004.

(135) Qin, Z. H.; Chen, R. W.; Wang, Y.; Nakai, M.; Chuang, D. M.; Chase, T. N. Nuclear Factor KappaB

Nuclear Translocation Upregulates C-Myc and P53 Expression during NMDA Receptor-Mediated Apoptosis in Rat Striatum. *J. Neurosci.* **1999**, *19* (10), 4023–4033.

(136) Herold, S.; Wanzel, M.; Beuger, V.; Frohme, C.; Beul, D.; Hillukkala, T.; Syvaoja, J.; Saluz, H. P.; Haenel, F.; Eilers, M. Negative Regulation of the Mammalian UV Response by Myc through Association with Miz-1. *Mol. Cell* **2002**, *10* (3), 509–521. https://doi.org/10.1016/S1097-2765(02)00633-0.

(137) Qi, Y.; Li, X.; Chang, C.; Xu, F.; He, Q.; Zhao, Y.; Wu, L. Ribosomal Protein L23 Negatively Regulates Cellular Apoptosis via the RPL23/Miz-1/c-Myc Circuit in Higher-Risk Myelodysplastic Syndrome. *Sci. Rep.* **2017**, *7* (1), 1–12. https://doi.org/10.1038/s41598-017-02403-x.

(138) Patel, J. H.; McMahon, S. B. Targeting of Miz-1 Is Essential for Myc-Mediated Apoptosis. *J. Biol. Chem.* **2006**, *281* (6), 3283–3289. https://doi.org/10.1074/jbc.M513038200.

(139) Eyss, V.; Wagner, N.; Wolf, E.; Gebhardt, A.; Kawauchi, D.; Walz, S.; Renninger, C.; Krohne, G.; Asan, E.; Roussel, M. F.; et al. Miz1 Is Required to Maintain Autophagic Flux ¨. **2013**, 1–12. https://doi.org/10.1038/ncomms3535.

(140) Sasikumar, A. N.; Perez, W. B.; Kinzy, T. G. The Many Roles of the Eukaryotic Elongation Factor 1 Complex. *Wiley Interdiscip. Rev. RNA* **2012**, *3* (4), 543–555. https://doi.org/10.1002/wrna.1118.

(141) Talapatra, S.; Wagner, J. D. O.; Thompson, C. B. Elongation Factor-1 Alpha Is a Selective Regulator of Growth Factor Withdrawal and ER Stress-Induced Apoptosis. *Cell Death Differ.* **2002**, *9* (8), 856–861. https://doi.org/10.1038/sj.cdd.4401078.

(142) Blanch, A.; Robinson, F.; Watson, I. R.; Cheng, L. S.; Irwin, M. S. Eukaryotic Translation Elongation Factor 1-Alpha 1 Inhibits P53 and P73 Dependent Apoptosis and Chemotherapy Sensitivity. *PLoS One* **2013**, *8* (6). https://doi.org/10.1371/journal.pone.0066436.

(143) Marin, P.; Nastiuk, K. L.; Daniel, N.; Girault, J. A.; Czernik, A. J.; Glowinski, J.; Nairn, A. C.; Prémont, J. Glutamate-Dependent Phosphorylation of Elongation Factor-2 and Inhibition of Protein Synthesis in Neurons. *J. Neurosci.* **1997**, *17* (10), 3445–3454.

(144) Martins-De-Souza, D.; Gattaz, W. F.; Schmitt, A.; Rewerts, C.; Marangoni, S.; Novello, J. C.; MacCarrone, G.; Turck, C. W.; Dias-Neto, E. Alterations in Oligodendrocyte Proteins, Calcium Homeostasis and New Potential Markers in Schizophrenia Anterior Temporal Lobe Are Revealed by Shotgun Proteome Analysis. *J. Neural Transm.* **2009**, *116* (3), 275–289. https://doi.org/10.1007/s00702-008-0156-y.

(145) Haroon, E.; Miller, A. H.; Sanacora, G. Inflammation, Glutamate, and Glia: A Trio of Trouble in Mood Disorders. *Neuropsychopharmacology* **2017**, *42* (1), 193–215. https://doi.org/10.1038/npp.2016.199.

(146) Guerrini, L.; Blasi, F.; Denis-Donini, S. Synaptic Activation of NF-Kappa B by Glutamate in Cerebellar Granule Neurons in Vitro. *Proc. Natl. Acad. Sci.* **1995**, *92*, 9077–9081. https://doi.org/10.1073/pnas.92.20.9077.

(147) Homayoun, H.; Moghaddam, B. Orbitofrontal Cortex Neurons as a Common Target for Classic and Glutamatergic Antipsychotic Drugs. *Proc. Natl. Acad. Sci.* **2008**, *105* (46), 18041–18046. https://doi.org/10.1073/pnas.0806669105.

(148) Klauck, S. M.; Felder, B.; Kolb-Kokocinski, A.; Schuster, C.; Chiocchetti, A.; Schupp, I.; Wellenreuther, R.; Schmötzer, G.; Poustka, F.; Breitenbach-Koller, L.; et al. Mutations in the Ribosomal Protein Gene RPL10 Suggest a Novel Modulating Disease Mechanism for Autism. *Mol. Psychiatry* **2006**, *11* (12), 1073–1084. https://doi.org/10.1038/sj.mp.4001883.

(149) Yang, J.; Chen, Z.; Liu, N.; Chen, Y. Ribosomal Protein L10 in Mitochondria Serves as a Regulator for ROS Level in Pancreatic Cancer Cells. *Redox Biol.* **2018**, *19* (May), 158–165. https://doi.org/10.1016/j.redox.2018.08.016.

(150) Jiang, Q.; Wu, G.; Yang, L.; Lu, Y. P.; Liu, X. X.; Han, F.; Deng, Y. P.; Fu, X. C.; Liu, Q. B.; Lu, Y. M. Elucidation of the FKBP25-60S Ribosomal Protein L7a Stress Response Signaling during Ischemic Injury. *Cell. Physiol. Biochem.* **2018**, *47* (5), 2018–2030. https://doi.org/10.1159/000491470.

(151) Dai, M.-S.; Zeng, S. X.; Jin, Y.; Sun, X.-X.; David, L.; Lu, H. Ribosomal Protein L23 Activates P53 by Inhibiting MDM2 Function in Response to Ribosomal Perturbation but Not to Translation Inhibition. *Mol. Cell. Biol.* **2004**, *24* (17), 7654–7668. https://doi.org/10.1128/mcb.24.17.7654-7668.2004.

(152) Clasen, S. J.; Shao, W.; Gu, H.; Espenshade, P. J. Prolyl Dihydroxylation of Unassembled US12/Rps23 Regulates Fungal Hypoxic Adaptation. *Elife* **2017**, *6*, 1–29. https://doi.org/10.7554/elife.28563.

(153) Landowski, M.; O'Donohue, M. F.; Buros, C.; Ghazvinian, R.; Montel-Lehry, N.; Vlachos, A.; Sieff, C. A.; Newburger, P. E.; Niewiadomska, E.; Matysiak, M.; et al. Novel Deletion of RPL15 Identified by Array-Comparative Genomic Hybridization in Diamond-Blackfan Anemia. *Hum. Genet.* **2013**, *132* (11), 1265–1274. https://doi.org/10.1007/s00439-013-1326-z.

**TABLE**

**Table 1:** Extra-ribosomal functions of ribosomal proteins.

**FIGURES**

**Figure 1. A)** Venn diagram of proteins identified among all cellular fractions. **B)** Biological functions of the proteins identified exclusively in each subcellular fraction. **C)** Principal component analysis of the patient proteome data from different fractions. **D)** The total number of proteins identified, quantified and dysregulated in each subcellular fraction.

**Figure 2.** Representation of the main proteins involved in apoptosis from the MIT fraction. During the apoptotic process proteins as VDAC1 and GAPDH interact, leading the increase of mitochondrial $Ca^{2+}$ uptake. VDAC1 also is linked with CNX in the MAMs, establishing the crosstalk between ER and mitochondria in the apoptosis. Calnexin (CNX), Voltage-dependent anion-selective channel protein 1 (VDAC1), Glyceraldehyde-3-phosphate dehydrogenase (GAPDH), Mitochondria-associated membrane (MAMs).

**Figure 3.** Imbalance in CREB activation. Cytoplasmatic βCaMKII quantified as down-regulated in CYT fraction was reported as a key kinase that phosphorylates γCaMKII. It is represented how the low availability of βCaMKII could affect γCaMKII phosphorylation which would impact γCaMKII/$Ca^{2+}$/CaM interaction. The inappropriate interaction between γCaMKII with $Ca^{2+}$/CaM leads an inefficient nuclear shuttle of $Ca^{2+}$/CaM by γCaMKII, who is translocated to the cell nucleus without the $Ca^{2+}$/CaM. On the other hand, nuclear αCaMKII is also decreased in the nucleus. The deficit in nuclear translocation of $Ca^{2+}$/CaM harms CREB activation by other $Ca^{2+}$/CaM dependent kinases such as CaMKK, CaMKIV, and αCaMKII. CREB: Ca2+/cAMP response element binding protein, βCaMKII: Calcium/calmodulin-dependent protein kinase beta, γCaMKII: Calcium/calmodulin-dependent protein kinase gamma, $Ca^{2+}$/CaM: Calcium/calmodulin, αCaMKII: Calcium/calmodulin-dependent protein kinase alpha.

**Figure 4.** Dysregulation in glutamate metabolism**.** In astrocytes, the glutamate is taken up from the synaptic cleft by the excitatory amino acid transporters and $Na^{+}/K^{+}$-ATPase and converted to glutamine by glutamine synthetase (GS). In the pre-synaptic terminal, the glutamine is transported and it is converted back into glutamate by glutaminase (GA). The deviation of the metabolism towards the preferential production

of glutamate is also favored whereby the decrease of GLDH and ASAT in astrocytes and neurons. Gln: glutamine, Glu: glutamate, EAAT1/ EAAT2: excitatory amino acid transporters, $Na^+/K^+$-ATPase: sodium/potassium-transporting ATPase, GLDH: glutamate dehydrogenase, ASAT: aspartate aminotransferase, TCA: tricarboxylic acid cycle.

**Figure 5. A)** NF-kB signaling pathway. The increase of RhoB, HMGB1, ERK-2 and UBE2N together with the glutamate activate the NF-kB signaling pathway and the decrease of protein kinase beta is involved in its regulation. NF-kB signaling pathway activation can promote the astrocytic production of complement C3. **B)** Quantification of complement C3 in NUC fraction **C)** Quantification of complement C3 in CYT fraction. NF-kB: Nuclear Factor kappa B, RhoB: Ras Homolog Family Member B, HMGB1: High Mobility Group Box 1, ERK-2: Mitogen-activated protein kinase 1, UBE2N: Ubiquitin-conjugating enzyme E2 N.

**SUPPORTING INFORMATION**

**Table S-1: Clinical information of patients and controls.**

**Table S-2: Group of proteins and peptides identified by iTRAQ in each enrichment of subcellular fraction.**

**Table S-3: Reactome pathway analysis of the proteome from each enriched subcellular fraction.**

**Table S-4: Group of proteins quantified after InfernoRND normalization.**

**Table S-5: Dysregulated proteins quantified by iTRAQ in each enriched subcellular fraction.**

**Table S-6: Selected reaction monitoring analysis of proteins as γCaMKII, MAPK2, C3, GS, UCH-L1 and NF-kB family.**

**Table S-7: Reactome pathway analysis of the dysregulated proteins quantified by iTRAQ of each enriched subcellular fraction.**

## FIGURE 1

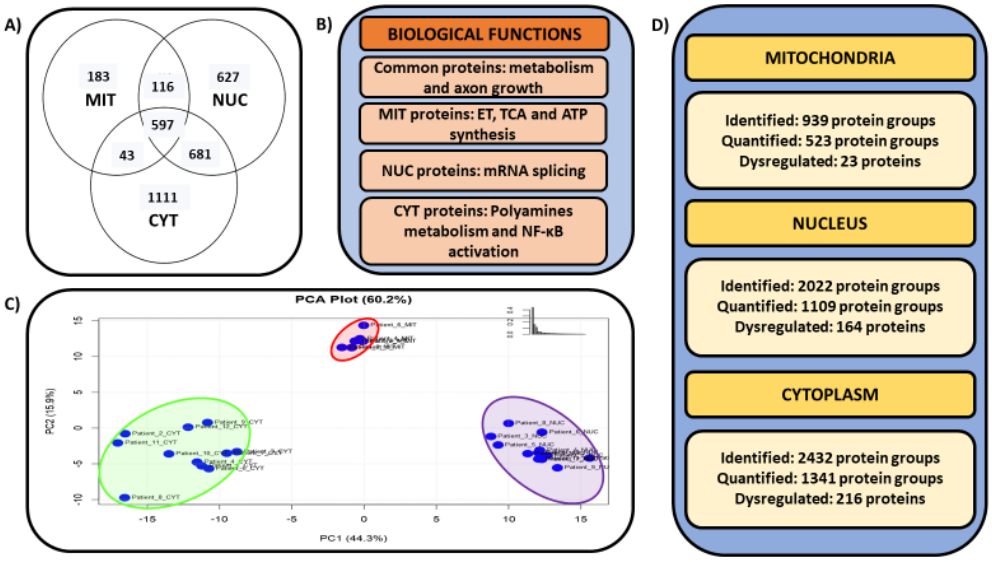


## FIGURE 2

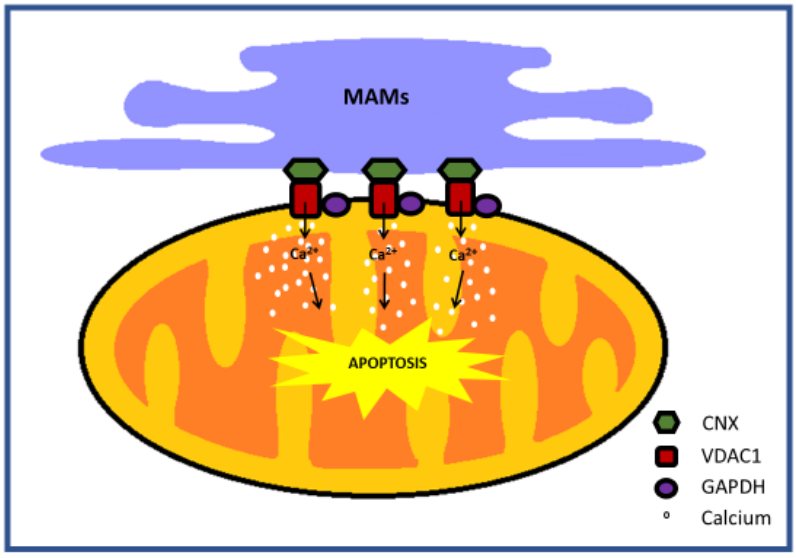

**FIGURE 3**

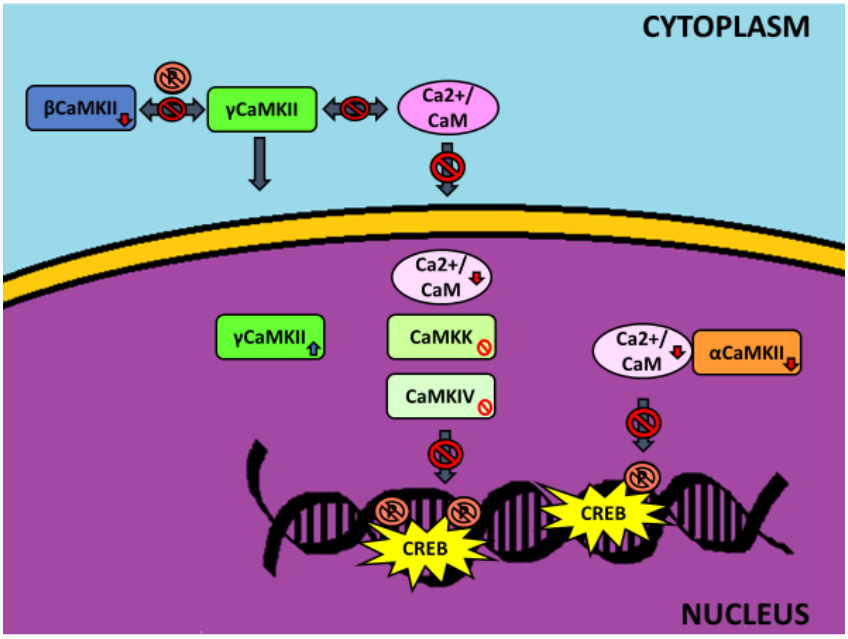


**FIGURE 4**

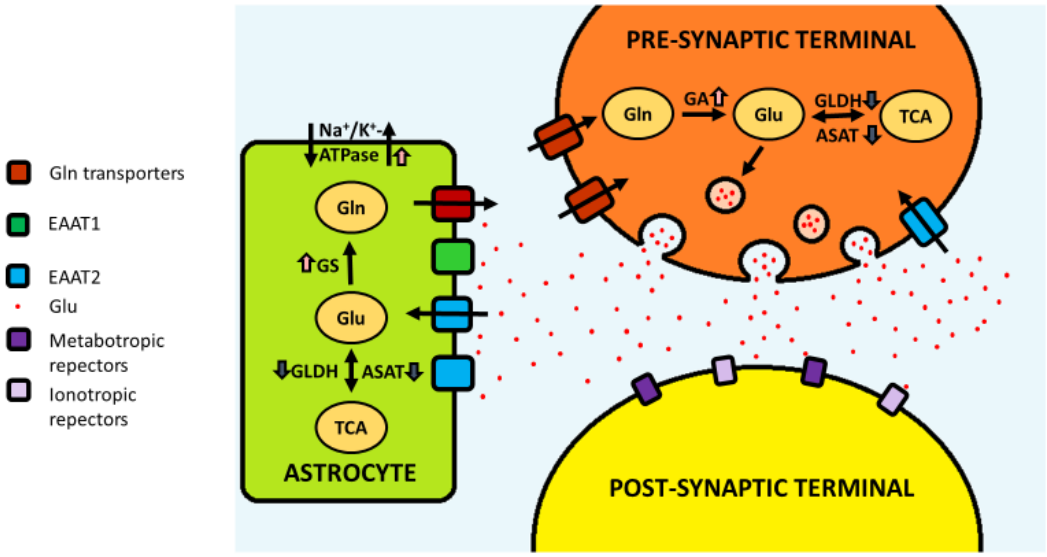

**FIGURE 5**

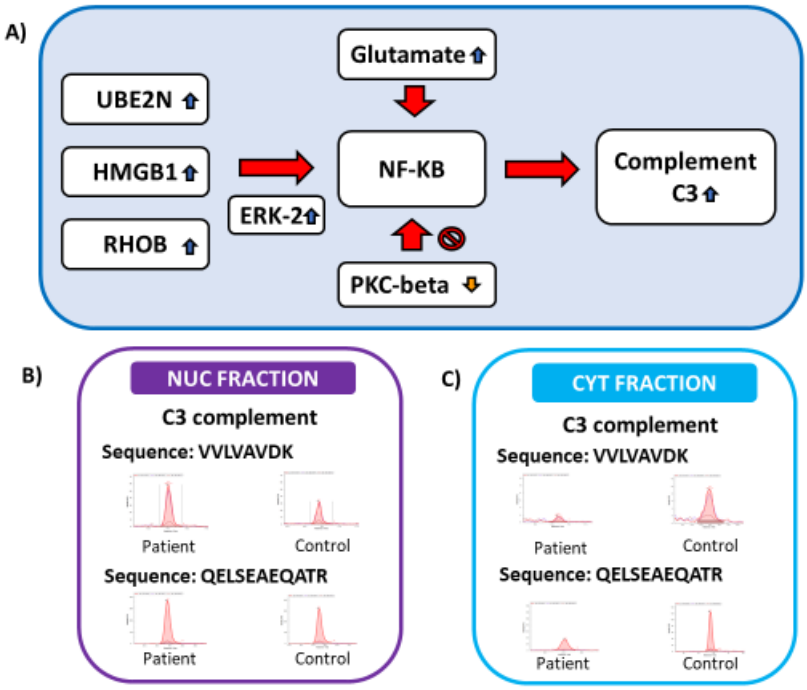
A)
Glutamate
UBE2N
HMGB1
RHOB
ERK-2
NF-KB
Complement C3
PKC-beta
B)
NUC FRACTION
C3 complement
Sequence: VVLVAVDK
Patient
Control
Sequence: QELSEAEQATR
Patient
Control
C)
CYT FRACTION
C3 complement
Sequence: VVLVAVDK
Patient
Control
Sequence: QELSEAEQATR
Patient
Control

**Table 1: Extra-ribosomal functions of ribosomal subunits.**

| Ribosomal protein | CYT fraction | NUC fraction | Extra-ribosomal function | Reference |
|---|---|---|---|---|
| **L10** | = | ↑ | ROS regulator, autism | (147); (148) |
| **S19** | ↓ | ↑ | Inhibition of Mif, ERK and NF-kB | (124); (125) |
| **L7a** | = | ↑ | Protective stress responses | (150) |
| **L23** | **n.q.** | ↑ | p53 activation. Regulation of Miz1 function. | (151); (128); (129) |
| **S23** | ↓ | ↑ | Sre1 activity modulation (yeast) | (152) |
| **L15** | = | ↑ | Diamond–Blackfan anemia | (153) |
| **L28** | **n.q.** | ↑ | Extraribosomal functions unknown | |

**n.q.: not quantified**
**=: non-significant quantitative changes**

## REFERENCIAS

AGHAJANIAN, G. K.; MAREK, G. J. **Serotonin model of schizophrenia: emerging role of glutamate mechanisms**. *Brain Research Reviews*, [s.l.], v. 31, nº 2–3, p. 302–312, 2000. ISSN: 01650173, DOI: 10.1016/S0165-0173(99)00046-
6.

BANERJEE, S.; MAZUMDAR, S. **Electrospray Ionization Mass Spectrometry: A Technique to Access the Information beyond the Molecular Weight of the Analyte**. *International Journal of Analytical Chemistry*, [s.l.], v. 2012, p. 1–40, 2012. ISSN: 1687-8760, DOI: 10.1155/2012/282574.

BANTSCHEFF, M. et al. **Quantitative mass spectrometry in proteomics: Critical review update from 2007 to the present**. *Analytical and Bioanalytical Chemistry*, [s.l.], v. 404, nº 4, p. 939–965, 2012. ISSN: 16182642, DOI: 10.1007/s00216-012-6203-4.

BEHAN, Á. et al. **Proteomic analysis of membrane microdomain-associated proteins in the dorsolateral prefrontal cortex in schizophrenia and bipolar disorder reveals alterations in LAMP, STXBP1 and BASP1 protein expression**. *Molecular Psychiatry*, [s.l.], v. 14, nº 6, p. 601–613, 2009. ISBN: 1359-4184, ISSN: 1359-4184, DOI: 10.1038/mp.2008.7.

BEHRENS, M. M. et al. **Ketamine-induced loss of phenotype of fast-spiking interneurons is mediated by NADPH-oxidase**. *Science*, [s.l.], v. 318, nº 5856, p. 1645–1647, 2007. ISSN: 00368075, DOI: 10.1126/science.1148045.

BORA, E. et al. **Neuroanatomical abnormalities in schizophrenia: A multimodal voxelwise meta-analysis and meta-regression analysis**. *Schizophrenia Research*, [s.l.], v. 127, nº 1–3, p. 46–57, 2011. ISSN: 09209964, DOI: 10.1016/j.schres.2010.12.020.

BORRÀS, E.; SABIDÓ, E. **What is targeted proteomics? A concise revision of targeted acquisition and targeted data analysis in mass spectrometry**. *Proteomics*, [s.l.], v. 17, nº 17–18, p. 17–18, 2017. ISSN: 16159861, DOI: 10.1002/pmic.201700180.

BREIER, A. et al. **Schizophrenia is associated with elevated amphetamine-induced synaptic dopamine concentrations: Evidence from a novel positron emission tomography method (raclopridebrain imagingstriatumin vivo microdialysispsychostimulants)**. *Medical Sciences Communicated by Seymour Kety*, [s.l.], v. 94, nº March, p. 2569–2574, 1997.

BRISCH, R. et al. **The role of dopamine in schizophrenia from a neurobiological and evolutionary perspective: Old fashioned, but still in vogue**. *Frontiers in Psychiatry*, [s.l.], v. 5, nº APR, p. 1–11, 2014. ISSN: 16640640, DOI: 10.3389/fpsyt.2014.00047.

CASTNER, S. A.; WILLIAMS, G. V.; GOLDMAN-RAKIC, P. S. **Reversal of antipsychotic-induced**

**working memory deficits by short-term dopamine D1 receptor stimulation**. *Science*, [s.l.], v. 287, nº 5460, p. 2020–2022, 2000. ISSN: 00368075, DOI: 10.1126/science.287.5460.2020.

CATHERMAN, A. D.; SKINNER, O. S.; KELLEHER, N. L. **Top Down Proteomics: Facts and Perspectives Proteomics in a Post-Genomics World**. [s.l.], v. 445, nº 4, p. 683–693, 2015. DOI: 10.1016/j.bbrc.2014.02.041.

CATTS, V. S. et al. **Postsynaptic density levels of the NMDA receptor NR1 subunit and PSD-95 protein in prefrontal cortex from people with schizophrenia**. *npj Schizophrenia*, [s.l.], v. 1, nº 1, p. 26–30, 2015. ISSN: 2334265X, DOI: 10.1038/npjschz.2015.37.

CHANG, W. C. et al. **Matrix-assisted laser desorption/ionization (MALDI) mechanism revisited**. *Analytica Chimica Acta*, [s.l.], v. 582, nº 1, p. 1–9, 2007. ISSN: 00032670, DOI: 10.1016/j.aca.2006.08.062.

CHELIUS, D.; BONDARENKO, P. V. **Quantitative profiling of proteins in complex mixtures using liquid chromatography and mass spectrometry**. *Journal of Proteome Research*, [s.l.], v. 1, nº 4, p. 317–323, 2002. ISSN: 15353893, DOI: 10.1021/pr025517j.

CHOE, L. et al. **8-Plex Quantitation of changes in cerebrospinal fluid protein expression in subjects undergoing intravenous immunoglobulin treatment for Alzheimer's disease**. *Proteomics.*, [s.l.], v. 7, nº 20, p. 3651–3660, 2007. DOI: 10.1002/pmic.200700316.

CHOHAN, M. O. et al. **Pathway-Specific Dopamine Abnormalities in Schizophrenia**. *Biological Psychiatry*, [s.l.], v. 81, nº 1, p. 31–42, 2016. ISSN: 00063223, DOI: 10.1016/j.biopsych.2016.03.2104.

DEMJAHA, A. et al. **Antipsychotic treatment resistance in schizophrenia associated with elevated glutamate levels but normal dopamine function**. *Biological Psychiatry*, [s.l.], v. 75, nº 5, p. e11–e13, 2014. ISSN: 00063223, DOI: 10.1016/j.biopsych.2013.06.011.

DONGEN, J. VAN; BOOMSMA, D. I. **The evolutionary paradox and the missing heritability of schizophrenia**. *American Journal of Medical Genetics, Part B: Neuropsychiatric Genetics*, [s.l.], v. 162, nº 2, p. 122–136, 2013. ISSN: 15524841, DOI: 10.1002/ajmg.b.32135.

EGGERS, A. E. **A serotonin hypothesis of schizophrenia**. *Medical Hypotheses*, [s.l.], v. 80, nº 6, p. 791–794, 2013. ISSN: 03069877, DOI: 10.1016/j.mehy.2013.03.013.

EIDHAMMER, I. et al. **Computational Methods for Mass Spectrometry Proteomics**. *Computational Methods for Mass Spectrometry Proteomics*, [s.l.], v. 009, p. 1–284, 2007. ISBN: 9780470512975, DOI: 10.1002/9780470724309.

ENG, J. K.; ASHLEY, MCCORMACK L. AND YATES, J. R. **An Approach to Correlate Tandem Mass Spectral Data of Peptides with Amino Acid Sequences in a Protein Database**. *Journal of the American Society for Mass Spectrometry*, [s.l.], v. 5, nº 11, p. 976–989, 1994. DOI: https://doi.org/10.1016/1044-0305(94)80016-2.

ENG, J. K.; JAHAN, T. A.; HOOPMANN, M. R. **Comet: an open-source MS/MS sequence database search tool.** *Proteomics*, [s.l.], v. 13, nº 1, p. 22–4, 2013. ISSN: 1615-9861, DOI: 10.1002/pmic.201200439.

EROGLU S., TOPRAK S., URGAN O, MD, OZGE E. ONUR, MD, ARZU DENIZBASI, MD, HALDUN AKOGLU, MD, CIGDEM OZPOLAT, MD, EBRU AKOGLU, M. **DSM-IV Diagnostic and Statistical Manual of Mental Disorder**. *American Psychiatric Organization*. [s.l.]: [s.n.], 1994. v. 33, 1–915 p. ISBN: 9781604138795, DOI: 10.1073/pnas.0703993104.

FARBER NB. **The NMDA receptor hypofunction model of psychosis**. *Ann N Y Acad Sci*, [s.l.], v. 6, nº 1003, p. 119–30, 2003. DOI: 10.1196/annals.1300.008.

FEINBERG, I. **Schizophrenia: Caused by a fault in programmed synaptic elimination during adolescence?** *Journal of Psychiatric Research*, [s.l.], v. 17, nº 4, p. 319–334, 1982. ISSN: 00223956, DOI: 10.1016/0022-3956(82)90038-3.

FÖCKING, M. et al. **Proteomic and genomic evidence implicates the postsynaptic density in schizophrenia**. *Molecular Psychiatry*, [s.l.], v. 20, nº 4, p. 424–432, 2015. ISBN: 0920-9964, ISSN: 1359-4184, DOI: 10.1038/mp.2014.63.

FUENTE-SANDOVAL, C. D. La et al. **Higher levels of glutamate in the associative-striatum of subjects with prodromal symptoms of schizophrenia and patients with first-episode psychosis**. *Neuropsychopharmacology*, [s.l.], v. 36, nº 9, p. 1781–1791, 2011. ISSN: 0893133X, DOI: 10.1038/npp.2011.65.

GASKELL, S. J. **SPECIAL FEATURE : Electrospray : Principles and Practice**. *Journal of mass spectrometry*, [s.l.], v. 32, nº April, p. 677–688, 1997. ISBN: 1096-9888, ISSN: 10765174, DOI: 10.1002/(SICI)1096-9888(199707)32:7<677::AID-JMS536>3.0.CO;2-G.

GAUR, N. et al. **THE BIOCHEMICAL WOMB OF SCHIZOPHRENIA : A REVIEW**. [s.l.], v. 23, nº 4, p. 307–327, 2008.

GIEGLING, I. et al. **Genetics of schizophrenia: A consensus paper of the WFSBP Task Force on Genetics**. *The World Journal of Biological Psychiatry*, [s.l.], v. 0, nº 0, p. 1–14, 2017. ISBN: 15622975 (ISSN), ISSN: 1562-2975, DOI: 10.1080/15622975.2016.1268715.

GROSS, J. H.; GROSS, J. H. **Tandem Mass Spectrometry**. *Mass Spectrometry*, [s.l.], p. 415–478, 2011. DOI: 10.1007/978-3-642-10711-5_9.

GUIDOTTI, A. et al. **GABAergic dysfunction in schizophrenia: New treatment strategies on the horizon**. *Psychopharmacology*, [s.l.], v. 180, nº 2, p. 191–205, 2005. ISSN: 00333158, DOI: 10.1007/s00213-005-2212-8.

HARRISON, P. J.; WEINBERGER, D. R. **Schizophrenia genes, gene expression, and neuropathology: On the matter of their convergence**. *Molecular Psychiatry*, [s.l.], v. 10, nº 1, p. 40–68, 2005. ISSN: 13594184, DOI: 10.1038/sj.mp.4001558.

HIRAYAMA-KUROGI, M. et al. **Downregulation of GNA13-ERK network in prefrontal cortex of schizophrenia brain identified by combined focused and targeted quantitative proteomics**. *Journal of Proteomics*, [s.l.], v. 158, p. 31–42, 2017. ISSN: 18767737, DOI: 10.1016/j.jprot.2017.02.009.

HOMAYOUN, H.; MOGHADDAM, B. **Orbitofrontal cortex neurons as a common target for classic and glutamatergic antipsychotic drugs**. *Proceedings of the National Academy of Sciences*, [s.l.], v. 105, nº 46, p. 18041–18046, 2008. ISSN: 0027-8424, DOI: 10.1073/pnas.0806669105.

HU, Q. et al. **The Orbitrap: A new mass spectrometer**. *Journal of Mass Spectrometry*, [s.l.], v. 40, nº 4, p. 430–443, 2005. ISSN: 10765174, DOI: 10.1002/jms.856.

HUBER, L. A. **Is proteomics heading in the wrong direction?** *Nature Reviews Molecular Cell Biology*, [s.l.], v. 4, nº 1, p. 74–80, 2003. ISSN: 14710072, DOI: 10.1038/nrm1007.

J.C. HAMMOND, D. SHAN, J. H. M.-W. and R. E. M. **Evidence of Glutamatergic Dysfunction in the Pathophysiology of Schizophrenia**. *Synaptic Stress and Pathogenesis of Neuropsychiatric Disorders*, [s.l.], p. 265–294, 2014. ISBN: 9781493910564, DOI: 10.1007/978-1-4939-1056-4.

JAYARAM, R. **Mass Spectrometry**. *Mass Spectrometry*. [s.l.]: [s.n.], 2013. ISBN: 9783642107092, DOI: 10.1007/978-1-4899-5672-9.

JOHNSTONE, E. V. E. C.; FRITH, C. D.; KREEL, L. **SCHIZOPHRENIA ment emerges principally in those items in the battery**. *The Lancet*, [s.l.], v. 2, nº 7992, p. 924–926, 1976.

JONGE, J. C. DE et al. **GABAergic mechanisms in schizophrenia: Linking postmortem and In vivo studies**. *Frontiers in Psychiatry*, [s.l.], v. 8, nº AUG, p. 118, 2017. ISSN: 16640640, DOI: 10.3389/fpsyt.2017.00118.

LAI, X.; WANG, L.; WITZMANN, F. A. **Issues and Applications in Label-Free Quantitative Mass**

**Spectrometry**. *International Journal of Proteomics*, [s.l.], v. 2013, nº c, p. 1–13, 2013. ISSN: 2090-2166, DOI: 10.1155/2013/756039.

LALLY, J.; MACCABE, J. H. **Antipsychotic medication in schizophrenia: A review**. *British Medical Bulletin*, [s.l.], v. 114, nº 1, p. 169–179, 2015. ISSN: 14718391, DOI: 10.1093/bmb/ldv017.

LANGE, V. et al. **Selected reaction monitoring for quantitative proteomics: A tutorial**. *Molecular Systems Biology*, [s.l.], v. 4, nº 222, 2008. ISSN: 17444292, DOI: 10.1038/msb.2008.61.

LEPREVOST, F. V. et al. **PepExplorer: A Similarity-driven Tool for Analyzing de Novo Sequencing Results** . *Molecular & Cellular Proteomics*, [s.l.], v. 13, nº 9, p. 2480–2489, 2014. ISSN: 1535-9476, DOI: 10.1074/mcp.m113.037002.

LEWIS, J. K.; WEI, J.; SIUZDAK, G. **Matrix-Assisted Laser Desorption/Ionization Mass Spectrometry in Peptide and Protein Analysis**. *Encyclopedia of Analytical Chemistry*, [s.l.], p. 1–14, 2006. ISBN: 9780470027318, DOI: 10.1002/9780470027318.a1621.

LI, H. et al. **Current trends in quantitative proteomics – an update**. *Journal of Mass Spectrometry*, [s.l.], v. 52, nº 5, p. 319–341, 2017. ISSN: 10969888, DOI: 10.1002/jms.3932.

LOO, J. A.; UDSETH, H. R.; SMITH, R. D. **Peptide and protein analysis by electrospray ionization-mass spectrometry and capillary electrophoresis-mass spectrometry**. *Analytical Biochemistry*, [s.l.], v. 179, nº 2, p. 404–412, 1989. ISSN: 10960309, DOI: 10.1016/0003-2697(89)90153-X.

MAKAROV, A. **Electrostatic axially harmonic orbital trapping: a high-performance technique of mass analysis**. *Anal Chem.*, [s.l.], v. 72, nº 6, p. 1156–62, 2000.

MARTINS-DE-SOUZA, D.; GATTAZ, W. F.; SCHMITT, A.; REWERTS, C.; MARANGONI, S. et al. **Alterations in oligodendrocyte proteins, calcium homeostasis and new potential markers in schizophrenia anterior temporal lobe are revealed by shotgun proteome analysis**. *Journal of Neural Transmission*, [s.l.], v. 116, nº 3, p. 275–289, 2009. ISSN: 03009564, DOI: 10.1007/s00702-008-0156-y.

MARTINS-DE-SOUZA, D.; GATTAZ, W. F.; SCHMITT, A.; REWERTS, C.; MACCARRONE, G. et al. **Prefrontal cortex shotgun proteome analysis reveals altered calcium homeostasis and immune system imbalance in schizophrenia**. *European Archives of Psychiatry and Clinical Neuroscience*, [s.l.], v. 259, nº 3, p. 151–163, 2009. ISBN: 1433-8491 (Electronic)r0940-1334 (Linking), ISSN: 14338491, DOI: 10.1007/s00406-008-0847-2.

MARTINS-DE-SOUZA, D.; GATTAZ, W. F.; SCHMITT, A.; NOVELLO, J. C.; MARANGONI, S. et al. **Proteome analysis of schizophrenia patients Wernicke's area reveals an energy metabolism**

**dysregulation**. *BMC Psychiatry*, [s.l.], v. 9, nº 1, p. 17, 2009. ISBN: 1471-244X, ISSN: 1471-244X, DOI: 10.1186/1471-244X-9-17.

MARTINS-DE-SOUZA, D. et al. **Proteome analysis of the thalamus and cerebrospinal fluid reveals glycolysis dysfunction and potential biomarkers candidates for schizophrenia**. *Journal of Psychiatric Research*, [s.l.], v. 44, nº 16, p. 1176–1189, 2010. ISBN: 0022-3956, ISSN: 00223956, DOI: 10.1016/j.jpsychires.2010.04.014.

MCCOLLUM, L. A. et al. **Elevated excitatory input to the nucleus accumbens in schizophrenia: A postmortem ultrastructural study**. *Schizophrenia Bulletin*, [s.l.], v. 41, nº 5, p. 1123–1132, 2015. ISSN: 17451701, DOI: 10.1093/schbul/sbv030.

MCCUTCHEON, R. et al. **Defining the locus of dopaminergic dysfunction in schizophrenia: A meta-analysis and test of the mesolimbic hypothesis**. *Schizophrenia Bulletin*, [s.l.], v. 44, nº 6, p. 1301–1311, 2018. ISSN: 17451701, DOI: 10.1093/schbul/sbx180.

MÖLLER, H.-J. **The Relevance of Negative Symptoms in Schizophrenia and How to Treat Them with Psychopharmaceuticals?** *Psychiatria Danubina*, [s.l.], v. 28, nº 4, p. 435–440, 2016. ISSN: 0353-5053.

NGAN, E. T. C. et al. **Decreased serotonin 2A receptor densities in neuroleptic-naive patients with schizophrenia: A pet study using [ 18F]setoperone**. *American Journal of Psychiatry*, [s.l.], v. 157, nº 6, p. 1016–1018, 2000. ISSN: 0002953X, DOI: 10.1176/appi.ajp.157.6.1016.

NUCIFORA, F. C. et al. **Treatment resistant schizophrenia: Clinical, biological, and therapeutic perspectives**. *Neurobiology of Disease*, [s.l.], p. #pagerange#, 2018. ISSN: 1095953X, DOI: 10.1016/j.nbd.2018.08.016.

PENNINGTON, K.; COTTER, D.; DUNN, M. J. **The role of proteomics in investigating psychiatric disorders**. *British Journal of Psychiatry*, [s.l.], v. 187, nº 1, p. 4–6, 2005. ISSN: 0007-1250, DOI: 10.1192/bjp.187.1.4.

PERKINS, D. et al. **Probability-based protein identification by searching sequence databases using mass spectrometry data**. *Electrophoresis*, [s.l.], v. 20, nº 18, p. 3551–67, 1999. DOI: 10.1002/(SICI)1522-2683(19991201)20:18<3551::AID-ELPS3551>3.0.CO;2-2.

PETANJEK, Z. et al. **Extraordinary neoteny of synaptic spines in the human prefrontal cortex.** *Proceedings of the National Academy of Sciences of the United States of America*, [s.l.], v. 108, nº 32, p. 13281–6, 2011. ISSN: 1091-6490, DOI: 10.1073/pnas.1105108108.

PETERSON, A. C. et al. **Parallel reaction monitoring for high resolution and high mass accuracy quantitative, targeted proteomics.** *Molecular & cellular proteomics : MCP*, [s.l.], v. 11, nº 11, p. 1475–

88, 2012. ISSN: 1535-9484, DOI: 10.1074/mcp.O112.020131.

PICHLER, P. et al. **Peptide labeling with isobaric tags yields higher identification rates using iTRAQ 4-plex compared to TMT 6-plex and iTRAQ 8-plex on LTQ orbitrap**. *Analytical Chemistry*, [s.l.], v. 82, nº 15, p. 6549–6558, 2010. ISBN: 4317904411, ISSN: 00032700, DOI: 10.1021/ac100890k.

PILOWSKY, L. S. et al. **First in vivo evidence of an NMDA receptor deficit in medication-free schizophrenic patients [2]**. *Molecular Psychiatry*, [s.l.], v. 11, nº 2, p. 118–119, 2006. ISSN: 13594184, DOI: 10.1038/sj.mp.4001751.

QUEDNOW, B. B.; GEYER, M. A.; HALBERSTADT, A. L. **Serotonin and Schizophrenia**. *Handbook of Behavioral Neuroscience*. [s.l.]: Elsevier B.V., 2010. v. 21, 585–620 p. ISBN: 9780123746344, ISSN: 15697339, DOI: 10.1016/S1569-7339(10)70102-8.

RAUNIYAR, N. **Parallel Reaction Monitoring : A Targeted Experiment Performed Using High Resolution and High Mass Accuracy Mass Spectrometry**. [s.l.], p. 28566–28581, 2015. DOI: 10.3390/ijms161226120.

RIPKE, S. et al. **Biological insights from 108 schizophrenia-associated genetic loci**. *Nature*, [s.l.], v. 511, nº 7510, p. 421–427, 2014. ISBN: 0028-0836, ISSN: 0028-0836, DOI: 10.1038/nature13595.

ROSS, P. L. et al. **Multiplexed Protein Quantitation in Saccharomyces cerevisiae Using Amine-reactive Isobaric Tagging Reagents * □**. [s.l.], p. 1154–1169, 2004. DOI: 10.1074/mcp.M400129-MCP200.

ROTARU, D. C.; LEWIS, D. A.; GONZALEZ-BURGOS, G. **Interneurons : Relevance for Schizophrenia**. [s.l.], v. 23, nº 1, p. 97–109, 2013. DOI: 10.1515/revneuro-2011-0059.

ROTHMAN, D. L. et al. **In vivo NMR Studies of the Glutamate Neurotransmitter Flux and Neuroenergetics: Implications for Brain Function**. *Annual Review of Physiology*, [s.l.], v. 65, nº 1, p. 401–427, 2003. ISSN: 0066-4278, DOI: 10.1146/annurev.physiol.65.092101.142131.

SAIA-CEREDA, V. M. et al. **Proteomics of the corpus callosum unravel pivotal players in the dysfunction of cell signaling, structure, and myelination in schizophrenia brains**. *European Archives of Psychiatry and Clinical Neuroscience*, [s.l.], v. 265, nº 7, p. 601–612, 2015. ISBN: 0940-1334, ISSN: 14338491, DOI: 10.1007/s00406-015-0621-1.

SAIA-CEREDA, V. M. et al . **The Nuclear Proteome of White and Gray Matter from Schizophrenia Postmortem Brains**. *Molecular Neuropsychiatry*, [s.l.], v. 3, nº 1, p. 37–52, 2017. ISSN: 2296-9209, DOI: 10.1159/000477299.

SEEMAN, P. et al. **Antipsychotic drug doses and neuroleptic/dopamine receptors**. *Nature*, [s.l.], v. 261, nº 5562, p. 717–719, 1976. ISSN: 00280836, DOI: 10.1038/261717a0.

SELEMON, L. D. et al. **Amphetamine sensitization alters dendritic morphology in prefrontal cortical pyramidal neurons in the non-human primate**. *Neuropsychopharmacology*, [s.l.], v. 32, nº 4, p. 919–931, 2007. ISSN: 0893133X, DOI: 10.1038/sj.npp.1301179.

SELTEN, J. P. et al. **The social defeat hypothesis of schizophrenia: An update**. *Schizophrenia Bulletin*, [s.l.], v. 39, nº 6, p. 1180–1186, 2013. ISBN: 3171890720, ISSN: 05867614, DOI: 10.1093/schbul/sbt134.

SHEVCHENKO, A.; VALCU, C. M.; JUNQUEIRA, M. **Tools for exploring the proteomosphere**. *Journal of Proteomics*, [s.l.], v. 72, nº 2, p. 137–144, 2009. ISSN: 18743919, DOI: 10.1016/j.jprot.2009.01.012.

SIDOLI, S.; GARCIA, B. A. **Middle-down proteomics: a still unexploited resource for chromatin biology**. *Expert Review of Proteomics*, [s.l.], v. 14, nº 7, p. 617–626, 2017. ISSN: 17448387, DOI: 10.1080/14789450.2017.1345632.

SIE, M. **Schizophrenia clinical features and diagnosis**. *Clinical Pharmacist*, [s.l.], v. 3, nº 1, p. 41–44, 2011.

SIMPSON, E. H.; KELLENDONK, C.; KANDEL, E. **A Possible Role for the Striatum in the Pathogenesis of the Cognitive Symptoms of Schizophrenia**. *Neuron*, [s.l.], v. 65, nº 5, p. 585–596, 2010. ISSN: 08966273, DOI: 10.1016/j.neuron.2010.02.014.

SIRIS, S. G. **Implications of Normal Brain Development for the Pathogenesis of Schizophrenia**. *Archives of General Psychiatry*, [s.l.], v. 45, nº 11, p. 1055, 1988. ISSN: 15383636, DOI: 10.1001/archpsyc.1988.01800350089019.

STĘPNICKI, P.; KONDEJ, M.; KACZOR, A. A. **Current Concepts and Treatments of Schizophrenia**. *Molecules*, [s.l.], v. 23, nº 8, p. 2087, 2018. DOI: 10.3390/molecules23082087.

TANDON, N. et al. **Brain metabolite alterations in young adults at familial high risk for schizophrenia using proton magnetic resonance spectroscopy**. *Schizophrenia Research*, [s.l.], v. 148, nº 1–3, p. 59–66, 2013. ISSN: 09209964, DOI: 10.1016/j.schres.2013.05.024.

WILKINS, M. et al. **From proteins to proteomes: large scale protein identification by two-dimensional electrophoresis and amino acid analysis.** *Bio/technology (Nature Publishing Company)*, [s.l.], v. 14, nº 1, p. 61–5, 1996.

WILM, M. **Principles of Electrospray Ionization**. *Molecular & Cellular Proteomics*, [s.l.], v. 10, nº 7, p. M111.009407, 2011. ISSN: 1535-9476, DOI: 10.1074/mcp.M111.009407.

WOLTERS, D. A.; WASHBURN, M. P.; YATES, J. R. **An automated multidimensional protein identification technology for shotgun proteomics**. *Analytical Chemistry*, [s.l.], v. 73, nº 23, p. 5683–5690, 2001. ISSN: 00032700, DOI: 10.1021/ac010617e.

WONG, J. W. . and; CAGNEY, G. **An Overview of Label-Free Quantitation Methods in Proteomics by Mass Spectrometry**. *Proteome Bioinformatics*. [s.l.]: [s.n.], 2009. p. 273–283. DOI: 10.1007/978-1-60761-444-9_18.

XU ET AL. **ProLuCID, a fast and sensitive tandem mass spectra-based protein identification program**. *Molecular Cellular Proteomics*, [s.l.], v. 5, p. 174, 2006.

XU, M. Y.; WONG, A. H. C. **GABAergic inhibitory neurons as therapeutic targets for cognitive impairment in schizophrenia**. *Acta Pharmacologica Sinica*, [s.l.], v. 39, nº 5, p. 733–753, 2018. ISSN: 17457254, DOI: 10.1038/aps.2017.172.

ZHAN, B. et al. **Protein Analysis by Shotgun/Bottom-up Proteomics**. *Chemical Reviews*, [s.l.], v. 113, nº 4, p. 2343–2394, 2013. ISBN: 00092665 (ISSN), ISSN: 0009-2665, DOI: 10.1021/cr3003533.

ZHANG, X. et al. **Progressive Grey Matter Volume Changes in Patients with Schizophrenia over 6 Weeks of Antipsychotic Treatment and Their Relationship to Clinical Improvement**. *Neuroscience Bulletin*, [s.l.], v. 34, nº 5, p. 816–826, 2018. ISSN: 19958218, DOI: 10.1007/s12264-018-0234-6.